

Neural coding in the *Drosophila* Mushroom Body

A Dissertation Presented

by

Kyle S. Honegger

to

The Watson School of Biological Sciences

in Partial Fulfillment of the Requirements

for the Degree of

Doctor of Philosophy

in

the Biological Sciences

at Cold Spring Harbor Laboratory

March 2012

Contents

Contents	i
Acknowledgements	iv
List of Abbreviations	v
List of Figures	vii
Foreword	viii
I Introduction	1
1 From sensation to action	2
Neural coding - a brief historical perspective	3
1.1 Stimulus encoding	9
1.2 Information processing	14
1.2.1 Transformations	14
1.2.2 Sparse coding	15
1.2.2.1 Efficient coding hypothesis	16
1.2.2.2 Sparse representation hypothesis	18
1.3 Decoding	19
1.3.1 The classification paradigm	19
1.3.2 Neural and perceptual classification	20
1.3.3 Ideal observers and the general classification problem	22
2 Neural Coding in the <i>Drosophila</i> Olfactory System	30
2.1 Olfactory anatomy of <i>Drosophila</i>	31
2.1.1 Sensory periphery	31
2.1.1.1 Olfactory organs	32
2.1.1.2 Olfactory sensilla	34
2.1.1.3 Cellular mechanisms of signal transduction	35
2.1.2 Antennal lobe	36
2.1.2.1 Glomerular organization	36
2.1.2.2 Local connections link glomeruli	37
2.1.2.3 Antennocerebral tracts	38
2.1.3 Mushroom body	38
2.1.3.1 Development of KC classes	39

2.1.3.2	Calyx microanatomy	39
2.1.3.3	Kenyon cell somata	40
2.1.3.4	MB lobes	40
2.1.3.5	Other cell types	41
2.1.4	Efferent neurons	41
2.1.5	Lateral horn	42
2.2	Olfactory Coding	42
2.2.1	Combinatorial coding by OSNs	43
2.2.2	AL Reformatting	46
2.2.3	Sparsening in MB	49
2.3	Outstanding questions in <i>Drosophila</i> olfactory coding	52
II Experimental results		55
3	Cellular-Resolution Population Imaging Reveals Robust Sparse Coding in the <i>Drosophila</i> Mushroom Body	56
3.1	Abstract	56
3.2	Introduction	57
3.3	Materials and Methods	58
3.4	Results	62
3.4.1	Optical monitoring of MB population activity	62
3.4.2	Determining population responses from somatic calcium signals	64
3.4.3	Random spatial distribution of MB odor responses	67
3.4.4	MB population responses to odors are sparse and correlated with net OSN output	72
3.4.5	MB population sparseness is preserved across a range of concentrations	74
3.4.6	Sparse MB responses to natural and artificial multimolecular odors	76
3.4.7	MB responses to natural and monomolecular odors are indistinguishable	79
3.5	Discussion	79
3.5.1	Spatial organization and tuning curve topography of sparse responses	81
3.5.2	Robustness of sparse representations to stimulus intensity and complexity	82
3.6	Acknowledgements	84
4	MB odor responses predict learned olfactory behavior in <i>Drosophila</i>	86
4.1	Abstract	86
4.2	Introduction	86
4.3	Materials and Methods	88
4.4	Results	92
4.4.1	Odor identity is represented by unique KC activity patterns	93
4.4.2	MB activity predicts generalization of olfactory associations	96
4.4.3	Probing olfactory discrimination using odor blends	100
4.4.4	KC activity predicts accuracy of learned odor discrimination	102
4.4.5	A binary code for odor identity in the MB	105
4.5	Discussion	106
4.5.1	MB odor representations in naïve animals predict learned behavior	107
4.5.2	Binary coding in MB enables a simple learning rule	108
4.5.3	Summary	109
4.6	Acknowledgements	110

III	Conclusions and perspectives	113
5	Conclusions and perspectives	114
5.1	<i>In vivo</i> imaging of population responses	114
5.2	Sparseness is a fundamental feature of the MB code	115
5.3	MB pattern overlap is predictive of simple learned olfactory behaviors	115
5.4	Associative memory as template matching	117
5.5	Toward a signal processing view of the olfactory system	118
5.6	Future directions	119
	Appendix A - Odor concentration and KC response magnitude	121
	References	128

Acknowledgements

I would like to thank my family, friends, and everyone at CSHL who made it possible for me to get to this point. First and foremost, I am indebted to my parents for always encouraging me to do what I love, and for allowing me to do so. I am grateful to my adviser, Glenn Turner, for his support and guidance throughout my time at CSHL, and for introducing me to the wonderful world of *Drosophila*. Whoever thought staring at tiny insects could be so much fun? Also in order is a hearty thanks to Rob Campbell, who trudged with me through all of the experiments described in this thesis (as well as many other experimental tribulations). And, since doing science is not always a walk in the park, we all need a good laugh every once in a while. Getting to work alongside the members of the Turner, Zhong, and Dubnau labs has made my daily graduate experience enjoyable and memorable. The members of my thesis committee - Josh Dubnau, John Inglis, Adam Kepecs, Pavel Osten, and Tony Zador - have provided experimental ideas and suggestions that have had a profound and positive impact on this work, and for that I'm very grateful. And last, but certainly not least, a special thanks to my wife, Laura, for all of her heartfelt support. The encouragement and inspiration she provides keeps me going, day in and day out. So, to those who I have mentioned (and also those who I have stupidly forgotten to mention), thank you. I couldn't have done it without all of you.

List of Abbreviations

ACT	Antennocerebral tract
AL	Antennal lobe
AMMC	Antennal mechanosensory and motor center
AON	Anterior olfactory nucleus pars externa
cVA	cis-vaccenyl acetate
dF/F	Proportional measure of fluorescence change
EN	Efferent neuron of the mushroom body
EPSP	Excitatory postsynaptic potential
GPCR	G protein-coupled receptor
IR	Ionotropic receptor
ISI	Interstimulus interval
JO	Johnston's organ
KC	Kenyon cell
LD	Linear discriminant
LDA	Linear discriminant analysis
LH	Lateral horn
LN	Local neuron of the antennal lobe
MB	Mushroom Body
MDA	Multiple discriminant analysis
MDS	Multidimensional scaling
OBP	Odorant binding protein
OR	Odorant receptor
OSN	Olfactory sensory neuron

PCA	Principal components analysis
PID	Photoionization detector
PN	Projection neuron of the antennal lobe
ROI	Region of interest
SD	Standard deviation
SVM	Support vector machine

List of Figures

Chapter 1	2
1.1 Two category classification problem illustrated in two dimensions	25
1.2 Difficult classification, model complexity, and overfitting	27
Chapter 3	56
3.1 Odors evoke consistent patterns of calcium activity in the mushroom body.	63
3.2 Detecting odor responses with cellular resolution in single trials	66
3.3 Reliably identifying KC odor responses	68
3.4 Random spatial distribution of responding MB neurons in the cell body layer	69
3.5 Responses to monomolecular odors are sparse in MB	73
3.6 The effects of odor concentration and recent stimulus history on MB population sparseness	75
3.7 MB responds sparsely to complex and natural odorants	78
3.8 MB population responses to natural and monomolecular odors are indistinguishable . .	80
Chapter 4	86
4.1 Two-photon calcium imaging demonstrates that MB population activity accurately conveys odor identity	95
4.2 Using MB activity patterns to identify candidate odors for generalization	98
4.3 Behavioral generalization across odors	101
4.4 Psychometric and neurometric measures of learned olfactory discrimination	103
4.5 Classification accuracy as a function of population size	111
4.6 A binary code in MB is sufficient to account for learned odor discrimination	112
Chapter 5	114
5.1 Probability of responding to a single odor, as a function of the number of odors	116
Appendix A	121
1 Total summed dF/F as a function of odor concentration	124
2 Mean dF/F as a function of odor concentration	125
3 Total summed dF/F in significantly responding KCs as a function of odor concentration	126
4 Mean dF/F in significantly responding KCs as a function of odor concentration	127

Foreword

Overview of thesis

This thesis is the ultimate product of several gallons of coffee and four years spent trying to understand the workings of an area of the *Drosophila* brain that people call the mushroom body. Though we have not fully figured it out, I feel we have made some good progress, and I remain confident that more investigation, and more coffee, will provide additional answers. This thesis is organized into three parts: Introduction, Experimental Results, and Conclusions. The aim of the Introduction is to summarize what has been learned so far about this system and what remains to be discovered. This is done in two chapters. Chapter 1 addresses general issues in systems neuroscience. It attempts to answer questions like: *Why do we care about the signaling activity of neurons? How does this neural activity convey information about the world?* and *What does this activity have to do with behavior?* Chapter 2 then goes on to introduce our experimental system, the olfactory system of *Drosophila*, at both the anatomical and functional (neural coding) levels. It is hoped that an in-depth discussion of both levels of analysis will help to frame subsequent results. The Experimental Results section also consists of two chapters. Chapter 3 presents the results of an initial study in which we looked at how a certain feature of mushroom body odor responses, the proportion of active cells, is affected by manipulating the odor stimulus. This manuscript has been published in *The Journal of Neuroscience* (Honegger et al. 2011). Chapter 4 then presents the results of another study we have done looking at how the patterns of responding neurons in the mushroom body are related to the perceptual abilities of the fly. The final part, Conclusions and Perspectives, consists of a single chapter, Chapter 5, that attempts to summarize our results and place these findings in a broad context.

Collaboration

I have been fortunate to benefit from the expertise of several people while at Cold Spring Harbor. As such, the work presented in this thesis is the product of fruitful collaborative effort. I would like to briefly clarify my role in this work. I have not performed any of the behavioral experiments presented in these chapters. That was done by the incredibly deft hands of Hongtao Qin and Wanhe Li of Josh Dubnau's lab, and Ebru Demir, when she was working in the Turner lab. Rob Campbell and I have, however, performed all of the imaging experiments. I think that it would not be an exaggeration to say that the experiments presented here were the minor part of my graduate work. Rob and I spent significantly more time developing/troubleshooting our imaging techniques (no one in the lab had any experience with two-photon imaging before we started) and developing the analytic framework for interpreting population-level calcium signals, which, as it turns out, is not an incredibly common thing to do. I think for the most part Rob and I expended equal efforts in this work, and because of this, he and I share first authorship of both manuscripts presented in the results chapters.

Part I

Introduction

Chapter 1

From sensation to action

In general, the job of the brain is to translate information about an animal's environment into useful behavioral activity. To do this, the environment must be sampled, information must be processed, relevant environmental parameters extracted, and appropriate motor outputs generated. Of course, this all involves an immensely complicated and intricately orchestrated sequence of events, involving signal transduction, biochemical cascades, and information processing governed by a seemingly unknowable network of interneuronal connections and set of gene expression profiles. The framework for this processing is embedded in a neural architecture honed by millions of years of selective pressures, of which we will never know the history. As biologists we both marvel and puzzle at the complexity of even the simplest nervous systems, but remain optimistic that some day the secrets of the mind will be revealed by our continuous efforts to chip away an often opaque edifice using the tools at our disposal. These tools are sometimes conceptual, but often end up guiding not only our thinking, but our experiments as well. Those in the neuroscience community today have come to think about, and analyze, brain function in a framework borrowed from engineering. Sensation, from the neuroscientist's perspective, is a three part process of *encoding* information about the environment into some form of neural activity, *processing* this information as part of some neural computation, and *decoding* this activity as needed to perform functions of use to the animal. Much as the digital computer represents inputs as a series of binary digits, the brain represents features of the outside world as patterns of neural activity, in the form of action potentials. Thus, we refer to the way in which stimuli affect the generation of action potentials in a certain brain area as the *neural code*. Obviously, the code need not be invariant across brain areas and, in fact, it is often observed that a code may be reformatted across areas as different information is processed. The code may rely on signal integration over long periods of time, or use the

fine timing of limited samples, and may be sensitive to various forms of modulation based on internal states, behavioral goals, and previous experience. Identifying the neural codes actually used by nervous systems, evaluating their properties, and enumerating the advantages and disadvantages of each with respect to certain kinds of computations is an active area of neuroscience research, and will be for years to come. This is because, at a core level, to really understand how and why the brain does what it does, our best bet today is to understand more about the ways in which information processing is carried out by the brain and how behavior is orchestrated as a result.

The subject of this thesis is neural coding. Specifically, I have investigated the neural code for odors in the mushroom body (MB) of the vinegar fly, *Drosophila melanogaster*. I will show that certain features (low probability of response, distributed representation, and high representational capacity) define this code and have important implications for the presumed role of the MB in olfactory learning and perception. By considering these results in context with what we know about the neural code for odors in other parts of the brain, the significance of these features may emerge. Before we begin, it will be useful to briefly examine the intellectual tradition off of which we are building and to ask why it is worth while studying brain function at the level of neural coding, as opposed to other levels of organization, e.g. gene expression, field potentials, or regional blood oxygenation. We will then explore in some depth a few general concepts in neural coding that will be central to our discussion and examine how they are thought to relate to the behavior of the animal.

Neural coding - a brief historical perspective

The neuron doctrine of Cajal Santiago Ramón y Cajal is widely recognized as the father of modern neuroscience for his contributions toward understanding the brain in terms of cellular organization, an approach that has come to be known as the *neuron doctrine*. Put succinctly, the neuron doctrine states that the fundamental biological unit of the nervous system is the neuron - a cell capable of performing independent computations and transmitting signals unidirectionally to other neurons through points of contact - synapses. Like his contemporaries, Cajal embraced the emerging cell theory of Schleiden and Schwann, the view that tissues are ultimately the product of many individual cellular components, and sought to identify its corollary in the nervous system. As every undergraduate neuroscience student

can relate, Cajal's breakthrough came from applying a new silver impregnation technique developed by Camillo Golgi to his neural tissue samples. Both he and Golgi found this histochemical method capable of sparsely labeling complete individual cells within a nervous tissue. However, after many years of optimizing and perfecting Golgi's technique, Cajal came to reject the idea embraced by Golgi and others that neurons of the same tissue are fused and communicate through shared cytoplasm, known as the reticular theory. This transition toward viewing the components of the nervous system as discrete elements signaled a paradigm shift in the study of nervous function. Rather than sharing membrane, cytoplasmic constituents, and excitability, neurons operate as autonomous units, and are thus capable of performing independent functions. Until the maturation of electrophysiological techniques in the late 1920's, though, the nature of these functions could only be guessed at.

The neuron doctrine of Barlow It wasn't until electrical potential recording from nerve preparations became possible that the functional importance of individual neurons could be evaluated. It was clear early on that the electrical activity of neurons is related to sensory stimulation of the preparation. Edgar Adrian first demonstrated that the rate of discharge (rather than the size of potentials, which were known to be all-or-nothing) from optic nerve and muscle preparations is proportional to the intensity of light on the eye and mass of a weight hung from the muscle (Adrian 1926; Adrian and Zotterman 1926; Adrian and Matthews 1927, 1928). The activity of individual neurons projecting from the retina remained obscured, however, by the preparation technique, which was limited to recording potentials from bundles of many axons. It wasn't until Hartline developed a method for isolating single axons from the optic nerve of *Limulus* that the responses of single retinal neurons could be recorded (Hartline and Graham 1932). He found that illumination of single ommatidia resulted in discharge of single fibers, at a rate proportional to the intensity of light. However, when single fiber recordings were performed in the more complex retina of the frog (Hartline 1938), it was found that individual neurons consistently signaled the intensity of light falling within a continuous area of the field of view, an area he called the *receptive field*. Furthermore, responses varied across neurons with the same receptive fields, with some neurons responding to increases in illumination (ON cells), some responding to decreases in illumination (OFF cells), and some responding transiently to both (ON/OFF cells). The observation that neural responses depend not on *whether* the receptive field is stimulated, but rather *how* it is stimulated indicates that

these neurons are conveying information much more complicated than the simple luminance values captured by photoreceptors. Thus, the individual neuron is capable of performing functions that extract information about the world pertaining to the location, intensity, and direction of change of the stimulus. At the time, these results from the optic nerve seemed perplexing from a teleological point of view and violated physiologists' expectations about the nature of information supplied to the brain from the retina. Why tile the visual field with individual photoreceptors, only to pool them *en masse* two synapses down the road? Wouldn't this ultimately blur the image of the world transmitted to the brain?

Horace Barlow was one of the first physiologists to consider this question, and the answer at which he arrived has profoundly influenced subsequent thinking about sensory neural codes.¹ Barlow began by following up Hartline's studies of individual retinal ganglion cells in the frog (Barlow 1953). In agreement with Hartline, he found three classes of ganglion cell response - ON, OFF, and ON/OFF. He also replicated Hartline's observation that receptive fields of individual neurons may be as large as 1 millimeter in diameter, and thus must integrate information across several thousand photoreceptor cells. However, Barlow added to his study a degree of stimulus control unachieved in earlier studies. By varying the position of a single, or multiple, stimulus spots within a receptive field, Barlow showed that individual neurons are capable of summing, or differencing, levels of illumination in different parts of the receptive field.² Furthermore, he found that the sensitive regions of ON/OFF cell receptive fields are typically much smaller than 1 millimeter in diameter and that these cells are acutely sensitive to motion within their receptive field. Therefore, the functions of which an individual neuron is capable involve integration and processing of information from across the receptive field, in ways that are cell-type specific. At the same time, Stephen Kuffler (1953), working in the retina of the cat, found similar receptive field properties, which he clearly identified as ON/OFF center-surround antagonism. Because this antagonism was relatively invariant to changes in intensity over several orders of magnitude, it was clear that the cells were responding to contrast, not overall levels of illumination. The convergence of these results pointed to the ubiquity of complex signal processing by single neurons. Arguably, though,

¹Though the work of many pioneering physiologists had led the field toward its current understanding, I believe Barlow deserves special mention. His seminal contributions to the understanding of receptive fields and signal processing in the nervous system refined views on sensory processing and directed future generations of physiologists. Barlow's unique contribution, though, was really to clearly advocate for the study of neural activity from a functional and behavioral viewpoint.

²A minor point, but this modern definition of receptive field differs slightly from Hartline's, who originally considered only the excitatory part of the visual field to be the receptive field. In light of the results of Barlow, Kuffler, and others we now consider both the center and annulus to be components of a cell's receptive field.

Barlow's most important contribution was really to take these findings one step further. In light of his results, he speculated:

“an optic nerve fibre is the final common path for activity aroused over a considered region of the retina, and if some *purposive integration* [my emphasis] has taken place it should be possible to relate this to the visual behaviour of the frog... When feeding, its attention is attracted by its prey, which it will approach, and finally strike at and swallow. Any small moving object will evoke this behaviour, and there is no indication of any form [of] discrimination. In fact, ‘on-off’ units seem to possess the whole of the discriminatory mechanism needed to account for this rather simple behaviour. The receptive field of an ‘on-off’ unit would be nicely filled by the image of a fly at 2 in. distance and it is difficult to avoid the conclusion that the ‘on-off’ units are matched to this stimulus and act as ‘fly detectors’.”

Thus, rather than fixating on the implicitly detrimental implications of presumed image ‘blurring,’ Barlow realized it should be far more productive to study the nature of the “purposive integration” performed by neurons and how this relates to sensory perception and behavior. As Barlow quipped in a now-classic epigram, “A wing would be a most mystifying structure if one did not know that birds flew.” One should study neural activity with the goal of identifying the functions that such activity performs for the animal. Following this work, a barrage of studies over the years revealed complex feature detection by neurons in a variety of systems. Inspired by Barlow, Lettvin and colleagues further refined frog ganglion cell responses into four classes, upon which they mapped possible perceptual operations (Lettvin et al. 1959). Using stimuli other than spots of light, Lettvin et al. identified sustained contrast detection, net convexity detection, moving edge detection, and net dimming detection as fundamental operations performed by ganglion cells in the frog retina. Furthermore, these four operations, they argued, coincided with the four layers of retinotectal projections which map retinal position continuously onto the tectum. What they found particularly striking was the implication that an animal thus perceives not the image illuminating the retina, but rather a spatial map of several combined qualities, qualities defined by the operations performed in the retina. It was a revolutionary idea to think that the job of the brain then is

not to reconstruct the world, but rather to interpret some abstract version of it.

In a series of similar experiments, Hubel and Wiesel (1959, 1962, 1968) extended this concept of feature detection to individual neurons recorded in the visual cortex of cats. They found neurons that responded preferentially to bars of light, rather than illuminated spots, within a receptive field and displayed selectivity for edges, orientation, and movement in certain directions as well. So it seemed that neurons within the brain continued to perform abstractions, beyond those performed within the retina, and detect features of even higher order. These features could be described hierarchically, they argued, from simple cells, to complex cells, and then hypercomplex cells. Each new level of abstraction was thus constructed from a combination of features detected by the previous layers. That this sort of organization is to be found in the mammalian cortex perhaps came as no surprise to psychologists, but physiologists who were expecting to drop an electrode into the brain and record how the visual image is remapped onto cortex were undoubtedly disconcerted.³ Though this interpretation seemed to satisfactorily explain their results, the logical extension of this principle raised some questions as to where this hierarchy of representation would stop. Presumably, the height of abstraction in detected features knows virtually no bounds - any number of features could be combined in any number of ways. If the goal of sensory coding in the brain were the simple amalgamation of features of higher and higher order, in every combination, then it seems unlikely that the brain would possess enough neurons to uniquely detect every combination of features, and the basis for generalization across unique stimuli would be lacking. The equivocal usefulness of infinitely hierarchical features is of course embodied by the *reductio ad absurdum* argument of Lettvin⁴ that such a scheme would ultimately culminate in *grandmother cells*, the existence of which remains questionable. The logical conclusion then is that the brain does not process information with the ignorantly generic goal of achieving ever increasing abstraction, rather the nature of these features must be somehow limited and directed by the circuits themselves. So what is it, then, that these neural circuits are relating to one another about the sensory world?

This question returns us to Barlow's original proposition. To understand how neurons code

³To quote Barlow (1972) once again, "Previously it was possible for physiologists to be satisfied with describing how the sense organs and their nerves present a picture of the external world to the brain, and they were happy to leave it to the psychologists to discuss what happened next; but these next things started to happen around the physiologist's micro-electrodes, and he has to join the discussion."

⁴An amusing account of the origin of this argument and of the term *grandmother cell* as related by Lettvin himself may be found in (Barlow 1994) and is discussed in broader context in (Gross 2002).

for aspects of the sensory world, we must consider them in the context of the functions they perform for the animal, whether that be the ultimate goal of driving a specific behavior, or the proximate goal of transforming the neural code to emphasize or extract certain relevant information. Barlow (1961) saw sensory-related activity in the brain as reflecting three possible types of computational process: 1) feature detection 2) selective filtering and 3) recoding to extract relevant information.⁵ The first process describes the feature-selective nature of neural responses, as discussed above. The second process seeks to explain observed invariances to possibly irrelevant features such as overall luminance. And the third process highlights a more nuanced role for neural coding in reducing redundancy in representation and reformatting for specific purposes. Though Barlow originally proposed these three processes as alternative explanations to the previous question, it became apparent that these categories were not mutually exclusive, nor were they unrelated. It is significant that, though we have perhaps redefined some of these points, and continue to map additional levels of detail onto our understanding, the spirit of these principles remains very much alive in contemporary systems neuroscience research. That is, most studies today seek to relate features of a stimulus to neural activity in certain areas, understand how this activity changes across synapses, and ultimately hope to relate some aspect of the neural code to the behavior of the animal.

Ultimately, Barlow (1972) attempted to assemble these thoughts and experimental observations into a coherent theory of the role of the nervous system in sensory perception and to codify this overall approach in what he considered an extension of the neuron doctrine, summarized by these five dogmas:

1. To understand nervous function one needs to look at interactions at a cellular level, rather than either a more macroscopic or microscopic level, because behaviour depends upon the organized pattern of these intercellular interactions.
2. The sensory system is organized to achieve as complete a representation of the sensory stimulus as possible with the minimum number of active neurons.
3. Trigger features of sensory neurons are matched to redundant patterns of stimulation by experience as well as by developmental processes.

⁵These labels are my derivations. Barlow used slightly different terminology.

4. Perception corresponds to the activity of a small selection from the very numerous high-level neurons, each of which corresponds to a pattern of external events of the order of complexity of the events symbolized by a word.
5. High impulse frequency in such neurons corresponds to high certainty that the trigger feature is present.

In a recent retrospective, several authors, including Barlow himself, note the time-tested veracity of the first three dogmas (Barlow et al. 2009). Though the final two points are more speculative, and experimental evidence for, or against, them remains sparse, they are included here for completeness and very little else will be said of them. Overall, we will consider the neuron the fundamental unit of the neural code. It is this level of analysis that we suspect will shed light on the relationship between neural activity, perception, and behavior - and illuminate the biological bridge linking sensation and action. In the following sections I will discuss the ways in which sensory stimulation is thought to influence the activity of neurons, and the ways in which this activity may reflect processes of importance to the animal.

1.1 Stimulus encoding

What follows is a brief account of some of what is known about the ways in which physical information about the world is translated into neural activity. The nature by which neurons perform this translation will be of importance in later discussion.

Signal transduction All sensory modalities share some core requirements and limitations when it comes to stimulus encoding. As a necessary first step, physical signals must be transduced into neural activity at the periphery. This is achieved cellularly through the activation of signal transduction cascades that ultimately result in changes in membrane potential and neurotransmitter release. These biochemical cascades are activated in photoreceptors by the photon-catalyzed isomerization of retinal molecules bound to opsin protein, in cochlear hair cells by vibration-induced activation of mechanore-

ceptors spanning stereocilia, in chemosensory neurons by ligand binding to dedicated G protein-coupled receptors, and in thermoreceptive and nociceptive neurons by activation of TRP family channels. Besides these basic human senses, other animals are capable of sensing additional stimulus modalities, including local electrical fields and magnetic polarity. The obvious general purpose of these processes is to encode some aspect of the physical world in the activity of neurons. This initial step in the sensory encoding process is nontrivial and involves highly orchestrated biochemical processes, as illustrated above, but for our purposes it is more interesting to discuss the aspects of this process that will become relevant to later steps of the neural coding process, rather than catalog the intricacies of sensory transduction.

Receptive range One aspect of this process worth considering is receptive range. I'll define receptive range as being both the range of stimuli to which a single receptor responds and the overall range of stimuli which a sensory organ is capable of detecting, taking into account all different types of a certain receptor. For modalities like somatosensation this is potentially not such a concern, and all receptors can have basically the same range - the relevant information for the animal is captured by simply knowing the intensity of the stimulus and the position on the body of the activated receptor. However, for other modalities the extent of receptive ranges and the ways in which they are distributed are highly important. A simple example to consider is color vision. The receptive range of the normal human eye includes wavelengths between roughly 400 and 700 nm. If we examine the receptive ranges (in this case, spectral sensitivities) of our three types of cones, we find that each cone type is excited by a different, yet partially overlapping, spectrum. From this, we can make two important observations. First, the overall range of colors detected by the eye is determined by the combined receptive ranges of these three cone types. This means that, unlike some other species, we cannot see ultraviolet or infrared light. Second, the continuous and overlapping nature of the individual receptive ranges ensures that there are no gaps in our receptivity. If the spectra of our M- and L-type cones were narrower and considerably red-shifted, for instance, we would be unable to detect green light.⁶ So the range of stimuli to which an animal can respond is specified at a very fundamental level by the receptors expressed in sense organs. In general, these receptors seem to have evolved to tile stimulus space so as to achieve continuous, but not

⁶Using cones. Of course, light of this wavelength would still be detected by rods which could, in this case, serve as a backup detector for green.

necessarily homogeneous, coverage over some range. The ways in which these primary encoders are combined and processed by later activity in the brain is a fascinating subject, discussed in subsequent sections. I will also return to these points in Chapter 2 in the context of olfactory detection.

The problem of representation Generally, a sensory neuron downstream of receptors fires in response to many stimuli, with a greater or lesser rate, within some range of stimuli. The stimuli to which a neuron responds can be arranged in a fashion that produces a *tuning curve*. Many neurons have single-peaked Gaussian tuning curves that are often related to some physical aspect of the stimulus. For example, orientation-selective neurons in visual cortex generally respond strongly to a preferred orientation (say, 90 degrees), not at all to the perpendicular orientation (180 degrees), and with intermediate rates to orientations in between. The width of the tuning curve indicates how broadly a neuron responds to stimuli, and these widths can vary drastically. A neuron with a broad tuning curve can be used to signal the presence of many stimuli, though this property makes it uninformative about the precise identity of the stimulus. A neuron with a narrow tuning curve may only signal the presence of a small number of stimuli, though this property makes it highly informative about stimulus identity when it does fire. Many such neurons would be needed to tile the stimulus space. So, as we can see, a system for representing the sensory world must balance the need for receptivity to a broad variety of stimuli, with the need to discriminate between these stimuli. A common solution to this problem seems to be to place broadly tuned neurons near the periphery and trim down the tuning curves in subsequent layers (discussed in the next section and in Results Chapter 3). This arrangement could have the desired effect of fully tiling the necessary receptive range, while reducing the number of neurons needed for unique representation. It is worth discussing some additional features of sensory representation before we explore how these representations may be transformed for certain purposes in the next section.

Distribution of responses Let us consider the problem of response distribution in the population. When many broadly-tuned neurons of the same type are considered, it is often the case that the receptive range for certain stimuli is spanned by their aggregate tuning curves. By chance, though, the tuning curves of many of the neurons will overlap. Thus, some information transmitted by these neurons to the

next layer may be redundant. The implications of this are twofold. First, information about the stimulus is encoded in the activity of many neurons. This forms the basis for a *population code*.⁷ Second, because neurons are not perfect encoders, this redundancy may help subsequent processors separate signal from irrelevant noise. This is especially true when considering neurons at the periphery, which we generally assume to be independent encoders. In the very rare case where stimulus information is not conveyed by populations of neurons, but rather by single neurons, this is known as a *local code*. This results when only a single neuron has a tuning curve that encompasses some feature of the stimulus. It is unclear whether complex stimulus representation in the human brain ever utilizes local codes, though some concrete examples can be found in the fly (the H1 and giant fiber neurons). An important distinction between these types of codes is the means for transmitting information. A local code must convey information about the features it is detecting through either rate or temporal information in the spike train. While populations of neurons certainly utilize this mode of coding as well, they are able to utilize an additional dimension of encoding that would be relevant to neurons downstream - the identity of active cells. Of course, these active cells must fire action potentials to transmit information, but this format of representation does not require information to be encoded in the rate or timing of the spikes. This implies that an all-or-none scheme could be used to encode stimulus identity in a population of neurons. This will become important in Results Chapter 4.

Neural distance A useful concept for considering stimulus representation by neuronal populations is the idea of *neural distance*. If we consider a population of neurons that encode a set of features about a visual scene, we would expect similar visual scenes (or the same visual scene slightly corrupted by noise) to evoke very similar patterns of activity in the population. If the activity evoked by two very *different* visual scenes was compared, we would probably expect the patterns to look quite different. One way of conceptualizing this difference is to imagine that each set of responses defines a vector (or a line, if preferred) in three dimensional space. Each axis is the firing rate of a single neuron in response to the stimulus, so this space is defined by the responses of three neurons. When the first scene is presented it activates one neuron strongly, and the other two not at all. Imagine this response pointing straight up from the origin. Now when we corrupt the image slightly, we get the same response from

⁷Alternatively, the terms *distributed code* and *ensemble code* are sometimes used.

the first neuron but now a second neuron responds weakly. Imagine this vector again pointing straight up, but now it is tilted slightly to the right. We can see that the angle between this vector and the first is small. Now imagine that we present a third, very distinct scene. This time our first neuron ceases to respond and only the third neuron, which did not respond to either of the other stimuli, responds. Imagine this vector as pointing straight back from the origin, parallel with the floor of our space. We can see that the angle separating this vector and the others is very large. Thus, it can be said that the *distance* between the representation of this stimulus and the other two is very large. This analogy will become quite useful when discussing the results of Chapter 4.

Types of codes There are many ways in which sensory information may be encoded in the activity of neurons. As discussed above, information can be encoded by single neurons or populations of neurons. The firing of a *single* action potential in a single neuron may signal the presence of a particular feature, as in the fly's giant fiber neuron. The firing *rate* of a single neuron may convey not only the presence of a feature, but the intensity, as well. Or, the simultaneous firing rates of *many neurons* may define a response vector that can convey information about a set of stimulus features, as illustrated above. The ways in which spike generation is related to time often forms the basis of many codes that have been studied. These include:

- rate coding
- temporal coding
- latency coding
- population coding
- local coding
- sparse coding
- dense coding
- correlation coding
- inter-spike interval coding
- ordinal coding⁸

⁸This list is not exhaustive, nor are its entries mutually exclusive. It is simply meant to convey the diversity of ways by which the nervous system may encode information.

Ultimately, as systems neuroscientists we are not interested in cataloging the possible ways the activity of neurons may represent the world. Rather, we are interested in the implications of using different modes of encoding for the behavior of the animal. It is wonderful to be able to categorize the activity patterns of neurons, but in the end it is understanding how and *why* these codes are used for different processing purposes that is relevant.

1.2 Information processing

After initial encoding of sensory stimulation by neurons at the periphery, this information generally passes through several layers of neural circuitry before producing, or influencing, some behavioral output. In most known cases, the representation of the stimulus is altered in some way at every layer, resulting in the emphasis or de-emphasis of certain features of a stimulus. The nature by which sensory information is transformed or recoded across layers is currently a topic of intense investigation.

1.2.1 Transformations

While there are many ways in which neural codes for stimuli may be processed, I will focus specifically on three transformations that are relevant to the olfactory system. The role that these are thought to play in *Drosophila* olfaction is discussed in Chapter 2.

Signal averaging (pooling) Noise poses a significant challenge for any set of encoders. Neurons are often especially noisy. Many sensory neurons have substantial baseline firing rates and display significant variation across stimulus responses. Noise can often be so great that one would be unable to tell, based only on the activity of a single neuron, whether the same stimulus was experienced twice. One way that a system can try to minimize the effects of noise is to *pool* responses of several similarly tuned neurons. If the noise is independent across these inputs, then computing their average would give a more reliable signal than any single neuron. This represents one way that a neural system might transform inputs to increase the reliability of a signal.

Histogram equalization Another factor to consider is the dynamic range of a neuron. Some neurons at the periphery tend to be excited weakly by some stimuli and very strongly by others. If one were to plot a histogram of the firing rates evoked by a set of different stimuli, the majority of observations would be stacked near the ends of the axis. To fully utilize the range of firing rates with which neurons can convey a signal, a transformation can be applied which selectively amplifies weak responses and attenuates strong ones. Because the histogram of response amplitudes then becomes flatter, this is called *histogram equalization*. As we will see in the next chapter, a neural circuit could accomplish this simply through the use of strong, but rapidly depressing, synapses.

Divisive normalization Sensory systems have to deal with large ranges of stimulus intensities and complexities. Often, visual stimuli in the real world are complex and light intensities vary over orders of magnitude. This could pose a problem for the cells of visual cortex, discussed earlier, which may be tuned to specific features of stimuli, including orientation, motion, and contrast. In the presence of many of these features (or at high intensities) the system needs to avoid saturated responses. One way this might be achieved is by normalizing a neuron's response to a stimulus by the total input to the system. Such a process would make the responses to complex stimuli, consisting of many features the neuron might potentially detect, look like the an average of the neuron's response to these features. This has been proposed as a mechanism for maintaining selectivity in visual cortex (Heeger 1992) and its involvement in processing in the *Drosophila* olfactory system is discussed next chapter.

1.2.2 Sparse coding

Though sparse coding is, itself, a type of transformation, I have chosen to treat it separately because it comes to occupy a significant portion of the Results and Conclusions chapters. We should clarify at the onset that sparseness in sensory systems has historically been studied in two contexts which may be classified as: 1) the *efficient coding* hypothesis and 2) the *sparse representation* hypothesis. The first context grew naturally out of early observations of neural coding in sensory systems (Barlow 1961). The second was an outgrowth of theoretical consideration of coding schemes that are optimized for storing large numbers of patterns (Marr 1969; Kanerva 1988). Because they are quite different in their

treatment of sparseness, we will consider them in turn.

1.2.2.1 Efficient coding hypothesis

It was noticed early on that responses to sensory stimuli deeper in the brain seemed to be much more sparse than responses near the periphery. Thus, after such a transformation, the number of neurons, and/or the number of action potentials, used to encode a stimulus is minimized. Several ideas have been proposed for why this might be a useful feature of neural codes, and many of them are centered around efficiency of representation. This topic, and its nuances, have recently been given thoughtful consideration by Willmore and colleagues, who identify several conceptual, and practical, divisions among many ideas that are generally placed under the larger heading of *sparse coding* (Willmore et al. 2011). While a full consideration of these topics is beyond the scope of this discussion, it will be helpful to discuss a few of the more prominent ideas.

Metabolic efficiency One proposal is that sparse coding of stimuli may result from selective pressures to minimize action potential usage (Levy and Baxter 1996; Attwell and Laughlin 2001). The reasoning is that since action potential generation is metabolically costly, and minimal coding schemes often suffice for performing certain functions, it would be evolutionarily advantageous to minimize the number of action potentials used to encode stimuli. Since the only condition to be met is that fewer action potentials are generated, this minimization could either take the form of many neurons firing few action potentials, or a few neurons firing many action potentials in response to a stimulus. While either of these schemes could be made to produce the same total number of spikes, they have the potential to affect information processing in very different ways.

Lifetime and population measures The situation just described, where a few neurons fire many action potentials in response to a stimulus, may be contrasted with a situation where a single neuron fires only rarely when presented many stimuli. It might seem paradoxical, but while these appear at the surface level to be the same aspect of stimulus response, they can actually have quite different consequences for the system. The first situation is said to have high *population sparseness* (few neurons

represent a stimulus), while the second has high *lifetime sparseness* (a single neuron represents few stimuli). It is possible to represent information in a group of neurons with *high* population sparseness and *low* lifetime sparseness, and vice versa (Willmore and Tolhurst 2001). This would be the case if the same small group of neurons responded to all stimuli. It all depends on how the responses are distributed. In fact, these two measures are only equivalent when responses are independent and identically distributed (Willmore et al. 2011). This means that the two measures, in practice, cannot substitute for one another, since real neural responses are rarely independent and identically distributed. It should be pointed out that in practice, these measures are generally calculated as the kurtosis (the peakedness) of the response distributions averaged over stimuli (population sparseness) or cells (lifetime sparseness). This differs from our measurements of sparseness reported in Results Chapter 3. Since we are able to quantify directly the proportion of the population that responds to a stimulus on single trials, we simply use this proportion as a measure of population sparseness. This corresponds to the *activity sparseness* measure used by Willmore and Tolhurst (2001).

Maximization of lifetime sparseness Another possible force driving sparse transformation of neural codes is the pressure to maximize lifetime sparseness. The goal would thus be for an individual neuron to adjust its responses so as to maximize the kurtosis of its tuning curve. In an incredible demonstration of possible relevance to real neural responses, Olshausen and Field (1996) showed that model neurons trained to represent natural scenes, using a rule that optimized for sparseness, converged on receptive fields that look incredibly like those of simple cells in primary visual cortex. This led to the proposal that the receptive fields of visual cortical neurons perhaps result from pressures to produce high lifetime sparseness.

Redundancy reduction in populations Another consequence of making neural responses highly selective is the reduction of overlap between their tuning curves at the population level. Thus, fewer action potentials are dedicated to signaling the same stimulus features. Barlow (1961) called this principle “the economy of impulses.” This somewhat contrasts the idea of pooling mentioned in the previous subsection. While pooling relies on having a batch of redundant encoders to increase detection reliability,

redundancy reduction seeks to minimize the number of encoders that transmit redundant information. The effect of this is not only the reduction in need for total action potentials, but a boost in signal separability across the population, due to increased independence of responses. In fact, there is evidence that such reduction of redundancy does occur in the auditory pathway of cats (Chechik et al. 2006).

1.2.2.2 Sparse representation hypothesis

In a slightly separate vein, the qualities of sparse representation have also been studied in the context of information storage. The major theoretical contributions came from the work of David Marr in the late 1960's and a single influential work by Pentti Kanerva. We will first consider Kanerva's treatment of the topic.

Capacity and similarity of representations Kanerva (1988) considered the problem of how a useful representational system for storing memories might be best formatted. He reasoned that, from a psychological perspective, the best format for human memory would be one which allowed not only for unique storage of many entries, but one that allowed linkages and generalizations to be made between stimuli. From a coding perspective, this corresponded to a sparse, distributed coding scheme. Kanerva envisioned a system which represents items as sets of binary features. The capacity of the system is determined by how many features are represented. So, a 10 feature code has the capacity to represent 2^{10} unique items. Each of these features can be considered the response of a single all-or-none neuron in the system. Kanerva identified two important qualities of such a coding scheme. First, this population could represent a vast number of features uniquely, using only binary features. A binary code represented by 100 neurons can represent $> 10^{30}$ items. Furthermore, because the coding space of such a system is so vast, it tends toward orthogonality, that is, the vast majority of potential items are orthogonal to, and very distant from, any single item. This desirable quality allows many items to be stored into memory which are all quite distinct. Second, for storage to be robust, an item should be stored not only at a single location, but at several nearby locations. Doing so confers not only robustness to noise (which will result in slightly different feature sets being active), but facilitates generalization and association between items in this vast space. This can be thought of as storing a particular item not only using its

set of features (its local *address*), but the entire set of items that are, say, one feature different (its *neighborhood*). When this is done, if any of the items in the neighborhood of the stored item are queried, they will recall the stored item. The implication for our binary neuron analogy is that one item is stored in a distributed way across a set of neurons, and that a given neuron participates in representing more than one item. Because most of the coding space is orthogonal to any given item, the neighborhood around that item represents a sparse sampling of that space, but it may still easily overlap with other neighborhoods. Thus, items may be stored into memory in a way that facilitates robust retrieval and allows for generalization between items.

Synaptic interference An additional property of sparse representation worth discussing is the impact it has on synaptic interference. Synaptic interference occurs when weight changes induced by learning *overwrite* existing weights that have been previously set to produce a certain pattern of output. This generally makes it difficult to find a set of weights that give a stable response. Because sparsening of inputs makes it less likely that two patterns to be stored will overlap, sparse representation in the inputs will result in less interference than dense representation (Marr 1969; Fiete et al. 2004).

1.3 Decoding

How are neural codes read out and how do they ultimately influence the behavior of the animal? Just as stimulus information may be encoded by neural activity in many ways, the ways in which neural activity may be decoded are numerous. In this section I will review briefly the relationship between neural activity, perception, and behavioral decisions in the context of stimulus discrimination. I will introduce the basic framework for analyzing stimulus discrimination at both the behavioral and neural levels and examine what is known about the relationship between discrimination at these levels.

1.3.1 The classification paradigm

Because of the obvious communication barrier between humans and other species, we are limited in practice to using behavioral methods to study sensory perception in other organisms. Unfortunately, we

cannot simply ask a mouse whether orange smells more similar to lemon, or to banana. One classical behavioral approach to studying this type of problem is to train the animal to make a discrimination-based decision and to report this decision in the form of a constrained, and often binary, choice. If an animal is unable to tell two stimuli apart, then performance on a discrimination-based task will be at chance. Similarly, in a statistical framework we can apply this same task to neural data and ask how accurately discrimination-based decisions can be made using the activity of certain neurons. The analysis results in a prediction about the identity, or class, of the stimulus presented to the animal on a given trial. If the correct classification technique is chosen (see below), the overall accuracy of these predictions is taken as a measure of how well an ideal observer could utilize the information contained in that neural activity. If activity contains no information for making a discrimination (either because there is no relevant signal or the signals themselves are statistically indistinguishable) then prediction accuracy will be at chance. Thus, we are able to compare directly the animal's ability to discriminate certain stimuli and the neural representation of those stimuli in a certain brain area. The general behavioral and statistical frameworks for approaching classification problems are discussed below.

1.3.2 Neural and perceptual classification

How do neural codes, and the manner in which they are decoded, relate to behavior? One of the most interesting examples comes from studies of non-human primates. Monkeys can be trained to stare at a fixation point on a computer screen and report a perceptual decision by making a saccade to one direction. Once the monkey has fixated on the point, the visual display is updated to present stimuli to the animal about which it has learned to make a judgement. This behavioral task can be performed while keeping the animal's head still, allowing simultaneous electrophysiological recording. In a pioneering study, Newsome and colleagues (1989) studied how the activity of single cortical neurons in visual area MT (V5) relate to the perceptual decisions made by a rhesus monkey. They devised a psychophysical task where the monkey has to report the direction of motion of a field of randomly moving dots. The coherence of this movement can be manipulated, from 0 to 100 percent correlation between the motion of the dots, allowing experimenters to precisely control the difficulty of the task. When the range of coherence values is optimized to encompass easy to difficult discriminations, a typical ex-

periment should produce the expected *psychometric function*.⁹ Because neurons in MT are sensitive to visual motion in certain directions, the activity of these neurons should provide information with which the animal can make a perceptual decision. In fact, direct microstimulation of direction-selective clusters of MT neurons has been shown to influence perceptual decisions about motion (Salzman et al. 1990). Importantly, the responses of individual neurons were recorded simultaneously with the animal's behavioral performance on single trials. To construct a neurometric function corresponding to the simultaneously acquired psychometric function, Newsome and colleagues utilized a simple response classification scheme which compared the overlap between firing rate distributions of a neuron's preferred direction and non-preferred direction. If the two distributions overlap completely (there is no information to make the decision) the function will perform at chance, while if the distributions are well separated the function will perform quite well. Using this procedure, the performance of a single neuron at classifying stimuli with different coherences can be compared directly to the animal's behavioral performance within the same set of experiments.

Newsome and colleagues found that many single MT neurons were able to perform as well as the animal at classifying the direction of movement. They found that the measured neurometric and psychometric functions largely overlapped. What's more, some neurons performed even better than the animal. These results were quite surprising. If single MT neurons can do well at discrimination on this task, why does the animal not pool many of these responses together and do better? Moreover, what makes the animal unable to listen selectively to the most informative neurons? The solution suggested by the authors was that indiscriminate pooling of all neurons in the population would cause the signal provided by informative neurons to be drowned out by the noise of other less-informative neurons. Notably, this would happen if the noise in responses is not independent between neurons, but correlated in the same direction as the signals (Averbeck et al. 2006). Because many neurons were recorded sequentially, rather than simultaneously, it is impossible to know the extent to which noise correlations impacted the animal's decision. Follow up studies did address this issue and indicated that fluctuations in the responses of individual neurons can correlate with the animal's perceptual decision, and that the noise in responses between two nearby MT neurons is, in fact, weakly correlated (Zohary et al. 1994; Britten et al. 1996). These results seem to suggest that some form of global correlation structure in the

⁹A psychometric function is a plot of the stimulus feature being manipulated (which should form a gradient of stimulus similarity on the axis) against the accuracy of the animal's performance. Generally, this function should take the shape of a sigmoidal curve.

responses of MT neurons contributes to the diminishing effects that pooling might have on the behavioral decisions the animal makes. Another implication is that performance on the task will asymptote (at a level determined by the degree of response correlation) at a very small number of neurons (Zohary et al. 1994).

Interestingly, a more recent study has examined a finer motion discrimination task using a similar experimental paradigm, and finds that, for this task, pooling of the most informative MT neurons is necessary to match behavioral performance of the animal (Purushothaman and Bradley 2005). These findings suggest that several models, including selective pooling of the most informative responses, may actually need to be used by the system to perform computations relevant to the task at hand. Without complete information about the anatomy and physiological properties of the system, however, we have to make assumptions about how activity in a given neural population can be decoded. Can the circuit really pool *every* neuron? Can one super-informative neuron really affect behavioral decisions?¹⁰ Thus, when evaluating the relationship between behavior and neural activity in a certain brain area, we have to contend with a model selection problem. How can we ever be sure that our method of decoding neural activity in a certain area is biologically relevant? Typically, because we lack all the information necessary to answer this, we make the best assumptions we can when building a model. Another common strategy, though, is to circumvent the issue by asking how well an *ideal observer* could perform. This approach, rather than trying to emulate the biology of the system, essentially tries to determine how much potential information is available for any decoder to utilize. This is very useful for exploring the ways in which different features of neural codes affect the ability to extract certain types of information from neural activity.

1.3.3 Ideal observers and the general classification problem

Generally stated, the problem for an ideal observer is this. We want to know the stimulus that most likely generated a given set of neural responses. So, we have a set of responses (say, firing rates of 2 neurons in response to a stimulus), some decision function,¹¹ and a list of potential stimulus labels. Classification

¹⁰Interestingly, there is evidence that a rat can learn to report the stimulation of a single neuron in somatosensory cortex (Houweling and Brecht 2008).

¹¹The terms *decision function*, *decision boundary*, *decision surface*, *classification boundary*, and *model* will be used interchangeably.

results from using this decision function to assign to the observed responses the most likely stimulus label from the set. If we did an experiment using 2 stimuli, we would pass the firing rates of our two neurons to the decision function and compute the output. The output of the function would be the label of one of the two stimuli used in the experiment. To anthropomorphize the process, the decision function first looks at the data, compares them with what it knows about responses to the stimuli (more about this below), and then decides which label to assign. Similarly, if the decision function were a neuron, that neuron would receive input from the other two neurons, add together these inputs (scaled by the weights at those synapses), and then decide to fire only if this sum exceeded some firing threshold. The neuron would try, through learning, to fire only to one stimulus. In this case, the weights hold the *memory* for the input features that should govern the neuron's response, while the linear summation of inputs and comparison with threshold constitute the neuron's decision function.

At this point, stating this problem with some formal rigor might be helpful. We have from our experiment the data set $X = \{x_1, x_2\}$ containing responses of the two neurons, x_1 and x_2 , the set $S = \{s_1, s_2\}$ containing the labels of both possible stimuli, and some function $f(X)$ that assigns a stimulus label s , from S , based on data contained in X .

Let's consider a simple example. Say two stimuli are presented while we record the spiking of two neurons. We find that stimulus A *always* evokes 20 spikes in Neuron 1 and 40 spikes in Neuron 2. Similarly, we find that stimulus B *always* evokes 40 spikes in Neuron 1 and 20 spikes in Neuron 2. This corresponds to a two-dimensional, two-class problem: If we make $S = \{0, 1\}$ correspond to the identity $S = \{\text{Stimulus A}, \text{Stimulus B}\}$, and input $X = \{x_1, x_2\}$ correspond to the number of spikes in $X = \{\text{Neuron 1}, \text{Neuron 2}\}$, then a simple function

$$f = \begin{cases} 1 & \text{if } x_1 \geq x_2 \\ 0 & \text{if } x_1 < x_2 \end{cases}$$

would classify these stimuli perfectly every time (Figure 1.1A).

Of course, biological systems are never deterministic and the exact number of spikes evoked in each neuron will vary across presentations of the same stimulus. Consider the more complicated, but more relevant situation, where some independent noise is added to each response (Figure 1.1B). In this case, we may again use the function f given above to classify, but now we are not guaranteed to get

perfect classification every time. There may be cases now when, just by chance, Neuron 1 fires more spikes than Neuron 2 in response to Stimulus A, or vice versa. We can see that this problem is made worse by using two stimuli that evoke more similar responses in these two neurons (Figure 1.1C). In this case, substantial overlap of the two stimuli near the boundary leads to many misclassifications. Note that increasing the variance of the responses in Figure 1.1B would produce a similar result. We can conclude from this example that the performance of a classifier is fundamentally limited by the amount of overlap between classes.

Now, how do we decide what function to use? The problem of finding a classification function is related to familiar regression analysis. Recall that a standard regression function seeks to predict a dependent variable y using a weighted version of the independent variable x . The problem for a classifier is very similar, however we would like our function to return to us a class label, rather than a continuous variable for y . As a result, many methods for fitting classifier functions are a direct outgrowth of regression techniques. To make a good prediction, we need to find a set of weights for our independent variables (the input data) that minimize the number of misclassifications using our function. In the examples above, a simple linear function sufficed. However, we can see that if we had a very complicated function, like that shown in Figure 1.2A, rather than our simple linear function, we could do much better at classifying these similar stimuli. But where would this incredibly complicated function come from?

It would not have been possible to create this complicated boundary function knowing only, say, the mean responses of each neuron. We are only able to derive this function from having full knowledge of the data we are trying to classify. If we were to do this experiment again, we would get a different set of points, and thus want a different complicated function with which to classify. This means that, were we to fit a massively complicated function using some particular subset of the universe of possible responses, the *training data*, when we use this function to classify another set of responses, the *test data*, we would observe many misclassifications (Figure 1.2B). This is known as *over-fitting* the model. So, while we might perfectly classify our training data using a custom-tailored, complicated function, a simpler, smoother function might actually perform better when tested with new data. There are several ways to avoid over-fitting, but a good general procedure is simply to limit the training set to a reasonable fraction of the data, and then use the remaining data as a test set. This is referred to as *cross validation* of the model. The key to classifying well is to find a good classification boundary. And, as it turns out, fitting a good classification boundary is all about tradeoffs. As we have seen, a complex over-fitted

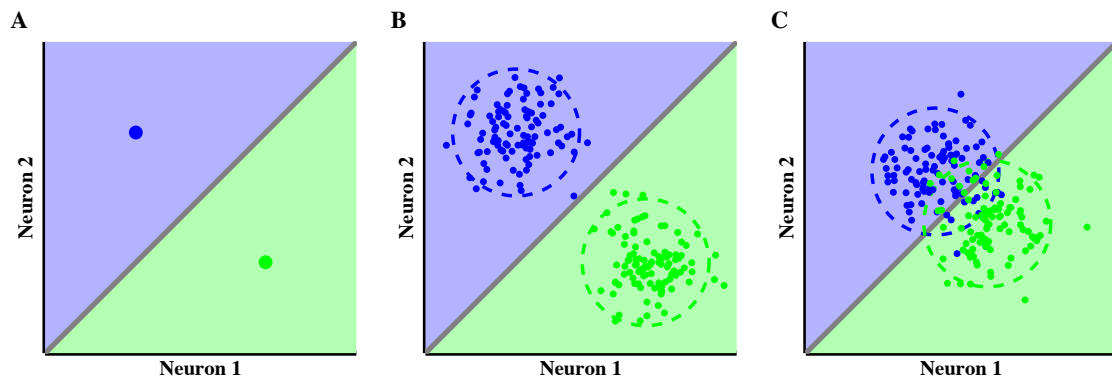


Figure 1.1: Two category classification problem illustrated in two dimensions. **A**, Each point is the response of two hypothetical neurons to two stimuli. Response to Stimulus A is shown in blue, and response to Stimulus B is shown in green. In this example, a classifier using the decision boundary shown in gray would perform perfectly classifying these data. **B**, For each of the two simulated stimuli, 100 points were sampled for each neuron from a Gaussian distribution. Dashed ellipse indicates 95% confidence region for responses to each stimulus. **C**, These simulated stimuli give responses that are much more similar than in **B**. This example would be misclassified a significant number of times using the decision boundary in gray. Simulation is the same as for **B**, only the means of the distributions have been made more similar.

model will perform extremely well at classifying its training set, but it performs poorly when applied to new data. Several methods may be used to find a classification function, all differing in their treatment of the fitting procedure. Three of these methods are described briefly below.

Linear discriminant analysis One of the first treatments of the classification problem came from the work of Ronald Fisher during the 1930s. Fisher developed a method for taxonomic classification of individuals in a population based on linear combination of their traits (Fisher 1936). The classification function, precursor to today's linear discriminant analysis (LDA), is parametric - it requires only the mean set of responses and covariance matrix for each stimulus. Thus, it predicts the class of an observation based on *estimates* of the distributions of stimulus responses. In doing so, it makes several assumptions about the structure of these distributions, including normality, and the assumption that covariances of the classes are identical. While these assumptions are not always valid, they quite often hold and the model may do quite well when classifying based on limited training data. It is easily adapted to predict multiple classes (multiple discriminant analysis; MDA), and a nonlinear extension of the method is easily applied. Despite its early origins, it remains a commonly used method for classification and dimensionality reduction.

Linear separability and the perceptron learning algorithm During the first surge of interest in neural networks in the 1950's, Frank Rosenblatt created a model network to perform binary classifications, that he termed the *perceptron* (Rosenblatt 1958). The model was developed in the context of emerging interest in the mathematical modeling of neurons and in the feature detection role that neurons seem to play. Though of course it is a mathematical function, the perceptron is conceptualized as a single McCulloch-Pitts neuron (one that fires only when the sum of its weighted inputs exceeds some threshold) that receives input from only a single layer. We could think of this as a ganglion cell that receives input directly from all-or-none photoreceptors that are activated by a lighted pixel. This model neuron can adjust the synaptic weights of its inputs so that it fires only when certain features are present. So our model ganglion cell might respond only to images of a fly projected onto the receptors. What was unique about the perceptron, though, is its ability to learn to respond to specific inputs by training with examples. The algorithm by which it learns searches iteratively for a set of input weights that satisfy

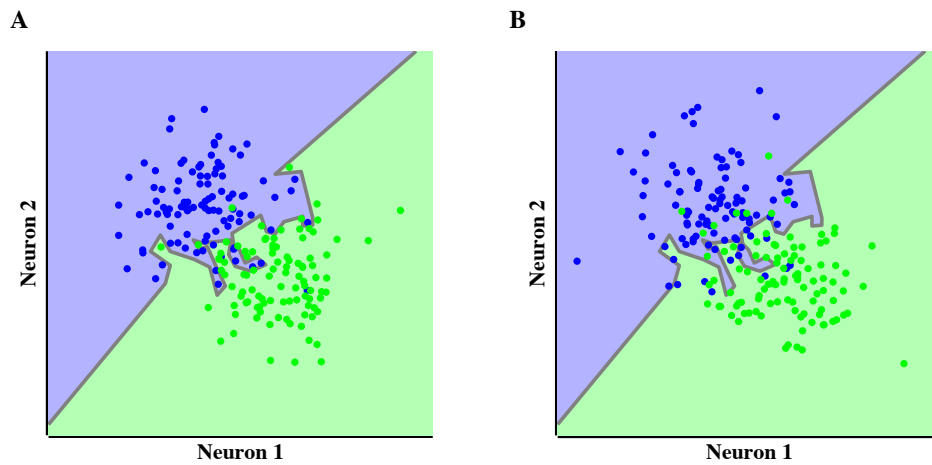


Figure 1.2: Difficult classification, model complexity, and overfitting. **A**, For responses to highly overlapping stimuli (blue and green points), a decision boundary (gray) may be found that classifies observations in a training set almost perfectly. **B**, However, when this complex boundary is used to classify a new set of data, it performs poorly. This model obviously suffers from over-fitting.

some performance criterion. If good examples are chosen for training, then the perceptron, using this algorithm, can learn to respond specifically and reliably when a feature is present, even if it has been corrupted by noise.

Formally, the correspondence between the perceptron and other models is that the decision boundary of a perceptron is represented by the set of input weights. The decision function of a perceptron is then simply the summation of its weighted inputs. The weight vector (and therefore, the boundary) is initialized during training with random values and adjusted iteratively until some performance criterion is met. This means that every time the algorithm is run, a slightly different boundary may be found. Because the model neuron can only simply sum its inputs, the decision boundary defined by the weight matrix is linear. One drawback of this iterative approach is that when a strict performance criterion is imposed, like requiring perfect classification of the training data, the learning algorithm may never converge on a solution. This happens when the input classes are not linearly separable. As it sounds, two classes are not linearly separable if a single line cannot be drawn to separate them, e.g. two concentric toroidal groups of responses - a donut inside of a donut. There is no way to separate these groups using a line, so the perceptron would not perform well in classifying these groups.

Maximum margin classification and support vector machines As mentioned above, if the responses to different stimuli are linearly separable, the perceptron learning algorithm will converge on a *different* set of weights, and thus a different decision boundary, every time it is run. It is possible to find the *optimal* decision boundary for a perceptron, though not using the perceptron learning algorithm. The method for doing so relies on first identifying so-called *support vectors*. These are essentially the positions of the trials that are most often misclassified by the perceptron. Once the support vectors are identified, the decision boundary can be found by maximizing its margin between the support vectors. Assuming nothing about the process generating the data, this decision boundary, known as the maximum margin, provides the optimal linear surface for classification of these groups.

The concept of the margin maximization is utilized by another type of classification algorithm known as a support vector machine (SVM). Because the SVM approach uses a boundary for classification which is often the best linear boundary for a given set of training data, it often serves as a benchmark for optimal classifier performance. An important added feature of SVM is its ability to classify data that

are not linearly separable. This is achieved by projecting the data into a higher dimension using a kernel function of one's choosing. This ability allows us to separate intertwined groups, as in the case of our donut inside of a donut example. Imagine taking this example and pressing it down on an orange juicer with an outer diameter that matches the inner donut's. We can now easily cut the inner donut free with a single flat blade (a plane is the three-dimensional extension of a line), and, in the presence of an orange, have a tasty breakfast. By projecting these data into a third dimension (using for the kernel a radial basis juicer) we are able to separate the two groups using a linear boundary.

Chapter 2

Neural Coding in the *Drosophila* Olfactory System

Of mice and mayflies - neuronal morphology and anatomy in insects Students of vertebrate neuroanatomy may find it both fascinating, and slightly disconcerting, that the organization of the insect nervous system looks, in many respects, inverted. The insect nerve cord sits ventrally, rather than dorsally. Neuropil, the axons and dendrites of neurons, forms the majority of recognizable structure in the insect brain, while neuronal cell bodies are strewn about the outside of the brain with little discernible pattern. This stands in stark contrast to the often highly-organized lamination observed in several regions of the mammalian brain. Insect neurons are almost entirely monopolar, lacking the often elaborate multipolar morphology characteristic of vertebrate central neurons. Axons of insect neurons are not myelinated and dendritic spines appear to be virtually nonexistent. The insect brain uses acetylcholine as its primary excitatory neurotransmitter, and uses glutamate at neuromuscular junctions - a complete inversion of the transmitter use observed in vertebrates.

But despite these prevalent differences, many commonalities are also discernible, especially in the olfactory pathway.¹ At both an anatomical and functional level, the olfactory system of insects and vertebrates seems highly analogous. A broad array of sensory neurons at the periphery, each expressing a single major type of odorant receptor, project axons to discrete glomerular structures inside the brain. A large number of these glomeruli are interconnected through excitatory and inhibitory neurons and a considerable amount of signal processing goes on at this layer. These neurons project to deeper areas of the brain and lead to the activation of small numbers of third-order neurons, thought to provide stimulus-

¹Sanes and Zipursky (2010) have recently highlighted an additional striking parallel between the visual systems of vertebrates and invertebrates.

specificity to olfactory memories. Whether these striking similarities indicate true homology of the system or convergent evolution is still a matter of debate. Of course, each system has its idiosyncrasies.² But quite often the principles of neural coding in this system seem to generalize across organisms. It is our hope that it will be of interest, not only to the *Drosophila* community, but the sensory neuroscience field as a whole, to study neural coding in the olfactory system of *Drosophila*.

2.1 Olfactory anatomy of *Drosophila*

The history of insect neuroanatomy extends far past the more contemporary work on the neurophysiology of these same systems. Cajal and his predecessors spent many decades studying the anatomy of insect brains. Cajal, in fact, very early on drew insightful parallels between the circuitries of the vertebrate and the fly retina, and suggested that these circuits were equivalent at a very fundamental level. Far from being outdated, however, contemporary molecular and microscopy techniques have reinvigorated neuroanatomical research in *Drosophila* and it remains an extremely active area of research today. This has led to an extremely detailed understanding of the anatomical and molecular organization of the early *Drosophila* olfactory system. As such, an in-depth review of *Drosophila* neuroanatomy is beyond the scope of this chapter, however a firm foundation must be laid to foster the development of subsequent ideas. I therefore endeavor to first lay out in fairly broad strokes the most basic elements of the adult *Drosophila* olfactory system at the molecular, cellular, and circuit levels. This is followed by a review of what is currently known about neural coding for odors in these same circuits.

2.1.1 Sensory periphery

Drosophila possess two bilaterally symmetrical olfactory organs: the antennae and maxillary palps. The antennae are the rostral most structure of the fly's head and are usually divided anatomically into three segments, discussed below. The maxillary palp is, in contrast, a single appendage of the rostrum of the proboscis. Thus, unless the proboscis is extended, the majority of the maxillary palp surface is shielded by the head capsule. Protruding from the surface of each of these structures are several hair-like sensory

²For instance, contrast the highly-specified logic of odorant receptor expression and existence of ionotropic odor receptors in insect olfactory sensory neurons with the random expression of metabotropic odor receptors in mammalian systems.

bristles, known as sensilla. Sensilla come in three types: trichoid, basiconic, and coeloconic, and each sensillum houses 1-4 olfactory sensory neurons (OSNs) along with various support cells. Each OSN expresses either a single classical odorant receptor (OR) or a set of ionotropic receptors (IR), which confers on that neuron its ligand binding characteristics (de Bruyne et al. 2001; Hallem and Carlson 2006; Laissue and Vosshall 2008; Benton et al. 2009). These sensory neurons send axons bilaterally directly to the antennal lobe (AL) of the brain, where they form discrete glomeruli with the dendrites of AL projection neurons (PNs). Though the output of both palps and antennae synapse in the AL, it is believed that their functions are not redundant. The identities of the sensory receptors expressed in these two structures are different, thus their receptive properties seem to be uniquely specified at the level of gene expression as discussed below.

2.1.1.1 Olfactory organs

Maxillary palps The maxillary palps are the simpler of the two olfactory organs, but comparatively much less is known of their function in *Drosophila*. The palp is attached to the lateral aspect of the fly's proboscis, the accordion-like mouth that is normally retracted into the head capsule. Unlike the antennae, the maxillary palps normally depend on food-evoked extension of the proboscis for full exposure and contain only basiconic sensilla. There are about 60 sensilla on the palps, containing roughly 120 OSNs with response profiles that overlap with those of the antennae (de Bruyne et al. 1999; Hallem and Carlson 2006; Laissue and Vosshall 2008). The function of the maxillary palps for the fly remains enigmatic. In mosquitoes, the maxillary palps house CO₂ detecting neurons, but in *Drosophila* these neurons are located on the antennae (Jones et al. 2007).³ Physical ablation of the maxillary palps has been shown to cause deficits in odor-induced food acceptance (Shiraiwa 2008), suggesting a role for the maxillary palps in modulating appetitive behaviors in *Drosophila*. Nothing else is known of the role the maxillary palps play in the life of the fly. Axons from maxillary palp OSNs follow the labial nerve to the AL where they become integrated with antennal inputs to other glomeruli.

³Interestingly, CO₂-sensing sensilla are induced in *Drosophila* maxillary palps by loss of expression of a single miRNA, miR-279, during development (Cayirlioglu et al. 2008).

Antennae The antenna is anatomically segregated into first, second, and third segments and serves dual sensory roles in sensing mechanical and olfactory stimuli. The second antennal segment, along with the arista of the third segment, constitute a chordotonal mechanosensory organ, which is essentially the closest thing the fly has to an ‘ear.’ A direct role for this segment in odor detection is not known, but the mechanosensory functionality of this organ is mapped onto the AL, and might affect odor processing there (Mamiya et al. 2008). The arista, a feather-like appendage on the third segment, acts as a receiver for sound waves and displacement of the arista activates stretch receptors tethered between the second and third antennal segments (Todi et al. 2004). It is thought that the arista functions to transduce auditory stimuli, mainly species-specific song, and thus could aid in conspecific mate recognition (Todi et al. 2004). The sacculus of the second segment contains the mechanosensory neurons of Johnston’s organ (JO). Deflection of the aristae activate stretch receptors in neurons of the JO and this information is relayed to an area in the central brain known as the antennal mechanosensory and motor center (AMMC). In a curious parallel to outer hair cells of the cochlea, the aristae resonate when stimulated, via an active feedback mechanism (Göpfert and Robert 2003; Göpfert et al. 2005). Little is known about the neural coding in this system. It has been shown that anatomical segregation exists in the AMMC projections of JO neurons (Kamikouchi et al. 2009; Yorozu et al. 2009). Also, it appears that AMMC neurons respond to stimulation with graded signaling, and seem to perform low-pass filtering of song-like pulse stimuli (Tootoonian et al. 2012). Surprisingly, stimulation of the antennae with pulses of pure air leads to significant activation in the AL, the first synaptic layer of the olfactory system (Mamiya et al. 2008), and antennal mechanosensory input may significantly impact odor-guided flight (Duistermars et al. 2009; Bhandawat et al. 2010; Mamiya et al. 2011). Thus, it seems quite possible that mechanosensory information about air velocity or plume dynamics may be juxtaposed with, and impact on, odor information as early as the AL.

The third antennal segment, or funiculus, is the main olfactory organ of the fly. It houses 410 olfactory sensilla of all three types, containing ~1200 OSNs, and is involved in detection of most odorants, pheromones, CO₂, temperature, and humidity. The three types of olfactory sensilla may be distinguished both morphologically and by their position on the antenna, as discussed below.

2.1.1.2 Olfactory sensilla

Olfactory sensilla are 5-20 μm long, porous, sensory bristles that protrude from the surface of antennae and maxillary palps. As mentioned above, three types of sensilla are recognized based on morphology: basiconic, trichoid, and coeloconic. These types are further divided into subtypes, and then classes based on the OSNs they contain. In total, 21 sensillum classes are recognized. Contained within a sensillum are the processes of up to four OSNs and several support cells. Cell bodies are located outside the sensillum, below the cuticle. There are many classes of each sensillum type, each determined by morphological characteristics and the set of sensory neurons contained within.

Basiconic sensilla Three subtypes of basiconic sensilla are recognized morphologically - small (SB), thin (TB), and large (LB). Basiconic subtypes are further divided into thirteen classes by morphological and physiological characteristics. Antennal LB sensilla are comprised of three sensillum classes (referred to as ab1-3), TB sensilla of three classes (ab4-6), and SB sensilla of four classes (ab7-10). Maxillary palps express basiconic sensilla that are morphologically similar to TB subtypes observed on the antenna, and are classified into three classes (pb1-3). Basiconic sensilla are the most numerous and most diverse type of sensillum. They house 28 distinct OSN types, many of which respond to quite a broad spectrum of food-related odorant molecules (Couto et al. 2005; Hallem and Carlson 2006). It therefore seems safe to say that most combinatorial encoding of food-related odorants (like those used in many studies cited in this thesis) is done by OSNs housed in basiconic sensilla.

Trichoid sensilla Three subtypes of trichoid sensilla are recognized based on whether they express one (T1), two (T2), or three (T3) sensory neurons. There are four classes of trichoid sensilla (at1-4), the T3 subtype being comprised of two classes. The number of trichoid sensilla on the antennae differs between males and females (Shanbhag et al. 1999). Trichoid sensilla house 9 OSN types (Couto et al. 2005). OSNs in trichoid sensilla respond selectively to *cis*-vaccenyl acetate (cVA; a pheromone) and fly-derived odors, but only weakly to food-related odors (van der Goes van Naters and Carlson 2007). Trichoid sensilla have a well-known role in mediating pheromone detection in other insects (Hansson and Stensmyr 2011), and it seems likely that they serve a similar function in *Drosophila*.

Coeloconic sensilla Coeloconic sensilla are divided into two subtypes, C2 and C3, containing two and three OSNs, respectively. Four classes are recognized (ac1-4) based on the set of OSNs contained. Coeloconic sensilla are unique in that they have a double-walled surface, unlike basiconic and trichoid sensilla, and house a set of 9 OSN types which express a family of receptors related to ionotropic glutamate receptors (IRs) (Benton et al. 2009; Abuin et al. 2011; Silbering et al. 2011). These IRs seem to respond selectively to water-soluble acids and amines, as well as select aldehydes and ammonia (Yao et al. 2005; Silbering et al. 2011). This, along with the observation of deep conservation of the IRs, has led to the recent suggestion that the coeloconic sensilla may represent an evolutionary first step in olfaction (Silbering et al. 2011).

A sensillum-receptor antennal map The map of relative sensilla position on the antennae is strikingly stereotyped. Trichoid and basiconic sensilla types are expressed in opposing patterns of subtype-bands running diagonally across the lateral-medial axis of the antenna. Basiconic sensilla are concentrated on the medial portion of the antennae while trichoid sensilla are predominantly located laterally. The smaller coeloconic sensilla appear to be concentrated in the center of the anterior face of the third segment.

2.1.1.3 Cellular mechanisms of signal transduction

Cellular organization of sensillum Each sensillum is supported by an external cuticular skeleton, perforated along its length to allow passage of odorant molecules, and filled with haemolymph. The length, pore density, and thickness of sensilla vary across types. A sensillum contains 1-4 OSNs and 3-4 auxiliary cells providing necessary support functions (Shanbhag et al. 2000). Each OSN extends branching dendrites up the length of the shaft into the haemolymph sinus. It is thought that upon adsorbing to haemolymph through pores in the cuticle, an odorant molecule binds dendritic receptors directly or is presented to dendritic receptors by an odorant binding protein (OBP). A bioinformatic screen has identified 51 putative OBP genes in *Drosophila*, making these molecules potentially as diverse as the ORs themselves (Hekmat-Scafe et al. 2002). It is notable, though, that heterologous expression of ORs in a non-cognate sensillum seems to have little effect on sensory ability (Dobritsa et al. 2003; Hallem

and Carlson 2006).

Molecular and cellular logic Certain pairing rules govern the receptivity of individual OSNs within a sensillum. An OSN generally expresses a single type of OR, or combination of IRs. The *Drosophila* genome encodes 62 OR gene products, 47 of which are expressed in adult OSNs (Laissue and Vosshall 2008). It is interesting to note that the membrane topology of *Drosophila* ORs appears to be inverted, with respect to mammalian ORs, with the N-terminus of the protein located cytoplasmically (Benton et al. 2006). The implication of this is that insect ORs may function as ligand-gated cation channels, rather than metabotropic G protein-coupled receptors (GPCRs). Ten types of IR are expressed in adult antennae either singly, or in combination (Benton et al. 2009). Each OSN type also contains an obligatory co-receptor, which interact with odorant receptors to form an odorant receptor complex. In OR-expressing neurons, this co-receptor is a closely related protein, called Orco (née Or83b), which forms a heteromeric duplex with ORs, and is at least necessary for proper targeting of ORs to the dendritic membrane (Benton et al. 2006). In IR-expressing neurons, IR8a, IR25a, or both are broadly expressed along with other IRs and may function as coreceptors, in a role similar to Orco (Abuin et al. 2011). The only known exception to these rules are the CO₂-sensing basiconic (ab1c) OSNs, which express only Gr21a and Gr63a receptors, without Orco (Jones et al. 2007).

2.1.2 Antennal lobe

2.1.2.1 Glomerular organization

OSNs project axons into the brain, in a bundle known as the antennal nerve, that terminate in the antennal lobe (AL). The AL is a bilaterally symmetrical, highly-stereotyped neuropilar structure, organized into 42 anatomically distinct spherical glomeruli, with 51-54 functional subdivisions (Laissue and Vosshall 2008). OR-expressing OSNs project bilaterally in symmetrical patterns to both AL hemispheres (Vosshall et al. 2000). This also appears to be generally true of IR-expressing OSNs; however there are some known exceptions (Silbering et al. 2011). While each OR-expressing OSN may, in some cases, express several ORs, an individual OSN terminates in a single AL glomerulus (Couto et al. 2005; Fishilevich and Vosshall 2005). Recently, it has been shown that 7 of 9 IR-expressing OSNs are also

uniglomerular (Silbering et al. 2011). Thus, a general 1:1 OSN:glomerulus mapping implies that each OSN type has the potential to function as an independent encoding channel. In general, glomeruli are diverse in size and general odor receptivity, but some organization is observable at the level of gross glomerular innervation. OSNs from trichoid sensilla innervate mainly lateral AL glomeruli. Antennal basiconic OSNs target medial anterior glomeruli, while palp basiconic OSNs innervate glomeruli located mainly in the center of the AL. IR-expressing coeloconic OSNs innervate a set of glomeruli in the posterior AL, which is non-overlapping, and spatially segregated from, OR-expressing OSNs (Silbering et al. 2011).

Within a glomerulus, OSN terminals make cholinergic synapses directly on the dendrites of AL output neurons, the projection neurons (PNs). Dendritic arbors of PNs generally display the same 1:1 glomerular innervation as OSN axons, however PN dendrites are restricted to a single AL hemisphere. There are roughly 150 PNs per AL hemisphere, with generally 2-4 PNs innervating a single glomerulus. All PNs innervating a glomerulus seem to get input from all OSNs terminating in that glomerulus (Kazama and Wilson 2009). Also present within a glomerulus are numerous processes from local neurons (LNs) which serve to link glomeruli through both inhibitory and excitatory channels (discussed below). The cell bodies of both types of AL neuron, PNs and LNs, are located on the periphery of the antennal lobe, making the glomeruli devoid of somata.

2.1.2.2 Local connections link glomeruli

It is estimated that there are at least 200 LNs, of several detectable classes, innervating each AL hemisphere - making LNs more numerous than glomeruli, or even PNs (Chou et al. 2010). All glomeruli are contacted by several LNs. LNs do not project outside of the AL and commonly display diverse pan-glomerular, periglomerular, and bilateral innervation patterns, thus providing extensive linkage between glomeruli within and across AL hemispheres. Both excitatory and inhibitory LNs serve to facilitate lateral interaction between glomeruli, however it seems that GABAergic LNs are significantly more numerous than cholinergic LNs. Excitatory LNs are electrically coupled to PNs of most glomeruli through gap junction and synapse directly onto inhibitory LNs, while inhibitory LNs seem to synapse primarily on presynaptic terminals of OSNs within the glomerulus (Olsen and Wilson 2008; Yaksi and Wilson 2010), though all PN types express GABA receptors (Okada et al. 2009). Many LN innervation patterns

are highly stereotyped, but the morphology of a certain class appears to be highly variably between individual animals, offering the intriguing potential for individual variability in odor processing. Additional evidence suggests that AL processing may be under control of diverse types of neuromodulation. In addition to the AL cell types mentioned above, glutamate, octopamine, dopamine, various neuropeptides, and serotonin immunoreactivity have all been observed in the AL (Roy et al. 2007; Daniels et al. 2008; Busch et al. 2009; Carlsson et al. 2010; Chou et al. 2010). At this time, though, only the roles of serotonin and two neuropeptides in AL processing have been experimentally demonstrated (Dacks et al. 2009; Ignell et al. 2009; Root et al. 2011).

2.1.2.3 Antennocerebral tracts

The axons of PNs project to the central brain via a set of bundles known as the antennocerebral tracts (ACTs). The ACTs consists of inner, middle, and outer bundles. Axons of the inner-ACT are most numerous and terminate in both the proximal mushroom body (MB) and the more distal lateral horn (LH) areas of the central brain where they make mostly cholinergic synapses. Typically, a single axon of this bundle will branch extensively in MB, then continue on to branch again in LH. Axons of the middle and outer ACTs generally project directly to LH, bypassing MB, though occasional projections to MB are observed (Tanaka et al. 2008). The termination sites in both MB and LH seem to be quite stereotyped, raising the possibility that certain olfactory functions could be anatomically specified to these two areas (Marin et al. 2002; Tanaka et al. 2004; Jefferis et al. 2007).

2.1.3 Mushroom body

The MB forms one of the most prominent anatomical structures of the *Drosophila* central brain. The architecture of the monopolar intrinsic MB neurons, known as Kenyon cells (KCs), divides the structure into three functionally, and anatomically, distinct regions. The *calyx* is a compact, bulbous (or mushroom-like) region of neuropil consisting of the dendrites of all KCs, from which the mushroom body derives its name. KC cell bodies overlie the posterior surface of the calyx, the *somatic* region. KC axons travel in bundles, forming output *lobes* of three distinct anatomical and developmental classes.

2.1.3.1 Development of KC classes

Mushroom body Kenyon cells are born throughout larval and pupal development. However, KCs derived from different neuroblast lineages have different anatomical, and seemingly functional, properties. Three primary KC classes are recognized based on birth timing and corresponding axonal projection patterns in the lobes: α/β , α'/β' , and γ (Lee et al. 1999). The γ class KCs are born first, during the mid-3rd instar stage of larval development, followed by α'/β' birth leading into puparium formation, and finally α/β KCs, born after puparium formation. During metamorphosis, larval axons and dendrites of the early-born γ class KCs degenerate and ultimately send axons only to a single medial lobe, termed the γ lobe (Lee et al. 1999; Zhu et al. 2003). The axons of α/β and α'/β' class KCs, in contrast, bifurcate and form a vertical and medial lobe, a process which depends on homotypic axonal repulsion mediated by *Dscam1* (Hattori et al. 2009). Sister KCs, those sharing a final precursor, develop axons with extremely similar branching patterns (Yu et al. 2009). Thus, the projection pattern, and ultimately function, of a KC seems to be highly specified by clonal lineage and timing of birth.

2.1.3.2 Calyx microanatomy

At a gross neuroanatomical level, the calyx looks rather unremarkable. Its uncanny resemblance to the cap of a mushroom was noted early in neuroanatomical studies of other insects (Kenyon 1896), but the primary focus in MB study has typically been on the prominent output lobes (discussed below). At a fine scale, however, the neuroanatomy of the calyx is quite intriguing. Similarly to the AL, the calyx is organized into several glomerular structures, referred to as microglomeruli. After branching from the primary neurite several micrometers from the soma, the KC dendritic branch enters the calyx and ramifies in 5-7 microglomeruli (Lee et al. 1999; Zhu et al. 2003). Each microglomerulus is easily recognized as an F-actin rich, ring-like structure, containing a single large PN bouton (2-7 μm in diameter) wrapped by several claw-shaped KC dendritic tufts (Yasuyama et al. 2002; Leiss et al. 2009; Butcher et al. 2012). Each KC claw synapses on a single PN bouton. It is not known whether different claws from the same KC contact boutons from different PN types, though this seems likely based on subthreshold tuning of KCs (discussed below). Presynaptic contact from KCs onto non-PN, non-KC cells within a microglomerulus has recently been reported, as well (Christiansen et al. 2011; Butcher et al. 2012). At a larger scale, there is some evidence for possible zonal stereotypy in KC dendritic innervation (Zhu et

al. 2003; Lin et al. 2007); however, whether innervation is stereotyped at the level of individual KCs remains a contentious issue; for discussion see (Cachero and Jefferis 2008; Murthy et al. 2008). This issue will also be discussed further in Chapter 3, in light of our experimental results which are generally in agreement with Murthy et al. (2008).

2.1.3.3 Kenyon cell somata

KC somata are extremely small, ~3-4 μm in diameter, and numerous. A majority of the somatic volume is occupied by the nucleus. The total number of KCs has been estimated at around 2000 per hemisphere (Aso et al. 2009), all of which are genetically labeled by a single GAL4 enhancer trap line, *OK107-Gal4* (Connolly et al. 1996). Cell bodies are packed tightly into a single cluster overlying the surface of the calyx directly under the posterior surface of the head. This fortuitous arrangement of tightly packed, small somata, has greatly impacted our ability to sample neural activity from a large number of KCs simultaneously, as discussed in Experimental Results, Chapters 3 and 4.

2.1.3.4 MB lobes

Perhaps the most prominent structure of the MB is the extensive axonal field, the MB lobes. Five major divisions are recognized per hemisphere: the γ lobes, the vertical α and α' lobes, and the medial β and β' lobes. As mentioned above, the three major KC classes (α/β , α'/β' , and γ) are defined by the lobes they innervate, with individual α/β or α'/β' KCs innervating both the vertical and medial lobes. The significance of the vertical/medial bifurcation is currently unclear, but the orthogonal lobes may simply serve to increase available synaptic volume, with which unique sets of downstream neurons can access equivalent information.⁴ The neurotransmitter(s) released from KC terminals in the lobes remains a mystery. Notably, KCs do not express vesicular transporter proteins for any common neurotransmitters, nor does pharmacological blockade of cholinergic receptors, the most common excitatory neurotransmitter class in the *Drosophila* brain, block MB output. It has been suggested, based on expression patterns of a

⁴Interestingly, a *Drosophila* mutant (*ala*) has been described that often entirely lacks either vertical or medial lobes (Pascual and Pr at 2001). Whether this hints at a functional subdivision within individual MB axons, or simply an underlying developmental process, is not known.

putative neuropeptide transporter, that KCs release neuropeptides, but this remains to be functionally verified (Johard et al. 2008; Brooks et al. 2011).

2.1.3.5 Other cell types

In addition to the cell types described above, many other non-KC neurons are known to innervate the MB. A large GABAergic neuron, known as APL, ramifies profusely throughout the MB calyx and lobes (Liu and Davis 2008). Another large neuron, the peptidergic DPM, is coupled to APL by gap junctions and fully innervates the MB lobes, and nothing else (Wu et al. 2011). Neurons immunoreactive for serotonin, dopamine, octopamine, and glutamate innervate various parts of the MB (Roy et al. 2007; Daniels et al. 2008; Tanaka et al. 2008; Busch et al. 2009; Aso et al. 2010). While the nature of these synapses remains to be worked out, local processing done within the MB is undoubtedly much more complex than currently understood.

2.1.4 Efferent neurons

KC axons in the MB lobes synapse onto a diverse group of approximately 30-100 MB efferent neurons (ENs) (Tanaka et al. 2008; Y. Aso, personal communication). This dramatic reduction of output channels from the relatively high number of KCs represents substantial convergence at this layer. If each KC synapsed on only a single EN, then KC:EN convergence would be at least 20:1 - considerably higher convergence of coding channels than that observed in the AL (1:1) or MB calyx (5-13:1). Most ENs seem to synapse selectively in a stereotyped way within restricted subdomains of certain MB lobes. For instance, the MB-V2 neurons bilaterally innervate regions of the vertical lobes, synapsing only on the tip of α' and below on the shaft of α , while the MB-MV1 neuron terminates only in the heel region of the γ lobe (Tanaka et al. 2008; Séjourné et al. 2011). However, though this innervation is highly specific, most termination sites within subdomains are dense and occupy rather large volumes, making it likely that ENs synapse with many individual KCs. The only published report of odor responses from ENs (the MB-V2 neurons) seem to indicate broad tuning to odors, consistent with a large number of KC inputs (Séjourné et al. 2011). These zonal innervation patterns in the lobes are reminiscent of the MB lobe innervation by dopaminergic neurons (Tanaka et al. 2008; Aso et al. 2010). Thus, the partitioning

of MB lobes into many subdomains may reflect functional sites of integration for neuromodulation, odor-specific information, and specialized effector output.

2.1.5 Lateral horn

Unfortunately, because specific GAL4 drivers for LH neurons are lacking, very little is known of the role of LH in olfaction.⁵ The dual projection of the AL PNs to both the LH and MB seems to represent parallel systems for processing olfactory information (Galizia and Rössler 2010). It has often been assumed that these parallel pathways serve distinct functions for the animal, with the MB being responsible for ‘memory’ and the LH being responsible for ‘innate’ odor response, receiving input from fruit-odor sensing PNs (de Belle and Heisenberg 1994; Jefferis et al. 2007). Sadly, testing this hypothesis directly has been challenging, but recent experimental evidence has confirmed that a class of LH neuron (DC1) receives input from cVA-sensing PNs and synapses on a neuron that provides descending output to the thoracic ganglia (Ruta et al. 2010). While the limited data seem to support this distinction, it seems to me that this view may be overly simplistic. It is interesting to note that the axons which innervate the MB (PN projections of the inner-ACT) almost always project to the LH, as well. This could simply reflect principles of wiring economy, or it could function to subserve a necessary comparison of information between MB and LH. It is possible that ENs (or some other cell type receiving EN input) that are connected to both MB and LH may use this parallel, differentially processed information to compute some kind of comparison of expectations, which would be necessary for MB-influenced olfactory behavior. Currently, at least one class of EN (the MB-V2 neurons) is known to send projections to both the MB and LH, displays associative plasticity in odor responses, and is required for olfactory memory retrieval (Tanaka et al. 2008; Séjourné et al. 2011).

2.2 Olfactory Coding

Despite our detailed understanding of the basic circuitry and molecular organization of the first few relays in the *Drosophila* olfactory system, comparatively less is known about the neural coding of odors

⁵This is sure to change in coming years, with the emerging development of highly-specific cell type drivers and brain-wide anatomical mapping techniques based on single neuron labeling (Pfeiffer et al. 2008; Chiang et al. 2011).

by this system. Of particular interest to this discussion will be the representation of combinatorially encoded odorants i.e., not the type of stimuli that have been referred to as ‘labeled lines.’ Labeled line stimuli seem to be processed through dedicated circuit subchannels from transduction to motor output, and include the increasingly well-characterized cVA and CO₂ subchannels. While the biological functions of such circuits are interesting and important for the fly, we are more interested in the generalist aspects of the system, because of the behavioral flexibility they provide.

2.2.1 Combinatorial coding by OSNs

OSN tuning OSNs are spiking neurons with average spontaneous rates of ~15 spikes/s, though this rate can be as high as 50 spikes/s (Hallem and Carlson 2006). Stimulation with odorants can evoke increases in firing rates exceeding 250 spikes/s, at their peak, thus these neurons have a broad dynamic range. Firing rates are temporally dynamic, usually resulting in a single peak, and typically show sustained responses to persistent stimuli that adapt within and across presentations (de Bruyne et al. 1999, 2001; Hallem and Carlson 2006; Nagel and Wilson 2011). Traditionally, the odor responses of individual OSNs were obtained through extracellular sensillum recording. This technique acquires multiunit responses from sensilla containing multiple OSNs, which can generally be separated based on the amplitude of the spike waveform. More recently, it has become possible to express individual OR genes in an ‘empty OSN’ and record responses from that OSN, thus isolating the receptivity of each OR (Dobritsa et al. 2003). Given the prevalence of single OR expression by OSNs, this is expected to be a good approximation of the responses of the OSNs expressing these ORs endogenously. Using this technique, the responses of 24 of the 47 ORs expressed in the adult have been tested using a panel of 110 monomolecular odorants of varying chemical compositions (Hallem and Carlson 2006). The results of these analyses, as well as sensillar recordings, indicate that OR-expressing OSNs exhibit a wide variety of tuning profiles, ranging from highly selective, to very broad (de Bruyne et al. 1999, 2001; Hallem and Carlson 2006). Typically, a given odorant molecule increases firing in many OSNs, and a given OSN will respond to many odorants within a certain chemical class, making the odorant identity conveyed by activity in any one neuron ambiguous. Thus, the identity of that odor at the periphery is said to be encoded *combinatorially* in the activity of many OSNs. The combinatorial nature of OSN coding is thought to be a necessary feature of odorant identity encoding, to reasonably ensure

detection of potentially enormous numbers of encountered odors by a limited number of OSN types. Were individual OSNs specialized to detect only single molecules, like the cVA-sensing Or67d receptor (van der Goes van Naters and Carlson 2007), the olfactory system could only detect about 50 different odorants. Distribution of responses across many OSNs increases the representational capacity of the system. A population of 40 broadly-tuned OSNs could, in theory, represent $> 10^{15}$ odorants using only binary responses.

In general, OR-expressing OSNs seem to be most highly receptive to esters, alcohols, and ketones, thus it may be said that their receptive range (discussed in Chapter 1) is limited largely to food-related odors. More recently, the tuning of IR-expressing OSNs has been studied extensively by sensillum recording,⁶ and with more limited stimuli by calcium imaging of OSN terminals in the AL. These results indicate that these OSNs seem to display generally selective responses, and are preferentially tuned to water-soluble, hydrophilic acids and amines not significantly detected by OR-expressing OSNs (Yao et al. 2005; Silbering et al. 2011). Though a given IR-expressing OSN may respond to several compounds, it seems that responses are determined largely by the class of molecule within this limited set. Whether coding of odor identity in these neurons is combinatorial remains to be determined.

Stimulus concentration OSN responses are also profoundly influenced by odor concentration. Higher concentrations of an odorant generally recruit activity in more OSNs, while an OSN which responds to an odorant at low concentrations generally responds at a higher rate to increased concentrations. Though this relationship is not necessarily linear, it does seem to be monotonic. So it seems that stimulus intensity could be represented both in the form of a rate code at the level of individual OSNs, and a distributed code represented by concentration-dependent sets of OSNs. Hence, there is potential for information about odor identity and intensity to be encoded independently. Because of the combinatorial nature of OSN coding, the same odorant encountered at different concentrations may be experienced by the animal as distinct percepts. It is notable that, despite considerable processing by the AL to maintain balanced levels of output (discussed below), *Drosophila* nonetheless display different behaviors to the same odor in a concentration-dependent manner (Wang et al. 2003; Masek and Heisenberg 2008; Sem-

⁶It should be noted that these extensive tuning curves are recorded at the level of sensilla, as the authors were unable to isolate spikes from the individual OSNs contained within a single sensillum.

melhack and Wang 2009). This suggests that concentration-dependent increases in OSN firing rate may perhaps be more relevant to signal detection than to the encoding of stimulus intensity.

Complex stimuli What is known about OSN encoding of *multimolecular* odors, like those naturally occurring in the animal's environment? Hallem and Carlson (2006) reported that most ORs they tested are activated by some type of fruit extract. These stimuli generally evoked activity that was at least as broad as any monomolecular odorants, and were dependent on concentration. Interestingly, monomolecular odors commonly evoke response suppression (decreases in baseline firing) in OSNs. While an odor may excite several OSNs, it may also lead to suppression (Hallem and Carlson 2006; Su et al. 2011). The significance of this for odor coding is currently unclear, though it is possible that responses to natural odors, consisting of many odorant molecules, may reflect the interaction of combined excitatory and suppressive effects on OSN activity. Notably, this interaction may be nonlinear - not simply a sum of the inhibitory and excitatory effects on an OSN (Su et al. 2011). Such nonlinear interactions may support a system for *masking* the effects of certain molecules, as has been observed for the food-odor masking effects on CO₂-sensing OSN activity and avoidance behavior (Turner and Ray 2009). Another interesting aspect of OSN responses to odorant blends is the apparent alteration of temporal dynamics of OSN activity (Su et al. 2011). Temporal dynamics of OSN responses vary dramatically across odors, and seem to do well at conveying high-frequency temporal information about odor plumes, indicating a possible role for odorant interaction in odor source localization (Hallem and Carlson 2006; Nagel and Wilson 2011). These observations highlight the potential importance of temporal information at the sensory periphery, but whether this information is utilized at subsequent stages of processing remains an unexplored topic in *Drosophila*.

Adaptation Like most sensory receptor neurons, OSNs display significant adaptation to prolonged or repetitive stimulus exposure, from which it can take several minutes to recover (de Bruyne et al. 1999; Störtkuhl et al. 1999; Murmu et al. 2011; Nagel and Wilson 2011). This could potentially target the dynamic range of OSNs to signal changes in odor concentration within a certain regime, or allow downstream filtering of responses to background odors. Though the mechanisms for OSN adaptation

in *Drosophila* have long remained elusive, recent evidence suggests that cellular factors involved in transduction, other than the odorant receptors themselves, may be responsible (Nagel and Wilson 2011).

2.2.2 AL Reformatting

Signal averaging The first synapse in the olfactory circuit is the excitatory cholinergic synapse between OSNs and neurons in AL glomeruli. As discussed in the previous section, within a glomerulus all sister PNs (3-5 depending on glomerulus) each receive input from all ~50 cognate OSNs of a certain type, essentially making each PN output *fully redundant*. OSNs of a given type seem to display odor evoked responses that are highly reproducible across animals, so we would expect most of them to respond similarly within an animal. Given the high cost of maintaining large numbers of essentially identical neurons in complex sensilla, this substantial convergence seems a bit surprising. We might be tempted to ask: isn't it wasteful to funnel the output of 50 neurons into 3 redundant units? But perhaps we would be better off asking why 50 identical OSNs are needed in the first place. We might expect the system to immediately utilize the vast combinatorial capacity of this organization by combining inputs from the numerous different OSNs, but this synapse obviously does not integrate multiple OSN coding channels. Rather, it pools all individual OSNs together and clones the pooled output across a handful of cells. Such pooling could serve to support the averaging of signals across many single OSNs. As mentioned earlier, though odor-evoked responses may be quite strong, OSNs have a substantial spontaneous firing rate. Many odorants that only weakly activate an OSN might be hard to detect amid spontaneous firing. If we assume that the noise inherent in OSN spikes is independent across neurons, averaging highly similar signals from many OSNs would substantially increase the reliability of the output. Thus, the integration of activity across channels, a necessary step for reading combinatorial codes, would suffer less from the effects of noise in the encoders. Indeed, PN responses have been shown to be more reproducible than responses of individual OSNs (Bhandawat et al. 2007).

Broadened tuning in PNs All PNs and LNs that have been described are spiking neurons. PNs fire with a mean spontaneous rate of ~4 spikes/s and LNs fire with spontaneous rates ranging from 2-17 spikes/s (Wilson et al. 2004; Wilson and Laurent 2005; Chou et al. 2010). Evoked activity in PNs

can reach > 250 spikes/s, while changes in LN firing rates are much more modest (up to 9 spikes/s). While OSNs display a wide variety of tuning breadths, most PNs are quite broadly tuned, more so than OSNs, with most PNs responding to $> 50\%$ of odors presented (Wilson et al. 2004; Bhandawat et al. 2007; Turner et al. 2008). Incredibly, rank-order inversions of odor preference seem to be quite common between a PN and its cognate OSN (Bhandawat et al. 2007). This broadened tuning and altered response profile implies that PNs receive additional excitatory input from neurons other than cognate OSNs. When the OSN input to a glomerulus is removed, odor-evoked excitation of PNs innervating that glomerulus may still be observed, supporting the existence of secondary excitatory input linking glomeruli (Olsen et al. 2007; Root et al. 2007; Shang et al. 2007). Indeed, excitatory LNs exist that innervate several AL glomeruli and are broadly tuned to odors (Shang et al. 2007; Yaksi and Wilson 2010). Unexpectedly, it was discovered that these excitatory LNs are electrically coupled to PNs, and thus function to spread odor-induced excitation through non-rectifying gap junctions, rather than through cholinergic synapses (Yaksi and Wilson 2010). Incidentally, weak, broadly-connected electrical coupling between glomeruli is expected to be much more robust to the effects of independent noise than chemical transmission, and thus could function to maintain the noise robustness gained by OSN pooling.

Intraglomerular transformation Besides displaying broadened tuning curves, PNs also differ from their cognate OSNs in the way that they utilize dynamic range for encoding stimuli. When OSN firing rate for several different odors is plotted against the firing rates of cognate PNs for those odors, it is apparent that the input-output relationship of a glomerulus is highly nonlinear (Bhandawat et al. 2007). While OSNs often operate at the extremes of their dynamic range, PNs generally utilize most of their dynamic range for encoding these same stimuli. Very weak responses in OSNs (< 20 spikes/s) may evoke high firing rates in cognate PNs (> 100 spikes/s). The mechanism for this seems to be strong, reliable synaptic coupling and rapid short-term synaptic depression at the OSN:PN synapse (Kazama and Wilson 2008). This balance allows the synapse to amplify weak inputs and dampen strong inputs. Though this is often considered to be an intra-glomerular processing step, it is also possible that this phenomenon involves inter-glomerular processes, namely presynaptic inhibition and lateral excitation described above (Olsen and Wilson 2008; Yaksi and Wilson 2010). This type of transformation has been

described as *histogram equalization*, because unevenly distributed input magnitudes become effectively flattened in the output. This process allows fuller use of the dynamic range within the output of a glomerulus. Such equalization may be intrinsically difficult for individual sensory receptor neurons to achieve.

Interglomerular normalization The odor response of a PN is also significantly impacted by interglomerular interactions. The substantial interglomerular connectivity of LNs allows elaborate crosstalk between glomeruli. Such interglomerular processing is responsible for the rank-order inversions observed between OSN and PN tuning curves, mentioned above. However, it also seems to be responsible for another phenomenon that serves to control the gain of overall AL output. In a parallel with coding in the visual system, it has been observed that the activity of PNs seems to be normalized by overall AL input (Olsen and Wilson 2008; Olsen et al. 2010). Olsen and Wilson (2008) found that the amount of lateral inhibition to a glomerulus scales with overall AL input. They also demonstrated that the odor response of a uniglomerular PN is disinhibited by removing input to other glomeruli, suggesting broad inhibitory input to each glomerulus, which they found acts on presynaptic OSN terminals within the glomerulus. This type of transformation has been referred to as *divisive normalization*. In another study, the same group experimentally fitted an AL model which incorporated divisive normalization and the intraglomerular transformation discussed above. They found, using a linear classifier, that both processing steps make it easier to identify odors (Olsen et al. 2010). These types of transformation could thus serve to increase separability of AL responses to different odors at the next stage of processing.

Extrinsic regulation One other point worth briefly mentioning is the role of extrinsic regulation of AL output. As mentioned in the preceding anatomy section, the AL is likely modulated by a plethora of neuromodulatory factors and neuropeptides. Evidence exists for neuromodulation of AL activity by serotonin and neuropeptide signaling, which seem to function as points of selective gain control for certain channels (Dacks et al. 2009; Ignell et al. 2009; Root et al. 2011). These may act at a presynaptic locus on OSN terminals, or directly on the different classes of cells within the AL. So far, the only demonstrated role of this modulation is to enhance detection of food-related odors in hungry flies (Root

et al. 2011).

2.2.3 Sparsening in MB

Physiological properties of KCs Mushroom body Kenyon cells (KCs) are spiking neurons that receive cholinergic input from ~3-7 PN terminals in calycal microglomeruli (see previous anatomy section). Input from individual PN synapses seems to be quite strong, with excitatory postsynaptic potentials (EPSPs) up to 5 mV in amplitude (Turner et al. 2008). Several properties of KC spiking activity are notable. First, most KCs show very little, to no, spontaneous firing, despite receiving substantial numbers of spontaneous EPSPs. When they do fire in response to an odor, spikes generally occur in a brief, high-frequency volley, with little evidence of temporal patterning (Murthy et al. 2008; Turner et al. 2008). Following discharge, a relatively long-lasting inhibition is observed in many KCs. Though inhibitory responses to odor have been observed, these seem to be much less common than excitatory responses. Notably, when KCs fail to fire in response to an odor, which is incredibly common, a considerable amount of subthreshold excitation is nonetheless observed.

Selective KC tuning Perhaps the most striking feature of KC odor responses is their selectiveness for certain odors. Quite unlike their PN synaptic partners, which are more broadly tuned than OSNs, KCs often respond to only one, or none, of the odors presented during an experiment. In an electrophysiological analysis of the odor responses of 71 KCs, Turner (2008) found that individual KCs responded reliably to only ~6% of odors presented, while individual PNs typically respond to ~60% of odors. This *sparsening* of odor responses at the level of individual MB neurons is striking, and has been observed in a number of other insects (Perez-Orive et al. 2002; Szyszka et al. 2005; Ito et al. 2008; Demmer and Kloppenburg 2009). The sparse responses of cells in the KC population are not distributed evenly across cell types (Turner et al. 2008). The three KC classes seem to display qualitatively different odor tuning. α'/β' KCs are the most broadly tuned class and seem to fire the most spikes during responses. α/β KCs are the next most responsive, followed by γ KCs, which seem to broadly, but rarely, respond to odorants. Notably, this ordering of responsiveness across KC classes agrees with results obtained by imaging calcium responses to odors in the MB lobes (Wang et al. 2008).

Mechanisms for generating selectivity As intriguing as MB sparsening may be, the mechanism by which the circuit achieves this transformation remains to be elucidated in *Drosophila*, though several hints may be gleaned from studies done in another system. In locusts, it has been estimated that an individual KC receives very weak input from ~400 PNs - 50% of total locust PNs (Jortner et al. 2007). This extremely high convergence corresponds to the maximal combinatorial complexity of inputs, assuming randomly chosen PNs, and seems to offer an explanation for why local field potential is highly correlated with low-amplitude oscillations of KC membrane potential. Odor-evoked oscillations observed in the AL serve to synchronize groups of PN inputs, which drive not only KCs, but inhibitory LH neurons, as well (Perez-Orive et al. 2002). Feedforward inhibition from the LH then serves to periodically reset KC membrane potential, thus limiting the window for integration of PN input by KCs and serving to sparsen KC output. While this fairly elaborate mechanism for generating sparse KC responses is intriguing, several properties of the *Drosophila* system make this strategy seem untenable. First, PN:KC convergence in *Drosophila* is at most 15:1, as discussed previously. Second, meaningful odor-evoked oscillations are not observed in the *Drosophila* olfactory system (but see Tanaka et al. 2009). Third, there is currently no evidence for feedforward MB inhibition in *Drosophila*, though the APL neuron might serve an overall gain control function. It is perhaps much more likely that MB sparseness is achieved in *Drosophila* through a simple combination of sparse input sampling and proper tuning of intrinsic physiological properties. This hypothesis remains to be tested.

The role of MB in learning and memory The striking transformation from dense AL output to sparse representation in MB seems to hint at its potential biological role for the animal. As discussed in Chapter 1, it has been suggested, based on theoretical consideration, that sparse representation is in some ways optimal for a neural system dedicated to storing memories. It is, in fact, generally agreed that the MB plays a primary role in olfactory learning and memory formation in *Drosophila*. This role is supported by a growing body of genetic lesion, activity block, and calcium imaging results. I will discuss each of these in turn.

Extensive genetic dissection of *Drosophila* olfactory learning and memory has led to the identification of distinct phases for the learning and maintenance of olfactory associations. In the standard Pavlovian conditioning paradigm an association is learned between a conditioned stimulus (an odor)

and an aversive unconditioned stimulus (an electric footshock). Following initial learning, the association passes through four phases of memory storage: short-term, middle-term, anesthesia-resistant, and long-term memory. These phases are characterized by their time courses, task-dependent induction and disruption, and requirements for unique sets of genes, many of which are involved in neuronal signal transduction (Margulies et al. 2005; Davis 2011). Anatomical dissociation using cell-type restricted drivers has revealed that requirements for expression of certain ‘memory molecules’ differ across KC classes at distinct phases of memory formation and maintenance. For instance, expression of *dumb*, a D1 dopamine receptor, during learning is required specifically in γ KCs to support the learning of the odor-shock association (Qin et al. 2012). In contrast, expression of *rutabaga*, an adenylyl cyclase, in γ KCs is required for the formation of short-term memory, while parallel expression in α/β KCs supports long-term memory (Blum et al. 2009).

Using a genetic strategy to target a blocker of synaptic transmission to the MB, several groups have directly demonstrated the necessity of MB output for associative olfactory conditioning and memory retrieval. It was originally observed that blocking output of MB disrupted memory retrieval, but did not affect acquisition or consolidation (Dubnau et al. 2001; McGuire et al. 2001; Schwaerzel et al. 2002). However, a subsequent study using slightly different genetic targeting determined that the output of α'/β' KCs is, in fact, required during acquisition and consolidation phases (Krashes et al. 2007). Additional evidence indicates that dopaminergic input to the MB lobes is necessary and sufficient to induce aversive olfactory associations (Kim et al. 2007; Claridge-Chang et al. 2009). Taken together with MB results, we are left with a model for olfactory associative learning in which the identity of the conditioned stimulus is represented by the pattern of active KCs, and dopaminergic input to the MB lobe serves to signal the aversive reinforcement (see Keene and Waddell 2007). From current evidence, it still is not clear, though, how changes in the output of KCs results in olfactory memories that are specific for a certain odor. In line with this, changes in axonal calcium responses to odor have been observed after an odor has been paired with shock. Imaging of the MB vertical lobes revealed an elevation in calcium responses to the conditioned odorant in α/β KCs (Yu et al. 2006). The time course of this elevated calcium signal did not become apparent for several hours after training, failed to be induced by a massed training protocol (a hallmark of long-term memory), and persisted for 24 hours. Thus, this KC class-specific change in calcium signal has been interpreted as the neural substrate for the long-term phase of memory processing. Subsequent calcium imaging studies have attempted to do the same for

the short-term phase of memory. Results of these studies indicate that an elevated calcium signal in response to the conditioned odor is observed in α'/β' KCs soon after conditioning (Wang et al. 2008; Tan et al. 2010). Interestingly, an alteration in calcium signal is also observed in γ KCs that appears to be consistent with long-term memory, though it does not appear until several hours after the onset of the changes observed in α/β KCs (Akmal et al. 2010).

Results from these genetic dissociations and calcium imaging studies have demonstrated differential molecular and micro-circuit contributions to MB support of associative memory phases. This has led to the conceptualization of MB-dependent olfactory association as a dynamic process of neural encoding and synaptic modification, involving both sequential, and parallel, processing in different KC classes. It will be important to keep in mind when considering the results to be presented in Chapters 3 and 4, that our imaging of calcium responses in naïve flies captures only a snapshot of the dynamic MB representation of olfactory stimuli. In fact, since electrophysiological results indicate that the majority of odor responses in naïve flies are observed in α'/β' KCs, we most likely are imaging responses of predominantly α'/β' KCs. While this limits us from asking questions about how the representation of the odors in MB might change after learning, we are able, nonetheless, to glean a sense for how different or similar MB representation of two odors may be before any learning-induced changes in activity reshape this representation.

2.3 Outstanding questions in *Drosophila* olfactory coding

What is the significance of these olfactory codes for the behavior of the animal? I suppose it is fair to say that, at this point, all we may do is speculate. The OSNs are, of course, the *initial encoders*. OSNs transduce the chemical identity of stimuli into patterns of neural activity, by selectively binding ligands with affinities based on physicochemical properties. Without the activity of certain OSNs, the animal will obviously lose the ability to detect certain molecules. The AL and MB *transform* this activity in different ways. Processing in the AL seems to increase the reliability, signal-to-noise ratio, and separability of input patterns, and thus could facilitate detection of weak odorants and aid in the differentiation of odorant identities downstream. The role of the MB transformations, on the other hand, remains enigmatic, and virtually nothing is known about how subsequent layers decode the information represented

in MB. Very little is known of the significance or mechanisms of the dramatic sparsening at this layer in *Drosophila*, though theoretical predictions suggest a role for sparse, distributed representation in supporting distinctive learned associations and increasing representational capacity (Marr 1969; Kanerva 1988). The dearth of knowledge in this area indicated to us a need for population-level analysis of MB activity and inspired us to address the broad questions outlined below.

What are the limits and roles of sparsening in the system? Given the potential importance of sparsening for learning and memory systems, we would naturally like to know what the limits are for performing this transformation in a biological circuit. Can sparseness ever break down, or are these circuits designed to buffer changing stimulus properties and maintain sparse representation? For example, what happens when a sparse area is driven by extremely strong stimulation (e.g. high odor concentration) or complex mixtures of stimuli? The MB is a prime area to ask this question. The MB is involved in olfactory learning and memory formation, its inputs are relatively well-defined, and responses to odors seem to be sparse. Direct manipulation of stimuli should alter the intensity and nature of drive to the MB, and thus allow us to test the limits of sparse coding in this system. Theoretical considerations of sparse coding in memory systems have focused primarily on a specific feature of representation, known as the population sparseness. To truly get a sense for this measure one must analyze the response statistics of simultaneously recorded neurons, as extrapolation of population sparseness from pooled single unit recordings can be misleading (Willmore and Tolhurst 2001; Willmore et al. 2011). Because electrophysiological recordings are limited to lifetime measures, we chose to measure sparseness of the population responses directly using calcium imaging. The results of these experiments are discussed in the next chapter (Chapter 3).

How does the formatting of MB odor responses affect behavior? While the circuit logic and role of coding in sensory neurons and AL are becoming increasingly clear, nothing is known about how the formatting of MB odor representations affects the animal's behavior. We know much about the role of the MB, and various genes expressed by KCs, in supporting associative olfactory memory, but this knowledge has been gleaned at the behavioral level. Integrating this knowledge with information

about how the MB encodes odorant identity would undoubtedly provide insight into the mechanisms by which stimulus associations are made. We chose to focus specifically on the question: how can stimulus associations be formatted to support robust subsequent *discrimination* and *generalization*? We think this is an interesting question to ask, because the requirements of discrimination and generalization make opposing demands on the system. This is an important unexplored topic that is potentially relevant to understanding neural coding across learning and memory systems. The results of this work are presented in Chapter 4.

Part II

Experimental results

Chapter 3

Cellular-Resolution Population Imaging Reveals Robust Sparse Coding in the *Drosophila* Mushroom Body

Kyle S. Honegger*, Robert A.A. Campbell*, and Glenn C. Turner

*K.S.H. and R.A.A.C. contributed equally to this work.

This work appeared nearly verbatim in *The Journal of Neuroscience* (Honegger et al. 2011).

3.1 Abstract

Sensory stimuli are represented in the brain by the activity of populations of neurons. In most biological systems, studying population coding is challenging since only a tiny proportion of cells can be recorded simultaneously. Here we used two-photon imaging to record neural activity in the relatively simple *Drosophila* mushroom body (MB), an area involved in olfactory learning and memory. Using the highly sensitive calcium indicator GCaMP3, we simultaneously monitored the activity of > 100 MB neurons *in vivo* (~5% of the total population). The MB is thought to encode odors in sparse patterns of activity, but the code has yet to be explored either on a population level or with a wide variety of stimuli. We therefore imaged responses to odors chosen to evaluate the robustness of sparse representations. Different odors activated distinct patterns of MB neurons; however, we found no evidence for spatial organization of neurons by either response probability or odor tuning within the cell body layer. The degree of sparseness was consistent across a wide range of stimuli, from monomolecular odors to artificial blends and even complex natural smells. Sparseness was mainly invariant across concentrations, largely because of the influence of recent odor experience. Finally, in contrast to sensory processing in other systems, no response features distinguished natural stimuli from monomolecular odors. Our results indicate that

the fundamental feature of odor processing in the MB is to create sparse stimulus representations in a format that facilitates arbitrary associations between odor and punishment or reward.

3.2 Introduction

A general feature of sensory systems is that dense representations by broadly tuned neurons at the sensory periphery are transformed into sparse representations by narrowly tuned neurons in deeper layers. Specifically, in the olfactory system, olfactory sensory neurons (OSNs) respond to a wide range of different odors (Hallem and Carlson 2006) and synapse onto projection neurons (PNs) of the antennal lobe within structures called glomeruli. At this layer, synaptic and circuit mechanisms produce even broader tuning curves in PNs (Bhandawat et al. 2007) while making responses of different glomerular channels more independent of one another (Olsen et al. 2010). Thus, in the antennal lobe, odor identity is represented by a dense code comprised of only ~51 different PN types.

The antennal lobe PNs project to the mushroom body (MB), an area involved in learning and memory, where a major reformatting of information occurs. The MB is composed of ~2000 small neurons known as Kenyon cells (KCs) (Aso et al. 2009). Electrophysiological recordings show that, unlike PNs, individual KCs have highly odor-specific responses and odors are represented by sparse population activity in the MB (Perez-Orive et al. 2002; Broome et al. 2006; Murthy et al. 2008; Turner et al. 2008). Theoretical work suggests that sparse representations are useful for accurate information storage (Marr 1969; Kanerva 1988; Olshausen and Field 2004) and appear to be a general feature of deeper brain areas.

Broad sampling of population activity is important to thoroughly characterize sparse representations and to establish that they are truly sparse. Recent advances have dramatically increased the sensitivity of genetically encoded calcium indicators (Tian et al. 2009). Here we use two-photon imaging with the GCaMP3 reporter to simultaneously monitor > 100 KCs (~5% of the total) with sensitivity approaching that of electrophysiology.

If sparse coding is truly a fundamental aspect of processing in the MB, it should be robust across a range of different stimulus features. There are two broad challenges to maintaining a sparse representation: variations in stimulus intensity and variations in stimulus complexity. We found that

population sparseness was largely robust to increases in odor concentration. To examine the effects of stimulus complexity, we tested responses to both natural and artificial multimolecular odors and compared them to monomolecular compounds. We observed similar levels of sparseness across all stimulus categories, including complex natural stimuli. Interestingly, there were no response features that distinguished representation of monomolecular and natural odors. This contrasts with other sensory systems where there are substantial differences in the coding of natural and artificial stimuli (Rieke et al. 1995; Machens et al. 2001; Yu et al. 2005; Garcia-Lazaro et al. 2006). Finally, we found no obvious spatial arrangement of KC somata based on odor tuning properties or responsiveness.

In contrast to other sensory systems, where familiar or behaviorally meaningful stimuli appear to be represented distinctively, the MB represents all stimuli sparsely, and responsive cells are randomly organized. This is similar to piriform cortex (Stettler and Axel 2009) and likely reflects the role of both these brain areas in learning arbitrary associations between odor and reward or punishment.

3.3 Materials and Methods

Fly stocks. Flies were reared on standard medium, supplemented with dry baker's yeast (Saf-Instant; Lesaffre Yeast), at room temperature (22-25°C). Flies carrying the genetically encoded calcium sensor UAS-GCaMP3 (Tian et al. 2009) were crossed with OK107-Gal4 (Connolly et al. 1996) to drive GCaMP3 expression in essentially all KCs (Lee et al. 1999; Aso et al. 2009). All experiments were conducted on female F1 heterozygotes from this cross, aged 2-5 d posteclosion. GCaMP expression has not been observed to affect normal neuronal function in *Drosophila* (Jayaraman and Laurent 2007).

Animal preparation. Procedures for animal preparation were based on earlier methods (Turner et al. 2008; Murthy and Turner 2010). Briefly, flies were transferred to a glass tube and anesthetized on ice until movement ceased (~15 s). A female fly was then gently inserted into a rectangular hole (~0.77 X 1.5 mm) cut into a piece of aluminum foil glued to the underside of the recording platform. The fly's head was tilted forward to provide access to the posterior surface of the brain where the KC cell bodies are located. The olfactory organs point downward in this preparation, allowing airborne odor delivery (Fig. 3.1A). The fly was fixed in place using fast-drying epoxy (5-Minute Epoxy; Devcon).

The bath surrounding the head capsule was continuously perfused with oxygenated saline (Wilson et al. 2004) and the cuticle at the back of the head was dissected away using sharpened forceps. We sometimes found it necessary to minimize brain motion by removing the pulsatile organ at the neck (care was taken to avoid damaging the gut) and the proboscis retractor muscles, which pass over the caudal aspect of the optic lobes. Air sacs and fat deposits occluding the MB were cleared from the brain's surface. We did not purposefully attempt to remove the perineural sheath, as is needed for electrophysiological experiments. Flies remained healthy and active throughout the experiment, as evidenced by abundant voluntary leg movements. Many preparations were discarded due to excessive brain motion that prevented us from tracking individual neurons throughout the imaging session.

Odor stimuli. The following chemicals were used as stimuli: 2-heptanone (CAS No. 110-43-0), 3-octanol (589-98-0), 6-methyl-5-hepten-2-one (110-93-0), α -humulene (6753-98-6), benzaldehyde (100-52-7), ethyl lactate (97-64-3), ethyl octanoate (106-32-1), hexanal (66-25-1), isoamyl acetate (123-92-2), 4-methylcyclohexanol (589-91-3), methyl octanoate (111-11-5), diethyl succinate (123-25-1), pentanal (110-62-3), and pentyl acetate (628-63-7). In addition to these monomolecular odorants, apple cider vinegar (Richfoods) and reconstituted dry baker's yeast (Saf-Instant; Lesaffre Yeast) were used. Fresh fruits (banana, mango, and orange) were obtained from a local grocer.

Odor delivery. We built a 12-channel odor delivery system capable of air-diluting pure odorants up to 1×10^{-4} . Odor stimuli were kept in 40 ml sample vials, each containing 3-4 ml of odorant and a strip of filter paper to aid evaporation and maintain a saturated headspace concentration. Using a smaller volume of odorant tended to produce inconsistent stimulus delivery, as measured with a photoionization detector (PID; Aurora Scientific). The delivery system required accurate airflow, which was achieved using fast mass flow controllers and meters (Alicat Scientific). In most experiments, saturated vapor from pure odorant was serially diluted in air to achieve a dilution ratio of 1:100. For the odor mixture experiments (see Fig. 3.7), headspace from separate vials containing monomolecular odors was combined, so the concentration of each component in the mixture was the same as the components presented individually. Headspace from vials containing orange, mango, yeast, and apple cider vinegar

was presented at 1:2 dilution.

Airflow into each vial was regulated by a two-way inert isolation valve (NResearch No. T360K012). Outflow was gated by a zero-dead-volume 4-way inert isolation valve manifold (NResearch No. 360T082). The manifold consists of a non-gated carrier (clean air) path into which four isolation valves connect. Thus, four odor vials can be connected to each manifold. Three manifolds were connected in series to allow up to 12 different odors to be used in a single experiment. A separate empty (control) vial was located upstream via two normally open isolation valves. To present an odor, a small quantity of odorized headspace was injected into the carrier path by closing the control vial valves and simultaneously opening the two valves gating one of the odor vials. We did not use check-valves at any point, as experience showed these to work poorly.

The total airflow coming out of the valve manifolds was always 1 L/min, so the first air dilution was controlled by varying the ratio of airflow between the carrier path and odor vial. This could be optionally diluted further by discarding a known proportion of the flow to vacuum via a needle valve using the principle of choked flow. The remaining odorized stream could then be further diluted by injecting it into a second carrier of up to 5 L/min. The total flow at the fly was regulated using vacuum and a second needle valve. Total airflow over the fly was 1 L/min, except for natural odor experiments, which used a 0.5 L/min flow rate.

A relatively square odor pulse (Fig. 3.1D) was created by switching between clean and odorized air streams using a synchronous two-way valve (NResearch No. 648T042SH). This final valve was located ~50 cm from the fly, leading to a delay of ~300 ms between valve switching and the odor reaching the fly. Inert tubing (SE-200; Tygon) was used for all connections. The flow path had an 1/8 inch internal diameter throughout. This diameter is sufficiently large to allow the system to work near to atmospheric pressure at our flow rates. This virtually eliminated pressure transients caused by valve switching, as measured by an anemometer (Kurz Instruments). The system terminated at a Teflon odor delivery nozzle (outer diameter, 1/8 inch; internal diameter, 1/16 inch), beveled so that its tip surrounded the fly's head. A suction tube was positioned opposite the odor tube to evacuate odorized air.

We monitored odor delivery on every trial using a PID. The flow path was split after the final valve, with half the stream delivered to the fly and half to the PID. The PID response was digitized at 1 kHz and boxcar filtered at 0.1 s.

Calcium imaging. All two-photon imaging was done using a Prairie Ultima system (Prairie Technologies) and a Chameleon Ti-Sapphire laser (Chameleon XR; Coherent) tuned to 920 nm. Beam strength was attenuated with a Pockels cell (Conoptics) to deliver ~8-10 mW at the sample. All images were acquired with Olympus water-immersion objectives (LUMPlanFl/IR: 60X; NA, 0.9; and LUMPlanFl/IR: 40X; NA, 0.8). Emission fluorescence was bandpass filtered using an HQ607/45-2p filter (Chroma Technologies). Imaging frames varied slightly for each experiment, but were generally ~300 X 300 pixels, with a pixel dwell time of 1.6 us, yielding frame rates of ~3.8 Hz.

Experimental protocol. Data were acquired using PrairieView software (Prairie Technologies). Custom MATLAB (MathWorks) routines were used to control odor presentation and synchronize stimulus delivery with data acquisition. Data were acquired in 25 s sweeps with a 1 s odor pulse triggered 8 s following sweep onset. There was no delay between sweeps so the interstimulus interval (ISI) was 25 s. Stimuli were presented in randomized odor blocks. The same odor was never presented twice in succession. The exception to this was the experiment displayed in Figure 3.6, which was designed to test the effects of presentation order, as discussed in the Results, below. Imaging sessions were generally limited to ~20 min (i.e., ~48 stimulus presentations with a 25 s ISI), due to gradual changes in brain shape and photobleaching.

Data analysis. All data analyses were conducted in MATLAB and R (<http://www.R-project.org>). To correct for motion artifacts, we aligned frames using a subpixel translational-based discrete Fourier analysis (Guizar-Sicairos et al. 2008). A region of interest (ROI) was drawn automatically around fluorescent neural tissue. The area outside the ROI was considered to be background fluorescence (autofluorescence plus shot noise) and its mean was subtracted from the overall image. To quantify the response of the KCs, we applied a small ROI, 6-8 pixels in diameter, to each cell body. This allowed us to average pixels from each cell and treat them as a unit. ROI selection was done manually as somata were packed closely together and of such low contrast that all automated algorithms we tried performed very poorly and required excessive supervision. In each optical section, we selected as many KCs as possible. Data were first motion-corrected and aligned using a rigid transform so that all frames

across all trials were in register. For each trial, we averaged all frames to yield a single mean image. For example, if an experiment consisted of 50 trials, then we ended up with 50 of these mean images. KCs were selected by identifying cells from a short looping movie built from the trial-averaged frames. This ensured that each selected cell remained within its ROI over the whole imaging session. Cells that moved excessively, whether responsive or not, were discarded from the dataset.

We used a simple statistical test to determine whether a KC responded significantly on a given trial. We first calculated the standard deviation of the baseline activity 8 s before stimulus onset. The response time course was then smoothed using a five-point running average and the peak dF/F in the 0.5-4.5 s window following stimulus onset was determined. The response was judged to be significant if the peak was 2.33 SDs greater than the baseline; this corresponds to a one-tailed significance test where $\alpha = 0.01$. This is discussed further in the Results, below. For a KC to be classified as responsive to a given odor, it had to exhibit significant responses to at least half the presentations of that odor. A previous electrophysiological study of KC responses used the same reliability criterion (Turner et al. 2008).

3.4 Results

3.4.1 Optical monitoring of MB population activity

To characterize the response of the MB population to a range of different olfactory stimuli, we used two-photon calcium imaging with the genetically encoded calcium indicator GCaMP3 (Tian et al. 2009). We targeted GCaMP3 expression to the MB using the GAL4 driver, OK107, which expresses in all KCs (Lee et al. 1999). We oriented the preparation so that the KC somata are superficial and the imaging axis is perpendicular to the disc-shaped field of cell bodies, maximizing the number of neurons that can be imaged simultaneously (Fig. 3.1A). A typical imaging plane captures ~100 of the 2000 total KCs in the MB; the location of the optical section varied across preparations, capturing a different set of KCs in each fly. Slightly deeper optical sections enabled us to image both cell bodies and the dendritic sites in the calyx (Fig. 3.1B,C).

We presented odor stimuli using a custom-built device that could deliver up to 12 different odors

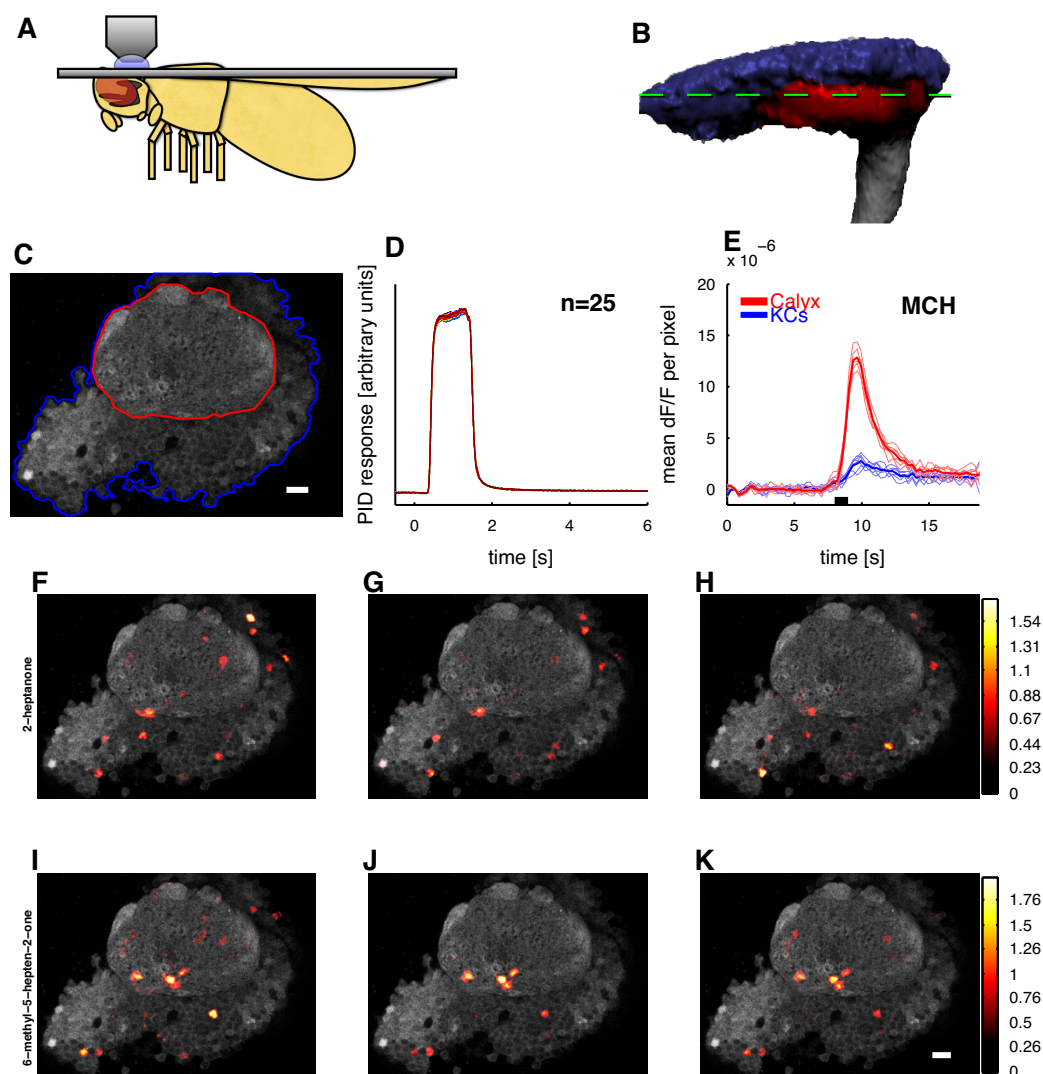


Figure 3.1: Odors evoke consistent patterns of calcium activity in the mushroom body. **A**, Schematic of a fly in the recording platform. Mushroom body is shown in dark gray behind the fly's eye. **B**, Three-dimensional reconstruction of the MB obtained using the OK107-Gal4 driver. The KC somatic region is shown in blue, the input neuropil region (calyx) in red, and axonal outputs in gray. The green dashed line indicates a typical imaging plane. **C**, Optical section through the MB showing the clearly distinguishable KC somatic region (blue) and dendrites in the calyx (red). Image is obtained by averaging 12 frames of basal GCaMP3 fluorescence. **D**, Time courses of 25 pulses of isoamyl acetate measured using a PID (arbitrary units) showing the high reliability of odor delivery. Odor delivery valve opens at $t = 0$ s and closes at $t = 1$ s. PID data are smoothed with a 0.1 s boxcar filter. **E**, Mean change in fluorescence per pixel following presentation of 4-methylcyclohexanol (black bar) in the calyx (red) and KC region (blue) from the optical section shown in C. Thin lines show five individual odor presentation trials and thicker lines show the means. The dF/F values are low because most pixels do not change in intensity. **F-K**, Basal fluorescence (gray) and mean evoked dF/F (heat map) from the experiment shown in C. Mean dF/F is calculated over 0.5-4.5 s following stimulus onset. Each row shows responses to three different presentations of the same odor. Responses are evident both in the dendritic region in the calyx (red outline in C) and the cell body area (blue outline in C). The pattern of responding neurons is similar within an odor and different across odors. Scale bars, 10 μm .

in one session. Different odors were delivered in pseudorandomized order, with a 25 s interstimulus interval (see Materials and Methods, above). Odor delivery was controlled by a series of valves triggered to open for 1 s, starting 8 s after trial onset. The actual time course and amplitude of odor delivery was directly monitored by splitting the odor flow line so half was delivered to the fly and half to a PID (see Materials and Methods). Odor delivery was highly reliable across multiple presentations as measured by the PID (Fig. 3.1D), although there was a consistent delay of ~300 ms between valve opening and the onset of the PID signal.

We could detect strong, reliable, odor-evoked signals in both the dendritic and somatic region of the MB. Figure 3.1 E shows the proportional change in fluorescence (dF/F) spatially averaged across the calyx and cell body region. The time course of the GCaMP3 signal generally lasted for several seconds after odor offset. The amplitude of the calyx signal was much greater than that observed at the cell bodies, which is consistent with calyx signals representing strong synaptic input from PNs, and cell bodies representing the sparse spiking output.

Responses were generally prolonged (Fig. 3.1E), so we quantified response amplitudes by averaging activity at each pixel from 0.5 to 4.5 s following stimulus onset. Figure 3.1, F-K, shows the mean evoked odor response (heat-map colors) superimposed on the basal fluorescence (gray scale) from a single fly. Figure 3.1, F-H, shows three responses to 2-heptanone and Figure 3.1, I-K, shows responses to the related compound, 6-methyl-5-hepten-2-one. Presentations of these odors were randomly interleaved with others (data not shown). Activity can be seen in both the cell body region and the calyx (Fig. 3.1C). Importantly, in the cell body region, there are focal, circular signals visibly attributable to individual KC somata. Note that the same odor activates similar patterns of MB activity across presentations and that response patterns are different between odors.

3.4.2 Determining population responses from somatic calcium signals

The strong baseline fluorescence, together with the high signal-to-noise ratio of the somatic responses, made it possible for us to analyze the data at the level of individual cells. This allowed us to evaluate sparseness of representations by directly visualizing the fraction of cells in the imaging plane that respond to a given odor. A cell was deemed to be responsive to an odor based on two criteria: the presence of a significant dF/F deflection from baseline after odor onset and the reliability

of this deflection across multiple presentations. To be deemed significant, the fluorescence change on a given trial had to exceed 2.33 SD of the dF/F fluctuations observed during the baseline period on that trial. This corresponds to a threshold crossing measure with $\alpha = 0.01$. To account for trial-by-trial variability, we required that this threshold be crossed on more than half of all presentations of an odor. These are similar criteria to those used in previous electrophysiology studies (Turner et al. 2008) and account for the fact that some KCs respond unreliably or weakly, a feature that can accompany sparse representations (Willmore and Tolhurst 2001), and may place a limit on the information carried by the KC population.

These statistical criteria effectively captured the features of the population response that were apparent from visual inspection. Figure 3.2 A shows the time course of fluorescence changes for 121 KCs in response to a single presentation of isoamyl acetate. The cells in Figure 3.2 A are sorted by the p -value for the significance of threshold crossing; the 24 cells below the dashed white line exceeded the threshold. Time courses from cells crossing the threshold are shown in Figure 3.2 B, while those failing to cross are shown in Figure 3.2C. Figure 3.2, D-F, shows dF/F time courses in response to the control stimulus (an empty vial). Pooling data over the entire experiment makes the distinction between responding and nonresponding cells clearer still. We recorded the responses of 121 KCs to five odors presented five times each, which yielded a total of 3025 KC-stimulus pairs. The distribution of threshold-crossing p -values for these data is shown in a cumulative histogram (Fig. 3.2G). The plot shows a clear elbow due to the presence of a small number of significant trials against a background of nonsignificant trials. The threshold of $\alpha = 0.01$ falls at this elbow, indicating that this threshold partitions the data naturally.

To estimate the fraction of KCs that respond to an odor, we also factored in the reliability of those threshold crossings over multiple odor presentations. On any given odor trial, ~20% of KCs may be active (Fig. 3.2 A-C). However, only a portion of these cells display significant fluorescence changes on more than two presentations of that odor (Fig. 3.2H). Moreover, we found that cells that respond significantly on more than half of trials are those with the larger median odor-evoked dF/F (Fig. 3.2 I), indicating that cells with larger response amplitudes also respond more reliably. Based on these observations, we considered a cell to be responsive to a particular odor if it passed the significance test on more than half of all presentations of that odor. The results obtained from applying our response criteria are shown in Figure 3.3. Figure 3.3, A and B, shows the dF/F time courses and response amplitudes

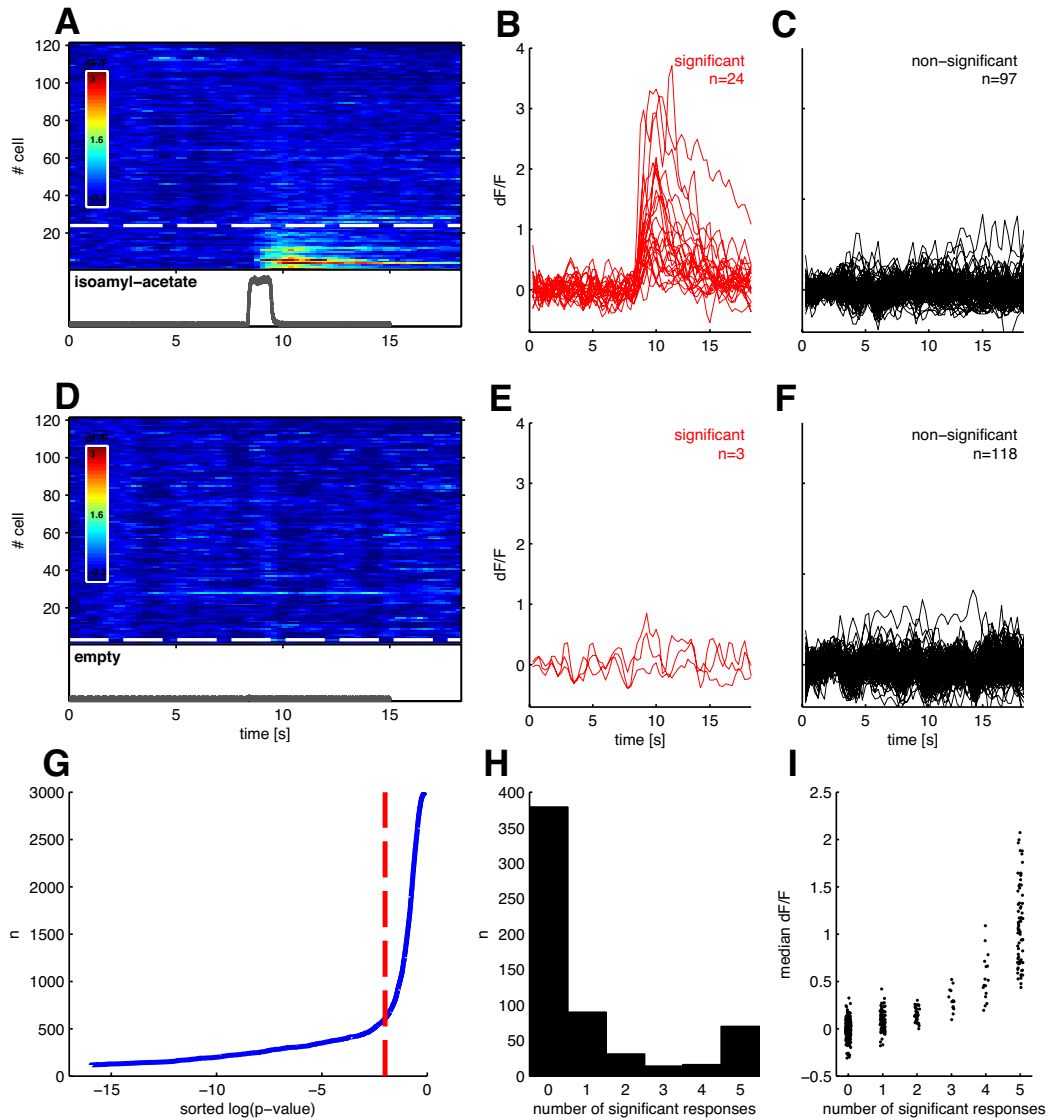


Figure 3.2: Detecting odor responses with cellular resolution in single trials. **A**, dF/F time courses of 121 KCs in response to the presentation of isoamyl acetate (PID trace in gray). KCs are sorted according to the p -value of the threshold crossing (see Results). Cells below the dashed white line show a significant response peak at $p = 0.01$. **B**, Time courses of the 24 significantly responding cells from **A**. **C**, Time courses of the 97 nonresponding cells from **A**. **D-F**, Responses of the same 121 cells to one presentation of clean air. **G**, Cumulative histogram of p -values from all cells and all odor presentation trials from a single fly. The $\alpha = 0.01$ (dashed red line) threshold falls at the elbow of the line, indicating that it represents a reasonable distinction between responding and nonresponding KCs. **H**, Histogram showing the number of trials in which each cell exhibited a significant response to an odor; data from 121 KCs presented with five different odors (605 KC-odor pairs) for five trials each. Data are bimodally distributed, with some cells responding to only one or two of the five total odor presentations. **I**, Relationship of response amplitude to response reliability from KC-odor pairs shown in **H**. Cells exhibiting a larger evoked dF/F also showed more reliable responses. Points are jittered along the x-axis for visibility.

of a cell we classified as responding significantly to 3-octanol but not to clean air. Response amplitudes were calculated as the mean evoked dF/F within the response window (0.5-4.5 s after odor onset). The response amplitudes of 45 cells are shown in Figure 3.3C, colored according to their classification as responding or nonresponding. Responding neurons generally displayed larger dF/F values than nonresponding cells, although occasionally their dF/F values were similar. Nonresponsive cells were classified as such either because those dF/F changes were not significantly greater than baseline fluctuations or because they were not reliable across presentations. This is evident in Figure 3.3D, which shows that the p -values for threshold crossing are invariably smaller over multiple trials for the gray, nonresponsive cells.

To summarize, to qualify as responsive to a particular odor, a cell had to exhibit a peak dF/F value that was 2.33 SD ($\alpha = 0.01$) greater than the baseline mean within a window 0.5-4.5 s after odor onset, on at least half of odor presentations. Both the threshold crossing and reliability criteria were chosen based on features that were evident in the underlying data (Fig. 3.2G,H). The fraction of responding KCs we detected with this method was extremely similar to that observed in previous electrophysiological studies (see Fig. 3.5) (Turner et al. 2008), suggesting that we detected the vast majority of KC responses. Overall, these results show that we can reliably track the activity of individual KCs on a trial-by-trial basis, enabling us to identify consistent KC responses within a large population of cells and generate an accurate measure of population sparseness.

3.4.3 Random spatial distribution of MB odor responses

We examined whether there was any relationship between the response properties of KCs and their spatial distribution within the cell body layer. Imaging can readily reveal whether there are clusters of highly responsive cells or groups of cells with similar response properties. We tested this by imaging responses to a panel of chemically diverse odors (a total of 18 different odors, four to seven odors per fly). We found that most KCs did not respond to any of the tested stimuli (Fig. 3.4 A), as observed previously with electrophysiological recordings (Perez-Orive et al. 2002; Turner et al. 2008). This skewed distribution could reflect a spatial organization consisting of small clusters of densely responding neurons.

We investigated this possibility by measuring the distances separating responding neurons and

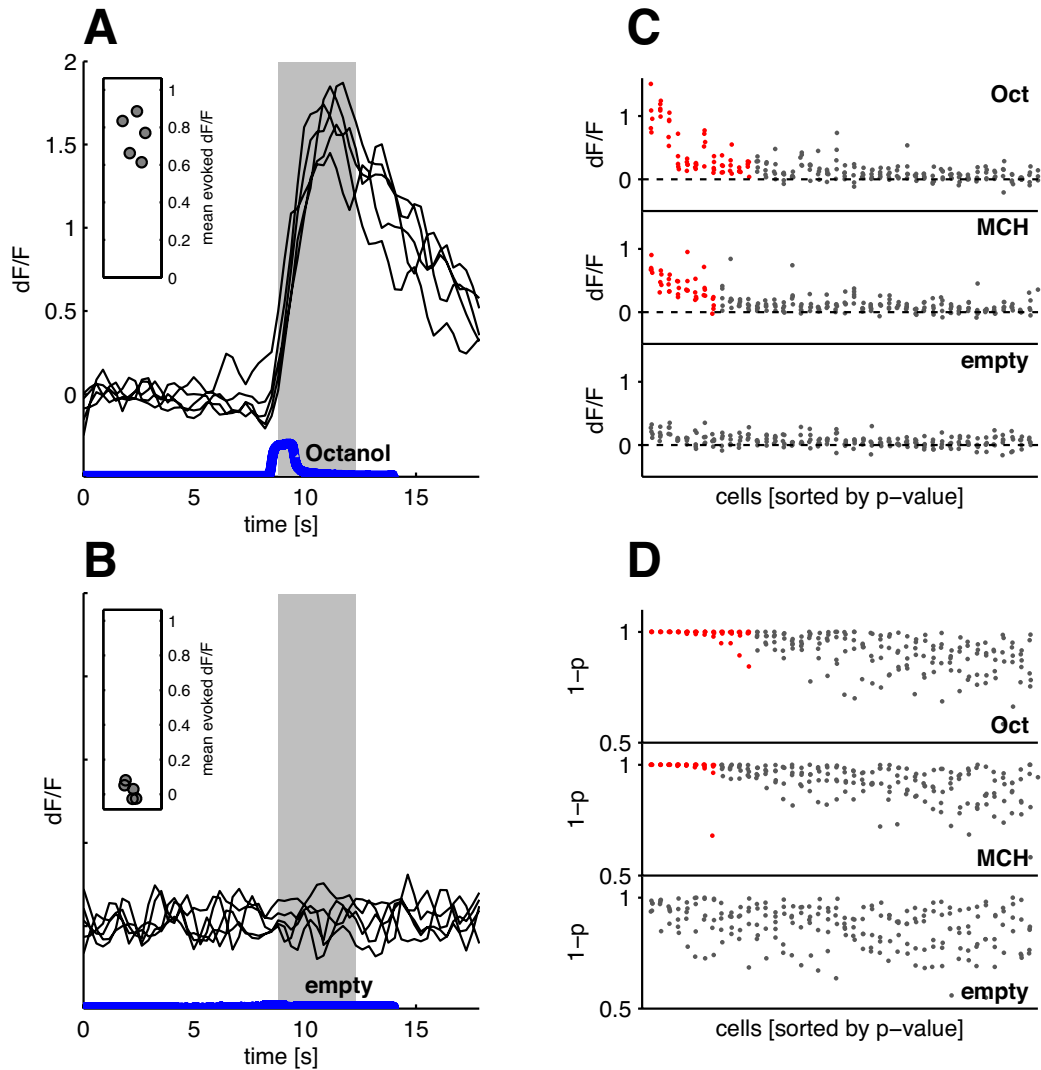


Figure 3.3: Reliably identifying KC odor responses. **A**, Responses of a single KC to five presentations of 3-octanol (black traces). The blue trace shows the kinetics of the odor pulse measured by PID. Response amplitudes (inset) are calculated by averaging activity between 0.5 and 4.5 s following stimulus onset (shaded gray area). **B**, Responses of the same cell to the clean air control. **C**, Response amplitudes of the 45 strongest responding neurons from a single optical section to 3-octanol (Oct), 4-methylcyclohexanol (MCH), and clean air. Each data point is the evoked response amplitude from a single cell on a single trial. A cell was deemed responsive to the odor if it responded significantly ($p < 0.01$) on more than half of the trials. Responsive cells are indicated by red points, nonresponsive cells by gray. Cells are sorted independently for each stimulus according to the mean p -value. **D**, Statistical significance of response peaks from the neurons shown in **C**. The y-axis shows 1 minus the p -value. Cells are sorted as in **C**. Note that responsive cells consistently have values close to 1 on almost all trials; this is not the case for cells classified as nonresponsive.

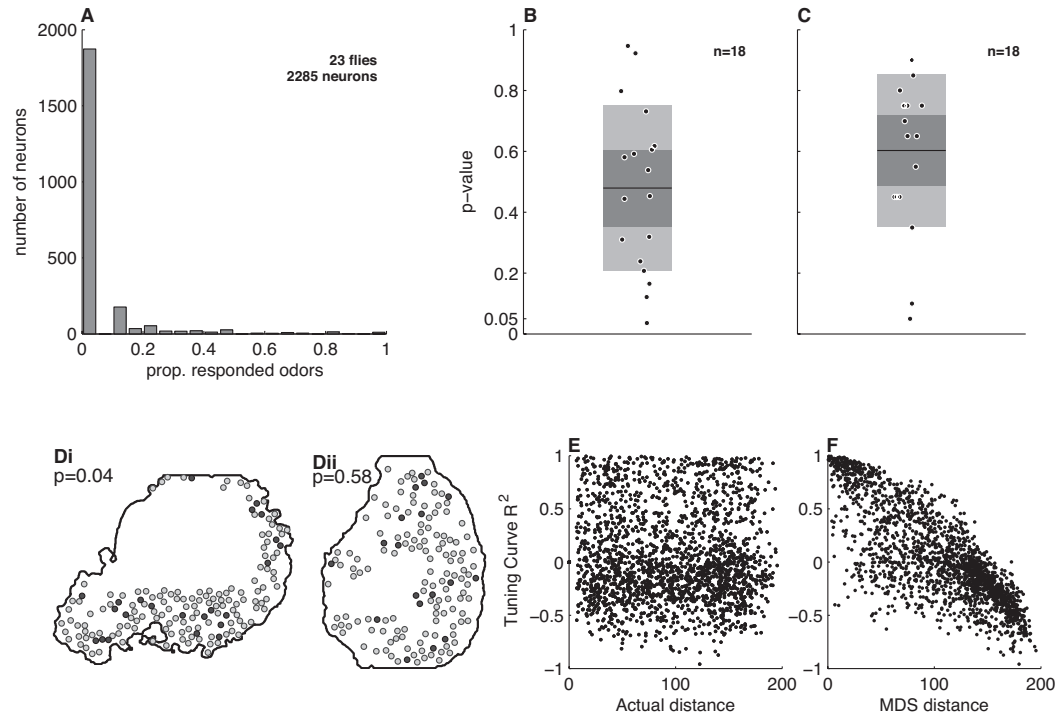


Figure 3.4: Random spatial distribution of responding MB neurons in the cell body layer. **A**, The proportion (prop.) of odors eliciting a response from each cell (lifetime sparseness). The vast majority of cells do not respond to any tested odor (peak at zero). **B**, Distribution of p -values from a permutation test for clustering of responsive neurons within an optical section. Each data point represents one optical section from an individual fly. Light gray boxes indicate standard deviation around the mean; dark gray box indicates the 95% confidence interval. Only a single imaging plane showed a nominally significant level of clustering ($p = 0.04$). See Results for details. **C**, Distribution of p -values from a permutation test for clustering of neurons with similar tuning curves. Each data point represents one optical section from an individual fly. We found no evidence for clustering. **D**, Example imaging planes showing distributions of responsive cells (dark gray). We observed a section with high clustering value (i) and one with a moderate value (ii); neither showed a visibly striking clustering of responsive neurons. **E**, Tuning curve correlation as a function of distance between cells from a single fly. **F**, Tuning curve correlation as a function of distance in MDS space (see Results) for the fly shown in **E**. This plot illustrates that obtaining topography is possible with the tuning curves we observed experimentally.

comparing them to the distances expected if these neurons were distributed randomly. Since each experiment involved optical sections from different locations and orientations in the MB, we analyzed each imaging plane individually. We began by identifying cells that responded to at least one odor (preparations with < 10 responding cells were excluded). We then calculated the distance from each responding cell to its nearest responding neighbor. For instance, an imaging field containing 16 responding cells would yield 16 distance values. We calculated the mean of these distances as a measure of clustering; a smaller value indicates tighter clustering. Using nearest-responding-neighbor distances ensured that our analysis would not overlook the possibility of multiple small clusters. We tested the significance of this value using a permutation test where the labels of all identified KCs were randomly reassigned, such that responding cells become located in new, randomly chosen, positions. We recalculated the nearest-responding-neighbor distances and took the mean of these to represent the value expected in the absence of clustering. This procedure was repeated 10,000 times for each fly. If the experimentally observed clustering value was smaller than 95% of the simulated values, we considered this to be evidence of significant clustering at $\alpha = 0.05$ for this particular fly. Figure 3.4 B shows the distribution of p -values from this response clustering test for 18 flies. Overall, these results showed no strong evidence for clustering of responsive neurons in the cell body layer, although one fly did have a p -value below the significance level ($p = 0.04$). The actual distribution of responding neurons in this section is shown in Figure 3.4Di, where it is apparent that the clustering is not striking. We note that electrophysiological studies have shown that KCs with axonal projections to the $\alpha'\beta'$ lobes tend to be more responsive than other KC types (Turner et al. 2008). However, our results indicate that this spatial organization is not present in the cell body layer.

It is also possible that KCs are topographically organized according to their odor tuning curves. Here we test the simplest hypothesis: that nearby neurons have tuning curves that are more similar to one another than those of more distant neurons. Tuning curves were calculated as the mean dF/F response evoked by each odor, and tuning curve similarity was measured as the Pearson's correlation coefficient between each pair of odor tuning curves. We then tested whether there was a relationship between tuning curve similarity and the Euclidean distance between cells using Spearman's ρ , which evaluates whether there is a monotonic relationship between these two variables. Spearman's ρ values were calculated for each imaging plane and, as before, we judged significance using a permutation test. We randomized the identity of the responding cells within the image plane to produce a new Euclidean distance matrix

while keeping the tuning curve correlation matrix fixed, and recalculated Spearman's ρ . This process was repeated 10,000 times to generate a distribution of ρ values expected if tuning curve topography were absent. If the experimentally observed ρ was $> 95\%$ of the simulated values, we considered there to be significant tuning curve topography in that optical section at the $\alpha = 0.05$ significance level. Figure 3.4C shows the distribution of p -values for the test of tuning curve clustering for the 18 flies. All points lie above the significance threshold, indicating that there is no strong tendency for KCs with similar odor tuning to be located near one another.

The odor tuning properties of KCs are extremely diverse, so it may not even be possible to arrange odor tuning curves topographically in 2-D. Therefore, to validate the results above, we confirmed that it was feasible to arrange the tuning curves we measured experimentally in a way that produces a topographic map. To generate an artificial topographic map with the data collected, we arranged KCs in a 2-D space based on the correlations between different tuning curves. Specifically, we projected the correlation matrix into a 2-D space that mimics the imaging plane. We achieved this using multidimensional scaling (MDS), a remapping technique that measures the distances between points in a high-dimensional space and projects this onto a low-dimensional space (typically 2-D) while attempting to retain the relationship between points (Martinez and Martinez 2005). We tested whether our regression analysis would reveal topography with the tuning curves arranged in 2-D MDS space. Again, we calculated the corresponding ρ value and compared this to a distribution of 10,000 ρ values generated using randomized Euclidean distance matrices. This analysis showed that the tuning curves we measured could indeed be arranged topographically. In every imaging experiment analyzed ($n = 18$), the MDS-based topographic map had a greater ρ value than all of the randomized tuning curve maps. Therefore, our inability to find topography in the original data was not due to the fact that tuning curve shapes are too varied or too uncorrelated to be regularly arranged in 2-D.

Together, these results demonstrate that neither do odor representations in the MB cluster spatially nor do KCs with similar odor tuning properties have apparent spatial localization. This suggests that the relationship between response properties of KCs and their spatial distribution within the cell body layer is random. Such a lack of spatial organization is a shared feature of the MB and mammalian piriform cortex (Stettler and Axel 2009) and highlights their likely role as associative areas where anatomical specialization plays a minimal role in information processing.

3.4.4 MB population responses to odors are sparse and correlated with net OSN output

Using GCaMP3, we routinely obtained response amplitudes with dF/F values two or three times greater than the baseline (for example, see Figs. 1, 2). This signal strength is four to six times higher than that obtained in a previous MB study using GCaMP1.3 (Wang et al. 2004) and suggests that this indicator has the sensitivity to detect most KC activity. Across the range of monomolecular odors shown in Figure 3.5A, we found that, on average, an odor evokes responses in ~5% of the KCs in an imaging plane ($n = 8$ flies and $n = 933$ neurons); given the lack of spatial clustering of responses, this likely reflects the overall probability of response across the entire MB. This is extremely similar to results obtained using single-cell recordings, where on average each odor activates 6% of cells (Turner et al. 2008). The mean proportion of responding cells did not exceed 0.1 for any odor, although the response from individual flies reached values up to 0.17. However, even the largest of these values is well below that observed in PNs, where a given odor often evokes a response in excess of 50% of the population (Wilson et al. 2004). Thus, although we do not exclude the possibility that some KC responses go undetected with GCaMP3, when expressed using the OK107 driver, this indicator clearly enables us to detect KC responses with a level of sensitivity comparable to that of electrophysiology.

Is it possible to predict the sparseness of an odor representation in MB? Although there was a high level of variability across individual flies, there was still a clear trend for certain odors to evoke a more extensive response in the MB than others. This suggested that sparseness levels could perhaps be predicted by some aspect of the stimulus. One such predictor could be the total activity of OSNs at the sensory periphery. To test this, we examined odorants for which the response properties of 24 adult OSN types are known (Hallem and Carlson 2006). We used linear regression to predict the proportion of responsive KCs as a function of the total evoked OSN activity (Fig. 3.5B). Since the data included repeated observations from the same fly, we used a mixed-effects linear model (Pinheiro and Bates 2000) to fit a random intercept for each animal. The slope of the model was significant ($p = 0.0001$, $df = 38$) and indicated that, on average, increasing the total OSN activity by 10 spikes/s caused the proportion of responsive KCs to increase by 0.03%. In other words, it would take 16 additional spikes at the OSN level to recruit one additional KC response within the entire MB population. However, the regression explained only ~27% of the variance. There are several possible reasons why this correlation is weak. One is that our prediction is based on the activity of only half the complement of OSNs. A second is that

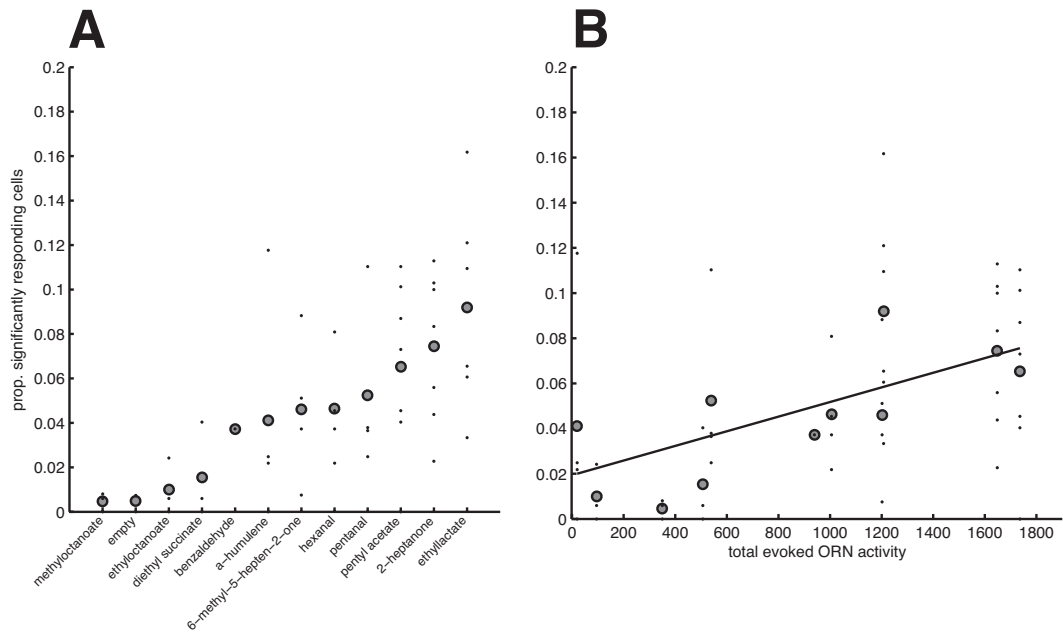


Figure 3.5: Responses to monomolecular odors are sparse in MB. **A**, Proportion (prop.) of KCs responding to a variety of different odors. Black points show sparseness values from individual animals ($n = 8$ flies); gray circles show the grand mean. **B**, Mean sparseness values as a function of total OSN activity [OSN data from Hallem and Carlson (2006)] for each odor. Some KC responses shown in **A** are not plotted since OSN data do not exist for these odors. The slope of the fit is significantly different from zero ($p < 0.0001$) (see Results).

processing by local neurons provides gain control within the antennal lobe, producing similar PN output levels for different intensities of OSN input (Olsen and Wilson 2008; Root et al. 2008). However, the fact that we find a significant correlation indicates that the gain control mechanisms are not complete.

3.4.5 MB population sparseness is preserved across a range of concentrations

The observation that the sparseness of MB odor representations is correlated with OSN output suggests that sparseness could be modulated by stimulus intensity. We therefore tested whether sparse representations are maintained across different odor concentrations. Individual KCs can exhibit both concentration-specific and concentration-independent responses (Stopfer et al. 2003). However, the effect of odor concentration on population-level activity has not been examined. Since olfactory memories are relatively concentration-invariant (Masek and Heisenberg 2008; Yarali et al. 2008), one might expect that MB representations have concentration-invariant qualities at the population level.

We tested MB responses to ripe banana odor and to a prominent monomolecular component of banana smell, isoamyl acetate, across a range of concentrations from 0.01X to 0.1X air dilutions of saturated vapor. Since adaptation could influence odor responses when repeatedly presenting the same odor at different concentrations, we used an experimental design where such effects are visible, enabling us to evaluate their contribution. We delivered odors in blocks, where odor concentrations stepped either from high to low or from low to high within each block, as illustrated by the PID traces in Figure 3.6A; the interstimulus interval, likely an important parameter, was 25 s as in other experiments. We presented each odor as a series of either five high-to-low blocks or five low-to-high blocks, with individual blocks separated by a single presentation of clean air from an empty control vial. Each fly received both banana and isoamyl acetate, but only one direction of the concentration steps. For these experiments, we calculated population sparseness on a trial-by-trial basis, allowing us to examine the effects of stimulus history on MB responses.

Figure 3.6, B-E, shows the effect of concentration on population sparseness, broken down to highlight either the odor presented (Fig. 3.6 B, C) or the direction of the concentration steps (Fig. 3.6 D, E). We used a mixed-effects ANOVA to evaluate the effects of stimulus concentration, stimulus order, and odor identity on sparseness. There was no effect of odor identity, so we pooled the data for subsequent analysis. We found there was a significant effect of stimulus concentration ($p < 0.0001$,

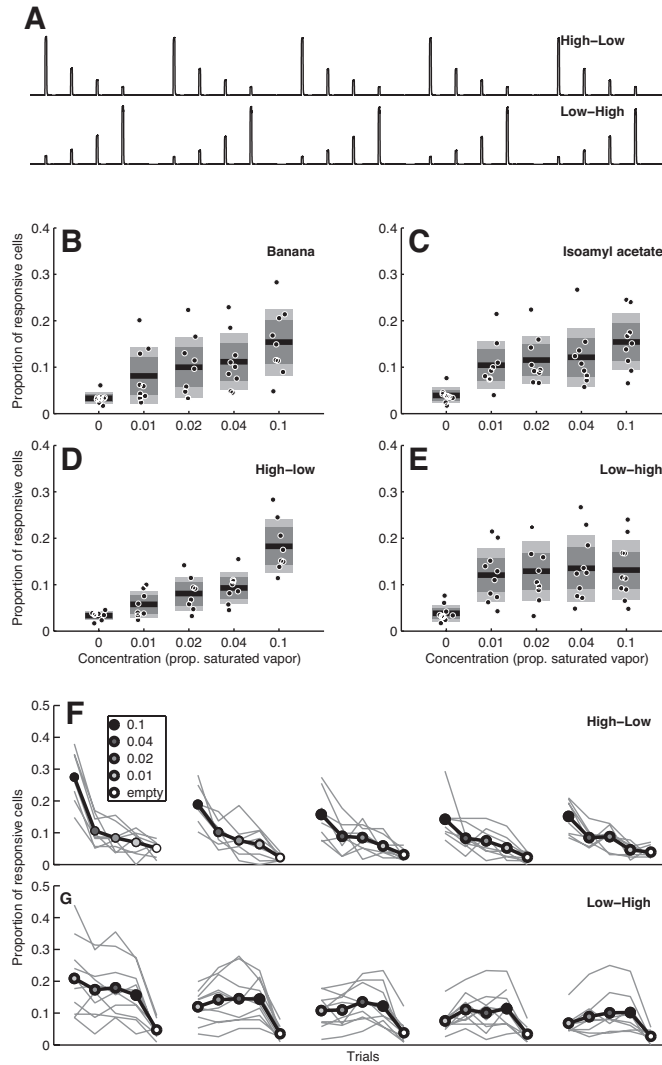


Figure 3.6: The effects of odor concentration and recent stimulus history on MB population sparseness. **A**, Stimuli were delivered in blocks of either increasing or decreasing concentration steps, shown here as the average PID traces acquired during each type of experiment (for details, see Results). **B**, Proportion of Kenyon cells responding to ripe banana over a range of different odor concentrations. Mean sparseness increases slightly with concentration, but never exceeds 0.2. Each point is the MB response from an individual fly for each concentration from both types of stimulus blocks (jittered along the x-axis for clarity); black bars indicate the mean of these points. Light gray boxes indicate standard deviations around the mean and dark boxes indicate the 95% confidence interval. **C**, Same as **B**, but for the monomolecular odor isoamyl acetate. **D**, Data from **B** and **C** showing specifically the results from the high-to-low concentration steps. **E**, As **D**, but the low-to-high steps. An effect of concentration is only apparent for the high-to-low condition. **F-G**, Responses on individual trials over the course of an experiment showing that the order in which stimuli were presented affects the sparseness of MB response. Response to the first trial was typically less sparse than subsequent trials. Additionally, the stimulus block type (high-to-low vs low-to-high) affected how sparseness changed with concentration. Gray lines show sparseness estimates from individual flies. Points connected by the black line indicate the mean responses on individual trials of different odorant concentrations (filled circles) or clean air (open circles). Trial blocks have been separated in time for clarity, but experiments were run continuously.

$F_{(4,73)} = 32.9$). However, this was profoundly affected by the order in which the stimuli are presented (Fig. 3.6 D, E). In the high-to-low condition, sparseness was significantly modulated by concentration ($p < 0.0001$, $F_{(3,25)} = 22.5$), but not in the low-to-high situation ($p = 0.71$, $F_{(3,32)} = 0.47$). Thus, whether one sees an effect of odor concentration on sparseness depends critically on the order of the concentration steps.

This effect was consistent and clearly visible on a trial-by-trial basis in individual flies (Fig. 3.6 F, G). This did not reflect any history-dependence of the stimulus delivery itself (Fig. 3.6 A). Rather, an adaptive process with a long time constant likely accounts for these results. For example, the very first odor presentation of the experiment typically evoked the broadest response, regardless of the concentration of odor. In fact, the sparseness of the very first odor response in an experiment was not significantly different between the 0.01X and 0.1X concentrations ($p = 0.20$, Wilcoxon rank sum). A similar effect has been seen at the single-cell level in the locust antennal lobe (Stopfer and Laurent 1999) and in the MB in honeybee (Szyszka et al. 2008). It is striking that the effect of changing concentration can be entirely occluded by changing the order of stimulus presentation, producing the essentially flat concentration dependence in the low-to-high condition. Our ability to track population-level responses reveals that this experience-dependent process can generate concentration-invariant levels of response in the MB.

3.4.6 Sparse MB responses to natural and artificial multimolecular odors

Our panel of monomolecular odors was chosen to activate a diverse set of OSNs (Hallem and Carlson 2006). Nevertheless, a surprisingly large fraction of KCs did not respond to any of these stimuli (Fig. 3.4 A), even when presented at high concentration. Most natural odors are composed of multiple volatile components and olfactory systems have presumably evolved to detect and respond to such complex odors. This raises the possibility that some KCs are tuned selectively for multimolecular detection. We therefore presented odor blends and natural odors to examine the effects of stimulus complexity on the sparseness of MB representations.

To assess how robustly the MB maintains sparse representations of multicomponent stimuli, we blended together different monomolecular odors that activate largely nonoverlapping populations of KCs. We used this strategy to maximize the possibility that mixing the odors increases the proportion

of responding cells in the MB. The odors 3-octanol and 4-methylcyclohexanol activate very different populations of KCs (Fig. 3.7 D, E). Presented individually, each of these odors activates 9% of KCs on average. When presented simultaneously, however, this proportion increases only slightly (11%) and is smaller than the linear sum of the two activity patterns, 15% (Fig. 3.7A). A different pair of odors, 2-heptanone and pentyl acetate (Fig. 3.7B), also did not show supra-additive responses. Individual cells displayed both suppressive and synergistic interactions, with most cells showing a weaker response to the mixture than predicted from the linear sum of the response to the components (Fig. 3.7C). This subadditivity is consistent with observations made in the antennal lobe (Silbering and Galizia 2007; Olsen et al. 2010) and olfactory bulb (Meredith 1986; Tabor et al. 2004) and is a well known olfactory phenomenon termed mixture suppression (Moskowitz and Barbe 1977). The strong effects of mixture suppression in the MB parallel observations in piriform cortex (Stettler and Axel 2009). Overall, these results indicate that blending odors has only a modest effect on the sparseness of MB representations, due to the subadditive recruitment of KCs.

The possibility remains, however, that because these odor blends are artificial, they may interact within the olfactory circuit in a nonoptimal way that accounts for the subadditivity of responses. This could result from a failure to synergistically activate KCs with an ethologically relevant set of input channels that the circuit evolved to process. We tested this possibility by examining responses to a variety of natural smells: apple cider vinegar, yeast, mango, and orange. Although these odors are not as chemically well defined as monomolecular odorants, we felt it was important to present volatiles from these genuinely natural stimuli. These appetitive odors drive robust behavioral responses and are clearly meaningful to the animal, although it should be noted that artificial compounds can also produce strong behavioral reactions (Stensmyr et al. 2003; Larsson et al. 2004; Fishilevich et al. 2005). To maximize the possibility that these odors would drive strong responses in MB, we presented them at an odor dilution ratio of 1:2, much less diluted than the 1:100 used for monomolecular odors. We found that the sparseness of natural odor responses fell within the range of the monomolecular test compounds (Fig. 3.7G-I). Although they were in the upper half of this range, this was likely because of their higher concentration, because comparable dilutions of a natural and artificial odor evoked responses in very similar fractions of KCs (Fig. 3.6). Thus, natural odors do not appear to present special ratios of components that could synergistically activate a large portion of the MB population. The absence of any specialization toward behaviorally relevant complex stimuli suggests that the fundamental processing

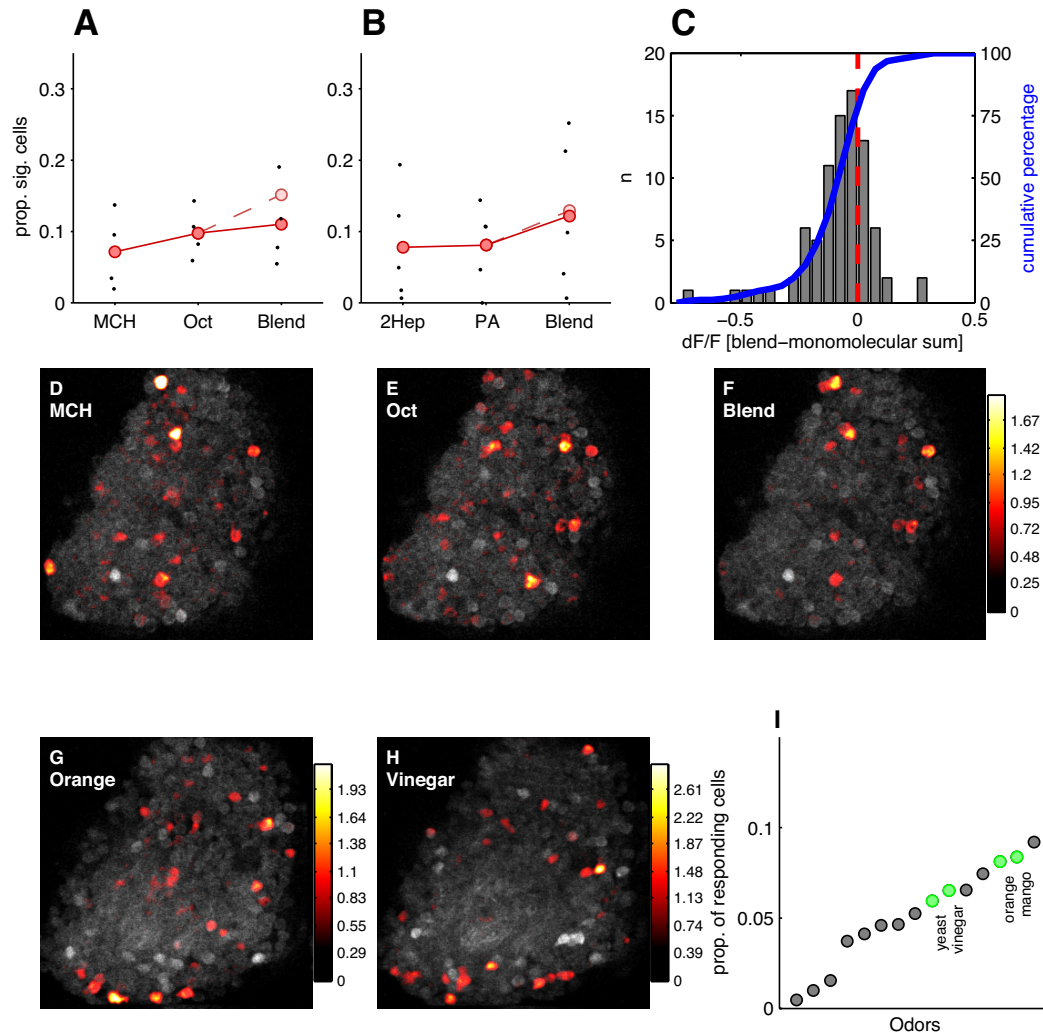


Figure 3.7: MB responds sparsely to complex and natural odors. **A**, Proportion of KCs responding to 4-methylcyclohexanol (MCH), 3-octanol (Oct), and a 50:50 blend of the two odorants. Points show sparseness values from individual optical sections ($n = 4$). Grand means shown in red. The sparseness of responses to the blend is very similar to that of the monomolecular components. The pale red point indicates expected proportion of responsive cells if the monomolecular odorants were to sum additively. **B**, Similar data as **A**, but from a different experiment using 2-heptanone (2Hep), pentyl acetate (PA), and their 50:50 blend. **C**, Responses to blends are predominantly subadditive. Histogram shows the distribution of deviations from linearity for responses to the 3-octanol plus 4-methylcyclohexanol blend compared with the response predicted by linear addition of responses to the individual components. Seventy-three percent of cells responded less to the blend than expected from the sum of the component responses, indicating that the majority of KC responses to the blend are subadditive. **D-F**, Basal fluorescence (gray) and dF/F overlay (heat map) for responses to 3-octanol, 4-methylcyclohexanol, and the blend of the two odors. Each panel shows data from an individual trial. dF/F values are on the same scale for all panels. **G-H**, Single-trial responses to two complex natural odors. **I**, The sparseness values of natural odors (green) compared with a range of different monomolecular odorants (gray). Natural odorants do not evoke responses that are substantially more or less sparse than monomolecular odorants.

feature of the MB is to create sparse stimulus representations regardless of the nature of the stimulus.

3.4.7 MB responses to natural and monomolecular odors are indistinguishable

The sparseness of responses to natural and monomolecular odorants was not noticeably different (Fig. 3.7I). Nonetheless, the perception of natural odors can be compellingly distinct from monomolecular odors. We therefore asked whether we could find any difference at all in the representations of these two odor classes. We compared statistics of responses using four different variables. These are shown in Figure 3.8A-D, where gray points represent data from monomolecular odorants and black points represent data from natural smells.

We tested whether the magnitude or duration of the odor response could predict whether the stimulus was a natural or monomolecular odorant. To quantify response duration and how consistent this duration was across cells, we calculated the mean and the standard deviation of the number of imaging frames in which the dF/F time course of cells was above response threshold (Fig. 3.8 A, B). To determine whether natural odors activate the same number of cells but evoke a stronger response at these cells, we calculated the mean evoked response per cell (Fig. 3.8C) and the standard deviation of the mean evoked response (Fig. 3.8D). These parameters did not appear to separate natural and monomolecular odors. Nevertheless, to maximize our chances of finding a difference, we conducted a linear discriminant analysis (LDA) on all four variables simultaneously. LDA is a classification technique that takes into account multiple variables and their interactions to best classify two or more groups of data; in this case, statistics of responses to monomolecular or natural odorants. We ran the classifier using a leave-one-out cross-validation to avoid overfitting. The resulting classification success was only ~78% (Fig. 3.8 E). We assessed the significance of this level of classification accuracy by rerunning the classifier 10,000 times with randomized odor labels, so there was no longer any relationship between the response parameters and the identity of the odors. The resulting distribution of classification success is shown in Figure 3.8E. The observed classification success is well within the range of the randomized values, indicating that natural and monomolecular odors do not evoke fundamentally different responses in KCs.

3.5 Discussion

We measured odor-evoked neural activity in the *Drosophila* MB using two-photon calcium

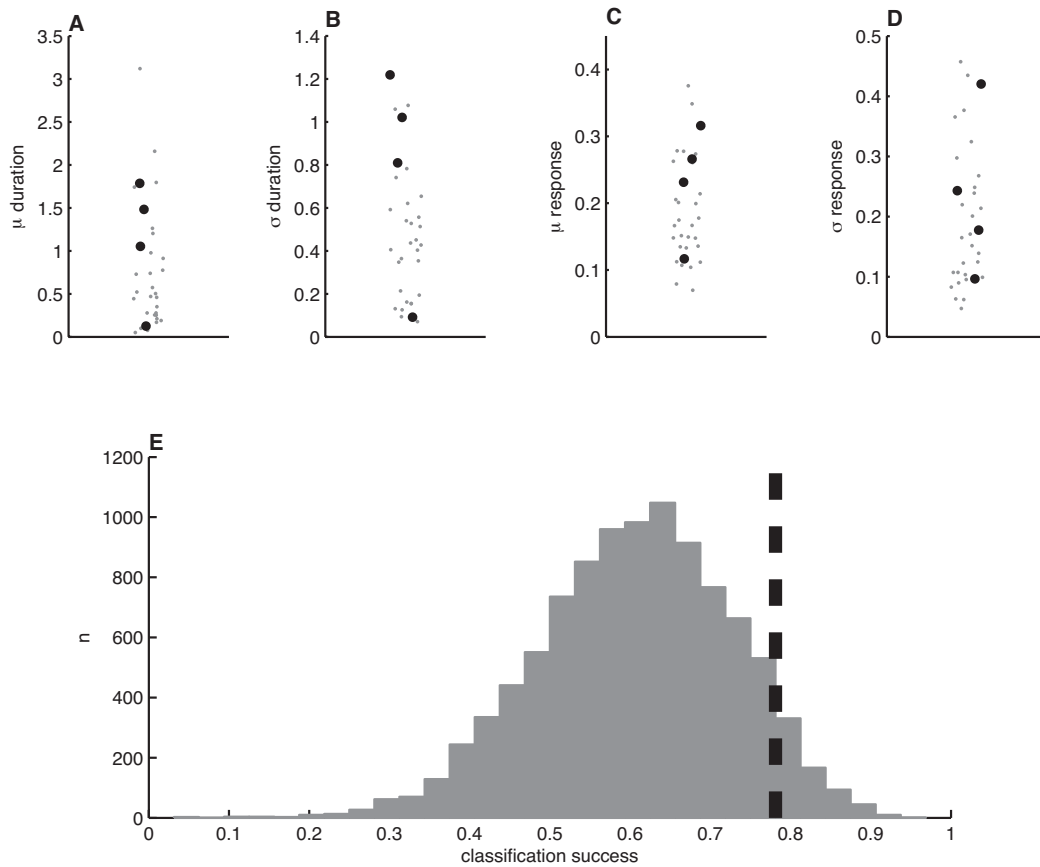


Figure 3.8: MB population responses to natural and monomolecular odors are indistinguishable. **A**, Mean response duration (imaging frames) for natural odors (black circles) and monomolecular odors (gray points). **B**, Standard deviation of response duration. **C**, Mean evoked response magnitude. **D**, Standard deviation of evoked response magnitudes. **E**, LDA-based classification accuracy of natural and monomolecular responses (78%, dashed black bar) compared against chance performance (gray histogram). Observed classification performance was not significantly greater than that of 10,000 chance bootstrap replicates.

imaging. Monomolecular odorants evoked sparse responses across the KC population. Activity remained sparse in response to multimolecular odor blends, complex natural odors, and even changes in odor concentration. Thus, sparseness was relatively unaltered despite large changes in stimulus complexity and intensity. This robustness is significant because sparse representations are thought to be important for information storage (Marr 1969; Kanerva 1988) and the MB plays a critical role in olfactory learning and memory (Erber et al. 1980; Heisenberg et al. 1985). Interestingly, unlike other sensory systems, we found that the MB encodes natural and artificial odors in a similar format. Furthermore, we found that KCs were not spatially organized according to responsiveness or odor tuning and that responsive KCs appeared to be distributed randomly within the cell body layer. We find no evidence of either functional or structural specialization within the MB, rather the main processing feature is to generate sparse stimulus representations.

3.5.1 Spatial organization and tuning curve topography of sparse responses

There is prominent spatial organization to the first two layers of the insect olfactory system. OSNs and PNs project to specific glomeruli that can be uniquely identified across different flies and have predictable response properties. However, it is unclear what role this spatial order plays in sensory processing, and whether it is preserved in the MB. Functional imaging is ideally suited to address this question; however, the reporter used must be sufficiently sensitive to detect most or all activity in the cells of interest. This appears to be the case in our preparation since the fraction of odor-responsive cells detected with GCaMP3 was similar to that detected using electrophysiological techniques (Turner et al. 2008). This is likely because, although KCs fire a small number of spikes, typically five to 10, evoked spike rates are high and spontaneous firing is extremely rare (Turner et al. 2008). Thus, our study provides a far more complete picture of the MB than previous work using the early generation calcium indicator, GCaMP1.3 (Wang et al. 2004), which found that only a tiny fraction of KCs responded to odors. Imaging of PN and KC responses in the honeybee using a synthetic calcium indicator corroborates our imaging results from *Drosophila* and highlights the dramatic sparsening that occurs in MB (Szyszka et al. 2005). However, previous studies did not analyze simultaneously recorded neurons to address the topography of odor representations or examine the robustness of sparseness across different stimulus features.

Previous electrophysiological studies showed that most MB neurons did not respond to any odor tested, while some KCs responded to multiple odors (Perez-Orive et al. 2002; Turner et al. 2008). This skewed distribution of response probabilities was also evident in our imaging results. However, electrophysiological recordings are unable to rule out the possibility that responsive neurons form spatially localized clusters. Using a bootstrapping approach, we showed that responsive neurons are in fact arranged randomly within the imaging fields we examined. PNs send axons to distinct but rather large zones within the KC dendritic field in the calyx (Tanaka et al. 2004; Jefferis et al. 2007; Lin et al. 2007). Although the spatial precision is certainly not to the level of individual KCs (Murthy et al. 2008), it is nevertheless conceivable that nearby KCs will have similar tuning curves. Even so, we again found that the relationship between the spatial arrangement of KCs and their response properties was random. Although we cannot rule out the possibility that KC responses are organized along a spatial axis we did not sample with imaging, our results suggest that neither overall responsiveness nor tuning curve shape are spatially organized at the level of the MB.

The vertebrate piriform cortex also displays this absence of functional topography (Stettler and Axel 2009). In contrast, there is clear anatomical evidence for spatial segregation in other areas at this depth in the olfactory pathway. Mitral cell projections are segregated to distinct zones in amygdala (Sosulski et al. 2011) and anterior olfactory nucleus pars externa (AON) (Ghosh et al. 2011). Similarly, in *Drosophila*, PN projections within the lateral horn appear more stereotyped than those in the MB (Tanaka et al. 2004; Jefferis et al. 2007; Lin et al. 2007). There is also clear functional segregation between projection patterns of food- and pheromone-responding PNs in the lateral horn (Jefferis et al. 2007). These lines of evidence suggest that the olfactory system may strive to construct odor representations that are heavily experience-based in piriform cortex and MB, while in parallel forming innate representations of odor quality in amygdala, AON, and lateral horn.

3.5.2 Robustness of sparse representations to stimulus intensity and complexity

Although sparse coding is useful for learning and memory, an important underlying assumption is that sparseness is robust to naturally varying features of the stimuli, including stimulus intensity and complexity. We tested this by examining sparseness of MB responses to a wide variety of odors, including complex odors composed of multiple components at a range of different concentrations. By

examining a broad array of odors, our goal was to uncover whether the MB is in some way tuned to particular stimuli that drive fundamentally different, potentially dense, patterns of activity.

The degree of MB sparseness was weakly correlated with the total population activity in the OSNs. Although there are clearly gain control mechanisms in the antennal lobe that act to normalize different levels of OSN input (Olsen and Wilson 2008; Root et al. 2008), our results indicate that this process is not complete since net input to the system influences the extent of activity in the MB. Consequently, we examined how robust MB responses were to changes in stimulus intensity. We found that response sparseness was relatively concentration-invariant. Within the concentration range we tested, the proportion of responding KCs remained < 0.2 , much lower than the levels observed in the antennal lobe PNs (Wilson et al. 2004). Interestingly, this upper limit is similar to that observed in piriform cortex (Stettler and Axel 2009).

Using a population imaging approach yielded an unexpected observation: stimulus history had a significant effect on sparseness. It appears that an adaptive process influences sparseness levels, whereby adaptation to strong sensory drive affects subsequent responses to weaker stimuli. When stimuli are presented in a series of increasing concentration steps, sparseness levels in the MB are essentially concentration-invariant. This could be a useful feature for a brain area involved in learning and memory, enabling accurate memory retrieval across a range of concentrations (Masek and Heisenberg 2008; Yarali et al. 2008). Alternatively, this process may play a role in odor localization; when closing in on an odor source, plume hits of increasing concentration would give a constant level of MB activation, but decreasing concentrations would cause a detectable drop in MB responses. This drop could be a signal to begin casting behavior to search again for the plume (Budick and Dickinson 2006; Duistermars et al. 2009).

Many sensory systems appear to be optimized for processing natural stimuli. There are examples in the auditory and visual systems where neurons transmit more information about stimuli with natural statistics than artificial stimuli (Rieke et al. 1995; Machens et al. 2001; Yu et al. 2005; Garcia-Lazaro et al. 2006). The olfactory system has clearly evolved to process naturally occurring smells composed of many compounds. We therefore examined how the complexity of an odor affected the sparseness of MB responses. Using monomolecular odors to study a deeper brain area such as the MB may yield an impoverished view of the cellular response properties, just as our understanding of inferotemporal cortex would be limited if the test stimuli were only spots and bars of light, rather than

meaningful visual objects. Additionally, anatomical evidence suggests that multimolecular blends could be particularly effective stimuli for KCs. PN projections are widely overlapping in the calyx, suggesting that individual KCs receive convergent input from multiple PN types. Thus, KCs could be tuned to detect coincident input from particular combinations of active PNs.

We examined MB responses to a variety of different natural odors, including smells of ripe fruits. At the OSN layer, it is possible to distinguish fruit odors from monomolecular odors when viewed at the population level (Hallem and Carlson 2006). We tested whether this distinction was detectable in the MB population. Interestingly, we found that no aspect of the response to natural smells enabled us to differentiate them from monomolecular odors. Moreover, the sparseness of natural odor representations was indistinguishable from that of monomolecular smells. This likely arises because the responses to individual components in a multicomponent blend are strongly subadditive. Overall, these results indicate that MB representations are not specialized for naturally occurring odors, even though these stimuli drive strong behavioral responses (Stensmyr et al. 2003; Fishilevich et al. 2005; Budick and Dickinson 2006). The indistinguishability of natural and artificial odors reinforces the view that the MB is a purely associative brain center.

Both the functional and anatomical similarities between the antennal lobe and olfactory bulb in mammals are well established and striking. A recent report suggests that the invertebrate MB is phylogenetically homologous to neocortex, based on expression patterns of important developmental genes (Tomer et al. 2010). Using detailed functional imaging, we have shown a striking functional similarity between the mushroom body and earlier reports of piriform cortex (Stettler and Axel 2009). These results suggest that the fundamental feature of olfactory processing at this layer of the system is to create sparse representations in a way that is robust to variation in the features of the olfactory stimulus.

3.6 Acknowledgements

This work was supported by NIH Grant R01 DC010403-01A1. K.S.H is supported by the Crick-Clay Fellowship from the Watson School of Biological Sciences at Cold Spring Harbor Laboratory and a predoctoral training grant (5T32GM065094) from the National Institute of General Medical Sciences, NIH. We are grateful to L. Looger, J. Simpson, and V. Jayaraman for providing the UAS-GCaMP3 strain. We thank V. Jayaraman, J. Dubnau, and Y. Zhong for useful comments on early versions of the

manuscript and E. Gruntman for vigorous statistical discussion. In addition, we have benefited from discussing this work with T. Hige and members of the Zhong and Dubnau Labs. We are grateful to R. Eifert for help building equipment. F. Albeanu, A. Khan, and D. Rinberg provided many useful suggestions about our odor delivery system.

Chapter 4

MB odor responses predict learned olfactory behavior in *Drosophila*

Robert A. A. Campbell*, Kyle S. Honegger*, Hongtao Qin, Wanhe Li, Ebru Demir, and Glenn C. Turner
*K.S.H. and R.A.A.C. contributed equally to this work.

4.1 Abstract

For memories to be useful, they must be both stimulus-specific and generalizable. How do brain areas involved in learning represent stimuli to meet these opposing demands? We address this question in an olfactory learning center in *Drosophila*, the mushroom body (MB), where we image activity of > 100 neurons with cellular resolution, 5% of the total population. We found that both specificity and generalization of olfactory associations are governed by a single feature: the degree of cellular overlap between different odor representations. When representations of two odors were significantly overlapping, an association formed with one odor generalized to a chemically distinct odor. Conversely, the degree of non-overlap predicted how well flies discriminate similar stimuli. We show that a simple discrimination rule exploiting the binary differences between response patterns is sufficient to determine odor identity. These results show how a simple coding scheme could form the basis of accurate but generalizable memory formation.

4.2 Introduction

Memories formed throughout an animal's lifetime need to be used both to respond appropriately to the same stimulus in the future, and to generalize that response to novel, but related stimuli. What is

remarkable is that both specific and general retrieval must be supported by the same memory, since the organism cannot know *a priori* the context in which retrieval will occur. Accordingly, a stimulus must be represented and stored in a way that retains a sense of perceptual distance to other stimuli. Although this aspect of learning and memory is fundamental for driving adaptive behavior, we do not understand how it is achieved in the brain.

We address this question in the relatively simple nervous system of *Drosophila*, focusing on the mushroom body (MB), an area essential for olfactory learning and memory (Heisenberg 2003; Davis 2005; Keene and Waddell 2007). The neural coding of stimulus identity is challenging in the olfactory system, where there is a tremendous diversity of stimuli, which are not related to one another in a systematic manner. The capacity of the olfactory system derives from the large number of different olfactory sensory neurons (OSNs), which are used combinatorially to represent different odors (de Bruyne et al. 1999; Malnic et al. 1999; de Bruyne et al. 2001). OSNs form synapses with projection neurons (PNs), analogs of vertebrate mitral/tufted cells, where the densely combinatorial representations are maintained (Bhandawat et al. 2007; Olsen et al. 2007). PNs project to the mushroom body (MB), which in *Drosophila* is composed of 2000 neurons termed Kenyon cells (KCs) (Lee et al. 1999; Aso et al. 2009). In contrast to earlier layers of the circuit, individual KCs exhibit highly odor-selective (sparse) responses in *Drosophila* (Wang et al. 2004; Murthy et al. 2008; Turner et al. 2008; Honegger et al. 2011), locust (Perez-Orive et al. 2002) and honeybee (Szyszka et al. 2005). Blocking KC synaptic output shows that KC activity is required for olfactory learning and memory (Dubnau et al. 2001; McGuire et al. 2001; Schwaerzel et al. 2002; Krashes et al. 2009). Additionally, functional imaging of KC axons indicates that the output of the MB changes after learning (Yu et al. 2006; Wang et al. 2008; Akalal et al. 2010; Davis 2011). Although these results indicate the MB plays a prominent role in olfactory learning, they do not address how odor identity is represented to produce the stimulus-specificity of learning.

Functional imaging experiments confirm that odors elicit sparse patterns of activity at KCs (Wang et al. 2004; Honegger et al. 2011). Imaging of diffuse activity in the KC somatic region suggested that different odors activate different groups of KCs (Wang et al. 2001). No study has asked, at single-cell resolution, what features of KC population activity convey odor identity. Furthermore, it is not known whether KC activity patterns convey odor identity in a way that reflects the specificity of olfactory learning. Understanding this relationship means recording simultaneously from large numbers of KCs

and linking these measures to behavior.

Our goals for this study were twofold: to determine how odor identity is represented in MB activity patterns, and to uncover how these representations can underlie both the stimulus specificity and generality of olfactory learning. We used two-photon calcium imaging to simultaneously monitor more than 100 KCs, ~5% of the population. The flies' ability to discriminate between, or generalize across, odors was assessed using the well-established T-maze assay for Pavlovian learning (Tully and Quinn 1985). We found that we could use KC activity recorded in naïve animals to predict both the accuracy and generality of olfactory learning in trained animals. Unlike PNs, where spike rate and timing information are important (Friedrich and Laurent 2001; Stopfer et al. 2003; Mazor and Laurent 2005; Broome et al. 2006; Bhandawat et al. 2007), we found that KC response magnitude was dispensable; it was possible to distinguish stimuli as accurately as the animal does using binary response patterns, even when approaching the limit of behavioral discrimination. These results show that relatively simple features of MB activity can provide the appropriate level of stimulus-specificity to olfactory learning.

4.3 Materials and Methods

Animal preparation Flies carrying the genetically encoded calcium sensor UAS-GCaMP3 (Tian et al. 2009) were crossed with OK107-Gal4 (Connolly et al. 1996), to drive GCaMP3 expression in essentially all KCs (Lee et al. 1999; Aso et al. 2009). All experiments were conducted on female F1 heterozygotes from this cross, aged 2-5 days post-eclosion. Procedures for animal preparation were as described previously (Turner et al. 2008; Murthy and Turner 2010). Briefly, flies were anesthetized temporarily on ice and inserted into a small hole cut in the recording platform. The animal's head was tilted forwards, exposing the olfactory organs to the odor delivery nozzle located on the underside of the platform. The fly was fixed in place with fast-drying epoxy (Devcon 5-minute Epoxy). The top of the fly was bathed in oxygenated saline (Wilson et al. 2004) and the cuticle overlying the brain was dissected away. Air sacs overlying the mushroom bodies were pushed aside, but we did not attempt to remove the peri-neural sheath. To minimize movement of the brain inside the head capsule, we removed the pulsatile organ at the neck, as well as the proboscis retractor muscles, which pass over the caudal aspect of the optic lobes.

Odor Delivery The following chemicals were used as stimuli: 2-heptanone (CAS No. 110-43-0), 3-octanol (589-98-0), 6-methyl-5-hepten-2-one (110-93-0), α -humulene (6753-98-6), benzaldehyde (100-52-7), ethyl lactate (97-64-3), ethyl octanoate (106-32-1), hexanal (66-25-1), isoamyl acetate (123-92-2), 4-methylcyclohexanol (589-91-3), methyl octanoate (111-11-5), diethyl succinate (123-25-1), pentanal (110-62-3), and pentyl acetate (628-63-7).

Odors were presented using a custom-built delivery system which uses a series of air dilutions to control odor concentration while maintaining a constant total airflow of 1 L/min. The experiments presented in Figure 4.1 were conducted with an air dilution of 1:100. For later experiments with octanol (oct) and 4-methylcyclohexanol (mch) blends, odor concentrations were adjusted to match concentrations in the T-maze, where odors were diluted 1:1000 in mineral oil. We used a photo-ionization detector (PID, Aurora Scientific) to match concentrations between the imaging rig and the T-maze, and to monitor odor delivery throughout each experiment. Odor pulses were created by switching between clean and odorized air streams using a synchronous two-way valve. This final valve was located about 50 cm from the fly, leading to a delay of roughly 300 ms between valve switching and the odor reaching the fly. The flow path was 1/8" diameter throughout, which enabled the system to work near to atmospheric pressure at these flow rates. This virtually eliminated pressure transients caused by valve switching, as measured by PID and hot-wire anemometer.

Calcium Imaging Two-photon imaging was carried out using a Prairie Ultima system (Prairie Technologies) and a Chameleon Ti-Sapphire laser (Chameleon XR, Coherent Inc.) tuned to 920 nm, delivering 8 to 10 mW at the sample. All images were acquired with Olympus water immersion objectives (LUMPlanFI/IR, 60X, numerical aperture (NA) 0.9 and LUMPlanFI/IR, 40X, NA 0.8). Imaging planes were selected so as to maximize the number of visible KCs. Typically they were around 300x300 pixels, acquired with a pixel dwell time of 1.6 μ s, yielding frame rates near 3.8 Hz. On average ~120 KCs (range: 65 to 168 KCs) were monitored in one plane.

Custom MATLAB (The MathWorks) routines were used to control odor presentation and synchronize stimulus delivery with data acquisition. Data were acquired in 20 s sweeps with a 1 s odor pulse triggered 8 s following sweep onset. The inter-stimulus interval was 25 s. Stimuli were presented in randomized odor blocks. The same odor was never presented twice in succession.

Data Analysis Data were analyzed using MATLAB and R (<http://www.R-project.org>). To correct for motion within the field of view, we aligned frames using a sub-pixel translational-based discrete Fourier analysis (Guizar-Sicairos et al. 2008). To quantify the noise in the acquired images, we automatically segmented fluorescent neural tissue from the surrounding regions. Pixel intensity values from the area outside this boundary were considered to represent background (tissue autofluorescence plus shot noise), and the mean pixel intensity value from the background was then subtracted from the overall image.

To quantify the response of the KCs, we applied a small circular region of interest (ROI), 6 to 8 pixels in diameter, to each cell body. This allowed us to average the pixel intensity values from each cell and treat them as a unit. Care was taken to ensure that each selected cell remained within its ROI over the whole imaging session. Response amplitudes were calculated as the mean change in dF/F in the 0.5 s to 4.5 s window following stimulus onset.

We used a statistical test, originally described in Honegger et al. (2011), to determine whether a KC responded significantly on a given trial. We first obtained the standard deviation (SD) of the baseline activity 8 seconds prior to stimulus onset. The response timecourse was then smoothed using a 5-point running average to control for outliers. The peak dF/F in the 0.5 s to 4.5 s window following stimulus onset was determined. The response was judged to be significant if this peak was 2.33 SDs greater than the baseline; this corresponds to a one-tailed significance test where $\alpha < 0.01$.

Odor Classification We employed classification algorithms to predict odor identity based upon neural population activity (the mean evoke dF/F values on each trial). All algorithms were implemented using leave-one-out cross-validation to avoid over-fitting. One trial is withheld and the model is fitted to the remaining data (the training set). The model is then used to predict the odor eliciting the evoked KC responses of the withheld trial (the test set). The procedure is repeated for each trial in turn. Classification accuracy fell to chance levels when odor labels are randomized.

In most cases we used discriminant analysis to fit a linear classification boundary between each odor pair (Venables and Ripley 1999). We chose this approach because it is well established (Fisher 1936), can in theory be implemented neurally simply by summing and thresholding, and, along with similar Euclidean-distance based approaches, has been commonly used both within olfactory neuro-

science (e.g. MacLeod et al. 1998; Friedrich and Laurent 2001; Bhandawat et al. 2007; Cury and Uchida 2010) and in other areas of systems neuroscience (e.g. Briggman et al. 2005; Hung et al. 2005; Walker et al. 2008). These models required an initial dimensionality reduction step since, in order to avoid over-fitting, there must be fewer input variables (neurons) than observations (odor presentation trials). We used principal components analysis (PCA) for dimensionality reduction. Fitting a model using more components increases the number of degrees of freedom and so increases classification accuracy. However, due to our use of cross-validation, beyond a certain number of components classification accuracy begins to drop. This occurs because higher-order PCs capture mostly noise, which is independent between training and test tests. Hence, higher-order models yield increasingly bad predictions for the identity of the test pattern. Classification accuracy peaks at a slightly different number of PCs for each animal, so some rational way of selecting the dimensionality of the model is needed. Choosing the optimal dimensionality for each fly in turn (which ranged between 6 and 15 PCs) is too aggressive since it runs the risk of even random data apparently classifying at above chance levels. Therefore, to avoid over-fitting, we chose the dimensionality which led to the highest average classification accuracy over all animals (see Results for specifics). For more detail on applying discriminant analysis to neural data see the supplementary material of Briggman et al. (2005); Campbell et al. (2008).

To create neurometric functions describing neural discriminability for the oct:mch blend stimuli (Figure 4.4), we used both discriminant analysis and a perceptron. The perceptron neural network was initialized with a random vector of small synaptic weights and a small bias term. Weights were then adjusted iteratively using the perceptron learning algorithm until all training trials were classified correctly. The final weight vector and bias term were used to classify the withheld trial. Classification accuracies are reported as the mean of 100 repeats of this procedure.

Behavioral Experiments Behavioral experiments were done using the T-maze olfactory learning paradigm (Tully and Quinn 1985) with the 2202U fly strain (Blum et al. 2009). Groups of approximately 100 flies were loaded into an electrifiable chamber, where odor presentation was paired with shock (twelve 60 V stimuli of 1.5 s duration presented over a period of one minute). Flies were then lowered to a choice point at the junction of two odorized chambers, each containing a different odor. Two conditioning protocols were used.

Generalization Protocol (Figure 4.3): This protocol involved pairing shock with a single odor and then directly giving flies a choice between different odors. We used a yoked design with two sets of flies run through the T-maze in succession: an experimental group that received shock in the presence of an odor, and a control group that simply received odor exposure without shock. This second group of flies established how flies distributed between the choice odors under control conditions. We compared the odor choices of trained flies to this control distribution to establish whether training modified their choices. For generalization, flies were trained with one odor, and then given a choice between two odors they had not experienced previously, one of which was predicted to be similar to the trained odor (Figure 4.3C-D). We also confirmed that flies could distinguish similar odors by training flies with one odor and testing their choice between that stimulus and a similar odor (Figure 4.3A-B).

Discrimination Protocol (Figure 4.4): Flies were presented one odor paired with shock (CS+), followed by presentation of a second odor in the absence of shock (CS-). They were then given a choice between the two odors experienced during the training phase. We quantified performance as the proportion of flies correctly avoiding the odor previously paired with shock. In these experiments, odor concentrations were set so that naïve flies distributed evenly between the two choices, so chance performance was 50%. A balanced experimental design was used where, for a pair of odors, one group of flies was trained to avoid one odor, and a separate group of flies was trained to avoid the other. For example, with the 70:30 blends, one half of the reciprocal design constituted shocking one group of flies in the presence of 70 oct : 30 mch and then exposing them to 30 oct : 70 mch without shock. These flies were then given a choice between these two blends. In the other phase of the reciprocal, a different set of flies was shocked in the presence of 30 oct : 70 mch, then exposed to 70 oct : 30 mch, and then given the same choice in the testing phase. The mean of the scores from the two halves of the reciprocal constituted a single data point in Figure 4.4B; performance was very similar for the reciprocal tests.

4.4 Results

Previous work indicates that associative conditioning can induce plasticity in the axonal output regions of the MB (Yu et al. 2006; Wang et al. 2008; Akalal et al. 2010; Davis 2011), however the basis for the stimulus-specificity of olfactory associations remains an open question. Physiological recordings show

that odors induce sparse activation of the KC population (Perez-Orive et al. 2002; Wang et al. 2004; Turner et al. 2008; Honegger et al. 2011). Here we use the calcium indicator GCaMP3 (Tian et al. 2009) and two-photon imaging to ask whether performance in a learning-related task can be predicted from the KC odor code, and to test what features of the KC population response encode odor identity. Can mushroom body activity predict how flies will generalize an association and the degree to which flies can learn to discriminate similar stimuli?

4.4.1 Odor identity is represented by unique KC activity patterns

To test whether activity patterns in the KC population convey odor identity reliably and precisely, we first examined population responses to a variety of different monomolecular compounds. To obtain a population-level view of MB representations, we targeted expression of GCaMP3 to the MB using the Gal4 driver OK107, which expresses in the entire population of ~2000 KCs (Lee et al. 1999; Aso et al. 2009). Individual KC somata were readily identified based on the resting fluorescence of the indicator, enabling us to track responses with cellular resolution. To maximize the number of KCs that can be imaged simultaneously, we oriented the preparation so that the imaging plane was parallel with the disc-shaped field of KC somata. In a single imaging plane, we typically captured > 120 KCs (range: 65 to 168), roughly 5% of the total population.

We detected strong, reliable, odor-evoked fluorescence changes in individual KCs (Figure 4.1A). Within a fly, the spatial pattern of evoked dF/F was reliably different between odors, and repeatable across presentations of the same odor. In the experiment shown in Figure 4.1, we identified 124 KCs in a single imaging plane, extracting responses on a cell-by-cell basis. Figure 4.1B shows response time courses corresponding to the cellular activation patterns depicted in Figure 4.1A. Qualitatively, the responses of individual neurons were fairly consistent across different presentations of the same odor. To summarize the responses to all 7 odors across all trials we quantified response amplitudes by averaging the fluorescence change (dF/F) in a 4 s window following stimulus onset. Figure 4.1C shows the responses observed in these cells to the 42 different stimulus presentations (7 different odors presented 6 times each in a randomized order; repeated presentations of the same stimulus are grouped for display. Across the dataset of 7 animals we show here, 6 repeats were obtained in 3 cases, 5 repeats in 1 case, and 4 repeats in the remaining 3 cases). The rows represent trials and the columns represent cells. Each

colored “square” is the mean evoked response of one cell on one trial, so a row represents the activity of the KC population on one trial. Taken together, the matrix indicates how distinct responses are to different odors, as well as how much variability there is between different responses to the same odor. This is important biologically because animals must make decisions based upon neural activity from a single trial. Identifying an odor accurately relies on two factors: low variability between responses to the same odor, and reliable differences between responses to different odors.

We set out to statistically quantify how much information there is about odor identity in the KC response patterns. To achieve this, we performed discriminant analysis, a classical technique related to ANOVA (see Methods for details) on the evoked dF/F responses (e.g. Figure 4.1C). This approach allowed us to assess, on a trial-by-trial basis, which stimulus was most likely to produce an observed pattern of population activity, and therefore how accurately KC response patterns convey odor identity. Fitting the classifier is straightforward. All responses to the same odor constitute a “group” and the goal of discriminant analysis is to obtain the best linear separation of each group from every other. This is achieved by finding the so-called linear discriminant (LD) directions which best separate each pair of groups. The direction of each LD is specified by N coefficients, corresponding to the N variables, or dimensions, with which the data were defined. In our case, the variables correspond to the evoked dF/F of each cell and the groups to the presented odors. However, since there are many more variables (cells) than observations (trials), dimensionality must first be reduced to avoid over-fitting. We used principal components analysis (PCA) for dimensionality reduction. The analyses shown in Figures 4.1D&E were conducted using 8 principal components, which on average explain 84% of the variance ($1SD = 4.3\%$). We chose this number of components because it yielded the highest average classification accuracy over all recordings (see Methods for further details). We ran the model fitting and prediction using leave-one-out cross-validation. One trial was withheld and the model fitted to the remaining data. This model was then used to infer the identity of the odor eliciting the responses in the withheld trial. The process was repeated for each trial in turn.

Using this approach, we can identify which trials were accurately classified and also the way in which misclassifications occur. An example of these results are displayed in Figure 4.1D in the form of a confusion matrix. Squares along the diagonal represent correct classifications. The digits indicate the number of trials (out of 6) which were classified correctly. Misclassifications are indicated by non-black tiles situated off the diagonal. Since we extensively sampled KCs from individual flies, we did not

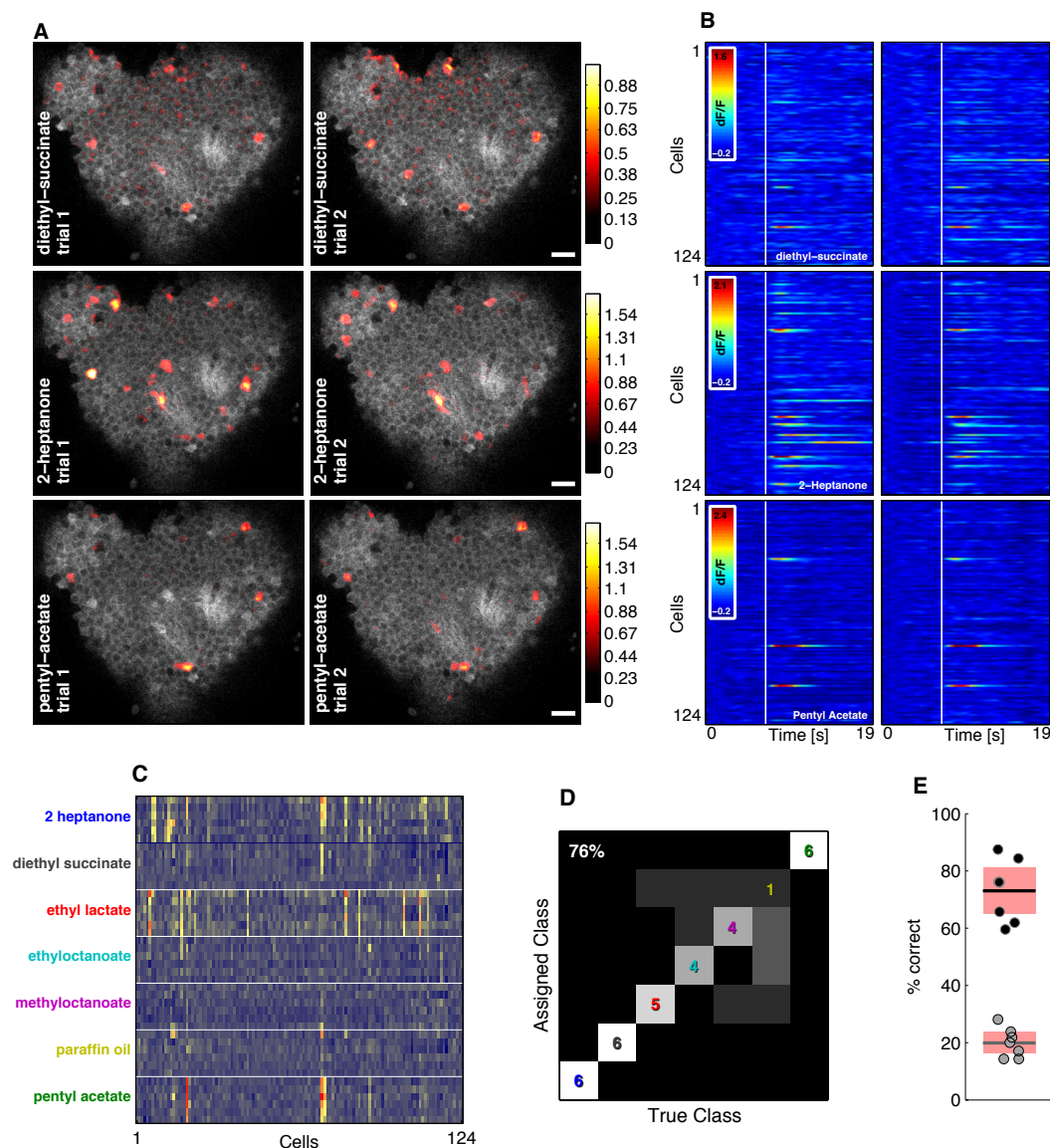


Figure 4.1: Two-photon calcium imaging demonstrates that MB population activity accurately conveys odor identity. **A**, Odor response patterns in the cell body layer of the MB. dF/F responses (colorbar) are shown overlaid on baseline fluorescence (grayscale). The different panels show the responses to 2 presentations of 3 different odors. Scale bar: $10\ \mu\text{m}$. **B**, dF/F timecourses of 124 KCs extracted from the data shown in the images in **A**. The white line indicates the onset of a 1 s odor pulse. **C**, Mean evoked dF/F responses of the KC population (columns) to individual odor presentations (rows), showing reliable, distinct responses to different odors. **D**, Confusion matrix showing odor classification assignments by discriminant analysis (see Methods) for one animal. For some odors, the classifier performs correctly on 6 of 6 trials. Overall classification accuracy across the entire stimulus set was 76%. Colors correspond to odor labels in **C**. **E**, Overall classification accuracy is consistently high in different flies (black points; $n = 7$). The classifier performs at chance when cell identity is randomized independently on each trial (gray points). Bars indicate means, and boxes represent 95% confidence intervals for the mean.

pool recordings across animals. Pooling can alter classification accuracy, since it assumes that signals from different neurons are statistically independent and therefore add linearly to the total amount of information (Averbeck et al. 2006). For the fly shown in Figure 4.1A-C, overall classification accuracy across all stimuli was 76% (Figure 4.1D), with similar accuracy obtained in other flies (black points, Figure 4.1E). These results are important because they are the first quantification of how accurately the KC population conveys odor identity. Furthermore, classification accuracy approached chance levels when we randomized the cell labels on each trial (gray points, Figure 4.1E), indicating that knowing the pattern of responding KCs is critical for accurate classification. Thus, despite the fact that individual KCs respond to few odors and only a small proportion of KCs respond to any given odor, at the population level, KC response patterns represent odor identity with a high level of specificity. If the patterns of activity in the MB reflect odor identity, we should be able to use those patterns to predict the odor choices of flies that were trained to form olfactory associations, a proposal we examined next.

4.4.2 MB activity predicts generalization of olfactory associations

We have shown that there is substantial information on odor identity in MB responses. Is it possible to use MB activity patterns to predict behavior? Specifically, can we use MB response patterns to predict whether flies that have formed an association with one particular odor will generalize that association to a new odor they have not experienced before? We searched our neural data for a trio of chemically distinct odors, two having similar activity patterns to one another with the third eliciting activity unrelated to the similar odor pair. We identified a set of odors matching these criteria: 2-heptanone (HP) and pentyl acetate (PA), which share similar response patterns, and ethyl lactate (EL) which evokes a pattern distinct from the other two. Will flies generalize across HP and PA?

The odors HP and PA evoked similar response patterns in the MB, in the sense that they activate similar subsets of KCs. This is shown in two examples from different animals (Figure 4.2A&B and 4.2E&F). In contrast, the third odor (EL, Figure 4.2C&G) evoked a relatively distinct KC response pattern. The evoked activity in each image is an average of all repeats of the same odor ($n = 4$ for the upper row and $n = 6$ for the lower row). To show the variability in the responses we can plot the data along the first two linear discriminant (LD) directions (Figure 4.2D&H). Each data point represents the

population response to a single odor presentation trial, the colors correspond to odor identity and match colors used in previous figures. The spread of the data points indicates the variability of responses across trials. The lack of overlap between the different groups of points indicates that these three odors should be reliably distinguishable from each other based on the neural activity.

We quantified the separability of MB responses to these three odors using discriminant analysis. We calculated the proportion of correct classifications for these odors alone (Figure 4.2I). This was done by restricting the “true class” (see Figure 4.1D) to only these three odors but leaving the “assigned class” possibilities open to the entire set of 7 odors in our test panel. This is a conservative approach, since misclassifications to any odor in our data set were allowed. Classification accuracy was over 90% (Figure 4.2I) for all 7 animals in this data set, indicating that all three odors are reliably distinguishable from one another. Note that classification accuracy does not reveal which activity patterns are similar to one another. Indeed, we see from Figures 4.1 and 4.2 that there is substantial overlap between activity patterns of several odors that are readily discriminated by the classifier.

We quantified the similarity between the activity patterns using two different measures: the correlation coefficient, and the number of neurons that respond uniquely to only one of the two stimuli. Averaging the KC activity patterns (rows in Figure 4.1C) across all presentations of each odor yields the mean evoked activity pattern for that odor. The similarity between two mean activity patterns can be represented by their correlation coefficient. The correlation coefficients measured for each pairwise combination of these odors are shown in Figure 4.2J. The similar odor pair (HP:PA) has R values significantly greater than both HP:EL ($t_{(11)} = 4.1, p = 0.002$) and PA:EL ($t_{(11)} = 5.1, p < 0.001$). There is no significant difference between the HP:EL and PA:EL distributions ($t_{(10)} = 1.2, p = 0.25$). This suggests that an association formed with HP may generalize to PA, and vice versa. We also evaluated similarity of response patterns by assessing the proportion of neurons responding uniquely to only one odor (Figure 4.2K). For a cell to be classed as responding uniquely to odor A and not odor B it must exhibit significant (see Methods) responses to A on either every trial or every trial but one, and not respond at all to odor B. By this measure, the HP:PA odor pair has significantly more overlapping response patterns than both HP:EL ($t_{(11)} = -3.7, p = 0.003$) and PA:EL ($t_{(11)} = -4.8, p < 0.001$), whereas there is no significant difference between the HP:EL and PA:EL distributions ($t_{(10)} = 0.35, p = 0.74$). Thus both types of analysis (Figures 4.2J&K) show that the odors HP and PA evoke response patterns that are more similar to one another, than to EL. Based upon the neural activity we can make two predictions. Firstly,

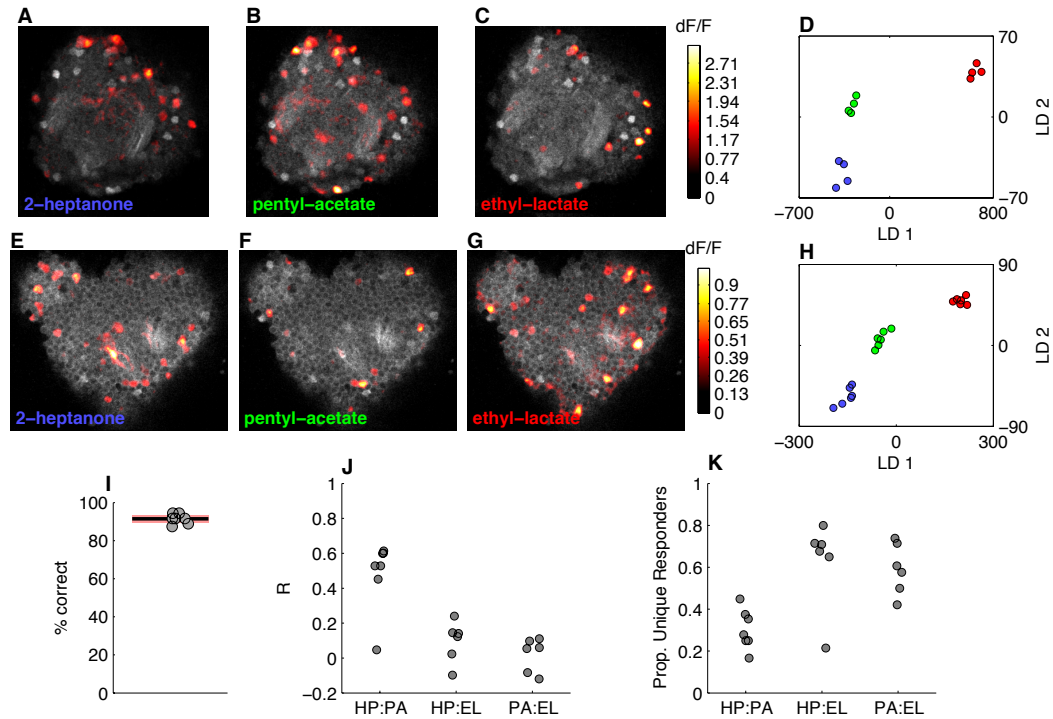


Figure 4.2: Using MB activity patterns to identify candidate odors for generalization. A-C, Mean evoked responses to three different odors with different functional groups. Population responses to 2-heptanone (HP) and pentyl acetate (PA) appear similar to each other and different from ethyl lactate (EL). D, The mean evoked KC responses plotted along the first linear discriminant directions. Each point represents the population response to a different odor presentation trial, colors code odor identity as in A-C. E-H, The same as A-D but for a different animal, in this case with 6 presentations of each stimulus. I, Classification of these three odors by discriminant analysis performs > 90% on average ($n = 7$ flies). J, Response pattern similarity quantified using the correlation coefficient between mean evoked activity patterns for different odor pairs. Response patterns to HP and PA are significantly more correlated with each other than either are to the pattern evoked by EL. Each point represents data from a different fly. K, Similarity between response patterns represented as the number of uniquely responding neurons (see main text) for each odor pair.

the high classification accuracy indicates that flies will readily be able to discriminate even the similar odors from each other. Secondly, associations formed with HP will generalize to PA, and vice versa. Note that we made these predictions strictly by examining neural activity - chemically these odors have different functional groups and are clearly distinct.

We tested these predictions using the T-maze Pavlovian olfactory learning paradigm (Tully and Quinn 1985), a well-studied task which is known to be MB-dependent (de Belle and Heisenberg 1994; Dubnau et al. 2001; McGuire et al. 2001). Groups of ~100 flies were trained to associate one odor (the conditioned stimulus: CS+) with electric shock (the unconditioned stimulus: US), and were then given the choice between the CS+ and another test odor (see Methods for details). The resulting distribution of the flies' choices was compared with how flies distributed when they were not exposed to shock. This comparison revealed how much the shock training modified the flies' innate odor preference. This training regimen is different from the standard discriminative training paradigm, where flies are first shocked in the presence of one odor and then exposed to a second odor in the absence of shock. Since our goal in this series of experiments was to study generalization, we did not include the second phase of training where flies could potentially learn that the second odor (the CS-) is 'safe.' Indeed, previous experiments indicate that the CS- is dispensable for forming associations (Masek and Heisenberg 2008). Our approach, which measures the degree to which innate odor preferences are modified by shock, enabled us to examine behavioral responses to odors presented at the 1:100 concentration used in imaging experiments, without correcting for the innate attractiveness or aversion of the different odors. This approach (also known as the Δ PI method) has been used previously in studies of long-term memory (Yu et al. 2006; Akalal et al. 2011).

We first tested whether flies could distinguish the two similar odors, PA and HP. We found that flies readily learned to discriminate these stimuli, with shock significantly modifying innate avoidance (Figures 4.3A&B). We then tested the prediction that flies generalized between PA and HP. We trained flies by pairing HP with shock and then asked flies to choose between PA and EL. If, as predicted, the flies perceive PA as being similar to the shock-paired odor (HP), then flies should generalize the association and increase their avoidance of PA. Alternatively, if all three odors are perceptually unrelated to one another, the association will not transfer and odor preferences will not change. Our results clearly show that flies generalize the aversive association formed with HP to PA (Figure 4.3C). Similar results were obtained with the reciprocal experiment, in which PA was paired with shock and flies chose

between HP and EL (Figure 4.3D). These results show that the MB response patterns observed in naïve animals can successfully predict how trained flies will generalize between chemically distinct odors in a learning task. Using patterns of neural activity is the only way of making such a prediction, since the perceptual relationship between different monomolecular odors is notoriously unpredictable when based on chemical structure (Arzi and Sobel 2011).

4.4.3 Probing olfactory discrimination using odor blends

The generalization experiments showed that perceptual similarity between readily discriminable odors is related to the degree of overlap in their MB representations. This raises the question: how much must two odor representations overlap in order for them to become indistinguishable? In other words, how different do two stimulus representations have to be in order to be perceived as distinct? Answering this question provides insight into the features of the neural activity patterns relevant to the animal. Experiments in other systems have addressed this issue using two-component odor mixtures, which make it possible to smoothly adjust the difficulty of a discrimination by controlling the relative levels of the two constituents in the blend (Uchida and Mainen 2003; Fernandez et al. 2009).

We tested odor discrimination using a series of two-component odor blends, made by systematically varying the ratio of the constituents: 3-octanol and 4-methylcyclohexanol (oct and mch, see Figure 4.4A). We chose this odor pair because it has been used extensively in the fly learning and memory literature (Tully and Quinn 1985; Yu et al. 2005; Thum et al. 2007), and it is well known that flies can discriminate these pure odors with high accuracy. Using stimuli where these two odors are blended together in different ratios, we were able to construct a psychometric function describing the flies' odor discrimination capabilities. We again used the T-maze to determine how accurately flies can distinguish these blends. Here we used the traditional discriminative training protocol, in which flies were shocked in the presence of one odor (CS+), then exposed to the second odor (CS-) in the absence of shock, before being given a choice between the two stimuli. Performance at the task was quantified as the proportion of flies correctly avoiding the stimulus previously paired with shock. Pure odors were diluted in mineral oil and delivered at a nominal concentration of about 1:1000. The actual concentrations were adjusted slightly so that so each pure odor evoked an equal innate response (mch was delivered at 1.5:1000 and

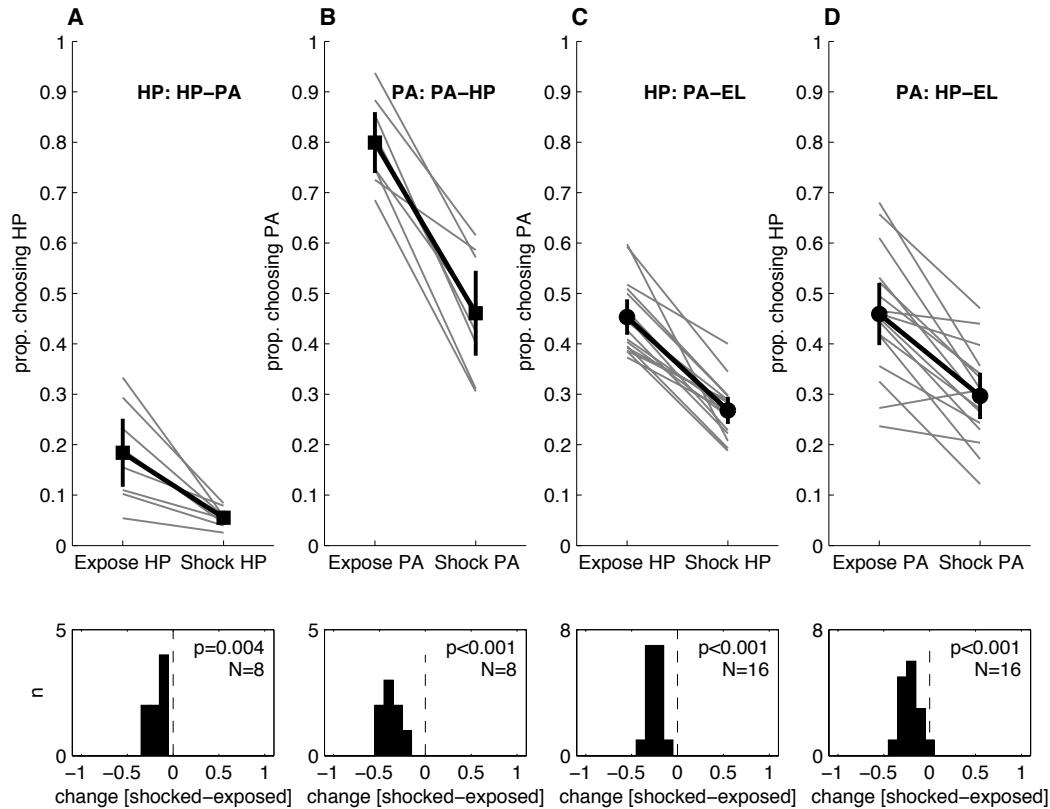


Figure 4.3: Behavioral generalization across odors. **A**, Flies were trained to avoid HP (2-heptanone; labels identical to those in Figure 4.2 and then tested on their choice between HP and PA (pentyl acetate). Control flies were merely exposed to HP without shock and then tested. The shock group constituted a different group of flies, trained and tested immediately after the control group, forming a yoked pair. Gray lines link these yoked pairs, black line represents mean across yoked pairs, bars indicate the 95% confidence interval of the mean. In each case training decreased the proportion of flies choosing HP. Although flies are initially biased against HP, the mean proportion choosing this odor drops from 0.2 to 0.05, indicating that they can effectively discriminate these two odors. Lower panel shows the distribution of the change in avoidance for each yoked pair. The p-values are derived from a t-test of the null hypothesis that the distribution of difference values has a mean of zero. **B**, As in **A** except odor PA is paired with shock. **C**, Odor HP is paired with shock and flies are given the choice between the similar odor, PA, and dissimilar odor, EL (ethyl lactate). The association with HP generalizes to PA, as fewer flies choose this odor following training. **D**, As in **C**, but showing generalization of the association formed with odor PA to tested odor HP, as predicted by the MB activity patterns.

oct at 1:1000). Odor blends were made by mixing these two oil dilutions at the desired ratios. Each group of flies was trained on one of three different odor blend ratios: 100:0, 70:30 or 60:40 (see Figure 4.4A). We assayed discrimination used a balanced experimental design. For example at the 60:40 ratio, one group of flies was trained to avoid 60 oct : 40 mch, and a second group of flies was trained to avoid 40 oct : 60 mch; each group was then tested on the choice between 60 oct : 40 mch and 40 oct : 60 mch. The mean of the two scores is treated as a single independent observation, so the choices of approximately 200 flies comprise each data point. Flies performed close to 100% correct for the pure odor pair (Figure 4.4B) with performance falling to just above chance for the 60:40 blend pair. Thus, using these stimuli we are able to systematically vary the difficulty of odor discrimination, with the 60:40 blends approaching the limit of the flies' discrimination capabilities.

4.4.4 KC activity predicts accuracy of learned odor discrimination

To quantify how accurately it is possible to discriminate odor blends based on patterns of MB activity, we presented the blend stimuli to naïve flies and examined how accurately they could be classified using discriminant analysis. Using this approach, we derived a classification accuracy value for each pair of the odor blends (the number of stimulus repetitions (n) varied between 5 and 8: $n = 5$ for 7 flies, $n = 6$ for 2 flies, $n = 7$ for 1 fly, $n = 8$ for 1 fly). This allowed us to construct a neurometric curve for odor discriminability (Figure 4.4C). Classification accuracy followed the same trend as the behavioral data: it was close to 100% for the pure odor pair but decreases as the blend pairs become more similar. In general, the variance of the behavioral data was lower since each data point was based on the odor choices made by approximately 200 flies, while for the neurometric data, each point was based on the MB response patterns in an individual fly. The discriminant analysis performed about 15% better on average than the animals' behavior. A more elaborate classification algorithm, capable of generating curved decision boundaries (SVM; Hamel 2009), produced almost identical results (data not shown). These results indicate that the KC population conveys sufficient information about odor identity to account for the behavioral responses of the animal. In fact, the performance of the classifier tended to be slightly higher than the behavioral performance of the flies. This may reflect the fact that information from the MB must pass through additional synapses before reaching the motor output, and

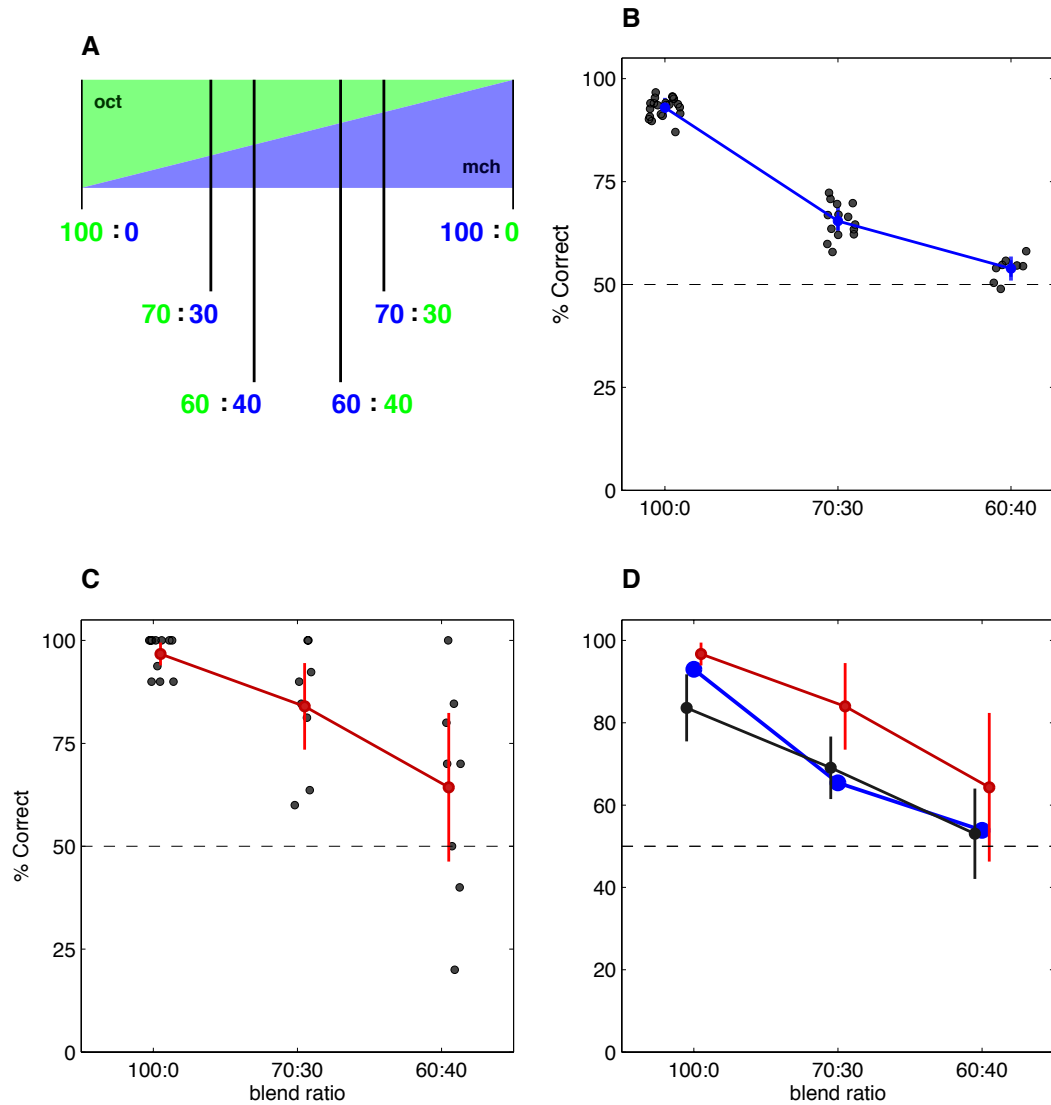


Figure 4.4: Psychometric and neurometric measures of learned olfactory discrimination. **A**, Increasingly similar odors were constructed by blending 3-octanol (oct) and 4-methylcyclohexanol (mch) over three pairs of increasingly similar blend ratios. **B**, Accuracy of olfactory learning. Flies accurately learn to discriminate pure oct from pure mch (100:0), but do progressively worse with blends of the two odors (70:30 and 60:40). Training on the more similar blend (60:40) produces performance just above chance. Bars represent 95% confidence interval of the mean. **C**, Discriminant classification accuracy of MB responses to different odor blends. Each point is the classification accuracy derived from a single fly recording. **D**, Performance of both the discriminant analysis (red) and the perceptron (black) match the trend of the behavioral data (blue).

downstream neurons are likely less than perfect at extracting that information. However it should be noted that the synaptic pathway from the antennal lobe PNs to motor output via the lateral horn is only two synapses (Ruta et al. 2010). If the route via the MB is similarly short, there may be little opportunity for information loss beyond the MB.

We next examined whether these patterns could be used to accurately identify odors by a non-optimal but biologically plausible classifier. Discriminant analysis sets classification boundaries based on estimating the mean and variance of odor responses over many trials. In contrast, artificial neural networks can be trained to classify data simply by iteratively changing the synaptic weights of connected units in the model. Although neural networks are more biologically realistic, they are not guaranteed to find the optimal solution to a classification problem. Perceptrons are class of neural networks which, like the discriminant analysis, solve linear classification problems (Hastie et al. 2009). Using the data from each fly, we constructed an artificial network with one input layer of units representing KC responses, connected to a unit in the output layer. We then asked whether, using the population responses recorded on individual odor presentation trials, we could adjust the synaptic weights of the inputs to obtain an odor-specific response in the output layer. As before, we trained the network using a drop-one-out approach, adjusting synaptic weights using all KC odor responses save the trial of interest, and then testing whether the network responded appropriately to the remaining odor presentation. The perceptron performed about 15% lower on average than the discriminant analysis, but the corresponding neurometric curve closely matched the behavioral results (Figure 4.4D).

An important factor that will influence the neurometric function is the size of the neuronal population analyzed. To evaluate the impact of population size on classification accuracy, we trained the perceptron using random subsamples of the KCs recorded in each fly. For a subpopulation of n cells, we drew 50 random subsamples and evaluated performance for each. This allowed us to derive a mean odor classification accuracy for each subpopulation of size n . We found that, for the pure odors, accuracy asymptotes at around $n = 25$ neurons (Figure 4.5A). Similar results are found for the 70:30 and 60:40 blends, where classifier performance saturates with subpopulations of 30 neurons (Figure 4.5B-C). Thus, despite the sparseness of KC responses, for this discrimination task, a relatively small subset of the KCs is capable of accurately conveying odor identity, and performance saturates at far fewer neurons than we typically sample in our imaging experiments. Downstream neurons have rather extensive dendritic arbors (Ito et al. 1998; Tanaka et al. 2008) and likely pool inputs from at least

this number of KCs, suggesting that this information could readily be transmitted to the next layer of the circuit. These results show that the odor identity information we extract from the KC population closely matches behavioral performance, even with stimuli that are close to the animal's behavioral discrimination limit.

4.4.5 A binary code for odor identity in the MB

Finally, we examined how different features of the KC response patterns contribute to the stimulus-specificity of learning. In *Drosophila*, KCs respond to odor with a brief volley of spikes against a background of little or no spontaneous firing, and there is no evidence of temporal patterning of responses (Murthy et al. 2008; Turner et al. 2008). We therefore focused on whether odor identity information is carried by the response amplitude of each cell, an analog code, or simply by the presence or absence of a response, a binary code. Our approach was to compare how effectively analog and binary KC response patterns could be used to train a classifier. First, we determined whether each KC responded significantly on each trial (see Methods). Figure 4.6 A and B show KC response patterns from two different animals from experiments in which we presented the pure odors, the 70:30 blends, and the 60:40 blends. In panels Ai and Bi, non-significant KC responses are set to zero, creating a thresholded view of activity patterns that retains analog response amplitude values. We noticed that individual KCs tended to respond to only one odor of the pair, which suggests that response amplitude may contribute little to determining odor identity. To explore this further, we binarized the response matrix, representing KC activity as either responding or non-responding for each trial (Figure 4.6Aii and Bii). Red is used to denote neurons which responded uniquely to one of the odors of a blend pair. For example, in the case of pure oct and pure mch, a cell responding on every trial (or every trial but one) to mch and never to oct would be considered a unique responder to mch. Across all flies, the proportion of neurons that responded uniquely to one odor within each blend pair decreased as the blends became more similar to one another (Figure 4.6C). This trend is also seen in the two example flies (Figure 4.6Aii and Bii). We also quantified the similarity between responses using the correlation coefficient (R) between the mean evoked activity patterns (Figure 4.6D). Both of these measures indicate that the pure odors show the least similarity and overlap while the 60:40 blends display the highest similarity and overlap.

We next tested whether binarizing the neural responses resulted in a loss of information content. We did this by using the thresholded and binarized response patterns to train a perceptron-based classifier. In both patterns, cells that do not respond significantly might be a source of noise during classification, so we set them to zero (as in Figure 4.6Ai and Bi). This controls for the possibility that the binary patterns are more informative because of a reduction in the noise contributed by non-responding cells. This enabled us to directly compare performance based on patterns that differ only by whether response magnitudes took analog or binary values. We found that classification accuracy was indistinguishable when either analog or binary input patterns were used to train the network (Figure 4.6E). A mixed effects ANOVA showed there was a significant effect of blend ratio ($F_{(2,38)} = 38, p < 0.001$) but no main effect of binarization ($F_{(1,38)} = 1.4, p = 0.24$) nor any interaction between binarization and concentration ($F_{(2,38)} = 1.1, p = 0.33$). Identical results were obtained with discriminant analysis (data not shown). Thus, response amplitude provided no additional information about odor identity and a binary view of KC responses is sufficient to explain behavioral performance in this task.

These results indicate that odor-specific information carried by the KC population is represented in a simple fashion: a binary code is no less informative than an analogue code, linear (integrate and threshold) models and the overlap between different population responses are sufficient to describe the stimulus-specificity of learned olfactory behavior.

4.5 Discussion

In what way do brain areas involved in learning and memory represent stimuli with distinct patterns of neural activity? We examined this question using functional imaging of the *Drosophila* MB, a brain area essential for olfactory learning and memory. Tracking the activity of ~100 KCs simultaneously enabled us to assess which features of those activity patterns were meaningful to the animal on a behavioral level.

4.5.1 MB odor representations in naïve animals predict learned behavior

Relatively few studies have linked neural activity patterns to behavioral measures of odor-specificity. In the mammalian olfactory bulb, spike timing in mitral/tufted cells conveyed information about odor identity in a way that is correlated with reaction time on an odor discrimination task (Cury and Uchida 2010). In the honeybee antennal lobe, there is a good correspondence between the similarity of different odor-evoked activity patterns and how similarly odors are perceived (Guerrieri et al. 2005). Although associative plasticity is thought to occur in the MB (Davis 2011; Cassenaer and Laurent 2012), much less is known about the representation of odor identity. In particular, population coding of odor identity and its link to behavior have not been explored. We note that the correlations we observe between naïve MB activity and learned behavior could potentially be observed in the OSN or PN population, as these earlier stages must contain an equal or greater amount of information about odor identity. We chose to focus on the MB because its odor code has not been well studied with respect to behavior, and because the stimulus-specificity of olfactory learning is a MB-dependent behavior.

The first work to image *Drosophila* KCs demonstrated that different odors activate different subsets of neurons (Wang et al. 2001, 2004). Individual MB neurons exhibit highly selective and sparse odor responses (Murthy et al. 2008; Turner et al. 2008), which are distributed widely throughout the cell body region (Honegger et al. 2011). This format of odor representations might be useful for learning since, compared to dense representations, sparse representations of different odors tend to be less overlapping. Theoretical work has suggested that the degree of overlap between stimulus representations in naïve animals could affect the specificity of subsequent learning; the more overlapping two representations are, the more difficult it might be for synaptic changes to be specific to one stimulus (Marr 1969; Kanerva 1988; Földiák and Young 1995).

Our large scale imaging approach enabled us to directly visualize the degree of overlap between different odor representations, and explore the behavioral consequences of this overlap. We used two separate approaches to explore how MB activity relates to behavior. First, we predicted generalization behavior of three chemically distinct odors based solely on the MB activity patterns observed in untrained animals. Second, we used a series of morphing odor blends to measure the flies' ability to discriminate similar odors and demonstrate that this could be predicted based on the KC activity patterns. Furthermore, no more than about 30 neurons were needed for our perceptron-based model network to

match behavioral performance in our task. Adding more neurons did not significantly improve classification accuracy. It is likely that this information can be read out by downstream neurons, which sample at least this many cells. This suggests that the sampling of the KC population we achieve with imaging may predict quite well the amount of information that can be transmitted to the next layer of the biological circuit, and ultimately guide behavior.

How does the neural code in the MB support both difficult olfactory discrimination and generalization? One appealing framework suggested by our results is that of memory retrieval by template matching. In this scenario, flies that form an association with one particular odor store a corresponding template in the MB. Both generalization and accuracy of memory retrieval depend upon the degree to which test odors match this stored template. When flies are trained with one stimulus and tested with other stimuli they have never before encountered, they respond to the stimulus whose representation most overlaps with the stored template, even if that match is not perfect. This corresponds to stimulus generalization. When confronted with a discrimination task, flies learn to accurately distinguish odors based on the parts of the representation that do not overlap. Our results suggest that the amount of non-overlap required for stimuli to be recognized as distinct is potentially quite small, since 30 MB neurons support high levels of odor discrimination when flies choose between two odors. However, this number of neurons is required for our classifier to make a binary choice. More neurons may be required to identify odors accurately in a natural setting, where animals are confronted with a much richer stimulus palette.

4.5.2 Binary coding in MB enables a simple learning rule

We have shown that the overlap between different odor representations influences both generalization and the ability to make fine discriminations. Increasing the difficulty of the discrimination was accompanied by a decrease in the number of cells responding uniquely to one of the two stimuli. The results from our model network suggest that little information about odor identity is conveyed by spike rate or timing in KCs. This possibility concurs with electrophysiological recordings of *Drosophila* KCs, which indicate that they respond to odors with a brief volley of spikes with no evident temporal patterning (Murthy et al. 2008; Turner et al. 2008). Instead, we found that simply modifying synaptic strengths

of all KCs responding to an odor would be sufficient to learn an odor-specific behavioral response. Although our model performs well without utilizing rate or timing information, we do not exclude the possibility that coding in either of these dimensions would be useful for more complex discrimination tasks, or for behavioral tasks other than discrimination. For example, rate information might be useful for distinguishing different concentrations of the same odor, or timing differences between hemispheres useful for navigating odor gradients.

Our results are consistent with the suggestion that the fly olfactory system forms associations using a simple learning rule that broadcasts a signal to all responding KCs to adjust synaptic weights when one odor is paired with punishment or reward. A promising candidate for the broadcast signal in aversive learning is the neuromodulator dopamine. Dopamine release is required for odor-shock conditioning (Schwaerzel et al. 2003), and pairing dopaminergic stimulation with odor delivery is sufficient for flies to form an aversive association with an odor (Claridge-Chang et al. 2009; Aso et al. 2010). Dopamine receptors are located predominantly on the axons of KCs, rather than their dendrites (Han et al. 1996).

The notion that KCs undergo synaptic plasticity simply based on being active during a period of aversive reinforcement has parallels in the mammalian brain. Experiments in hippocampal slices have suggested that individual CA3-CA1 synapses only assume two states - low and high strength (Petersen et al. 1998; O'Connor et al. 2005). The transitions between the binary states of these synapses parallels the model of the MB, where KCs undergo plasticity simply if they were activated by odor during aversive reinforcement. In both cases synapses assume either high or low weights. Such binary networks can perform well in many conditions, forming accurate associations (Baldassi et al. 2007). Although finer-grain information from the KC activity patterns may be used in more subtle behavioral contexts, in this simple associative learning context, our results show that analog information is dispensable for accurate discrimination.

4.5.3 Summary

Taken together, these results demonstrate the importance of minimizing the overlap of stimulus representations for maximizing the specificity of associations. Animals generalized across stimuli which

exhibited moderate overlap, and had difficulty discriminating between stimuli which were highly overlapping. Our results show that the sparsening of odor representations in the MB creates binary differences between response patterns, which can allow specific associations to form using a very simple, biologically plausible learning rule.

4.6 Acknowledgements

We would like to thank J. Dubnau, A. Kepecs, E. Gruntman, T. Hige, V. Jayaraman, J. Schnupp, A. Zador and Y. Zhong for advice and comments on the manuscript. K.S.H is supported by the Crick-Clay fellowship from the Watson School of Biological Sciences and predoctoral training grant 5T32GM065094 from the National Institute of General Medical Sciences. E.D. was supported by an EMBO Long-Term Fellowship and a Patterson Trust Fellowship. This work was funded by NIH grant R01 DC010403-01A1.

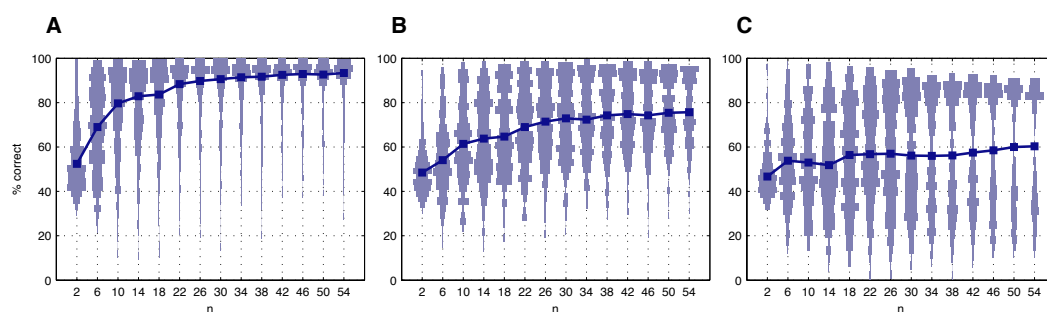


Figure 4.5: Classification accuracy as a function of population size. **A**, Classification accuracy for the pure odor pair as a function of the number of neurons used to train the model network. The perceptron was trained using 50 randomly chosen subsets of n KCs from each fly. The distribution of classification performance over these runs is shown by the blue violin plot. The solid curve is the mean. Classification accuracy asymptotes after about $n = 25$. **B**, As **A**, but for the 70:30 blend. **C**, As **A**, but for the 60:40 blend.

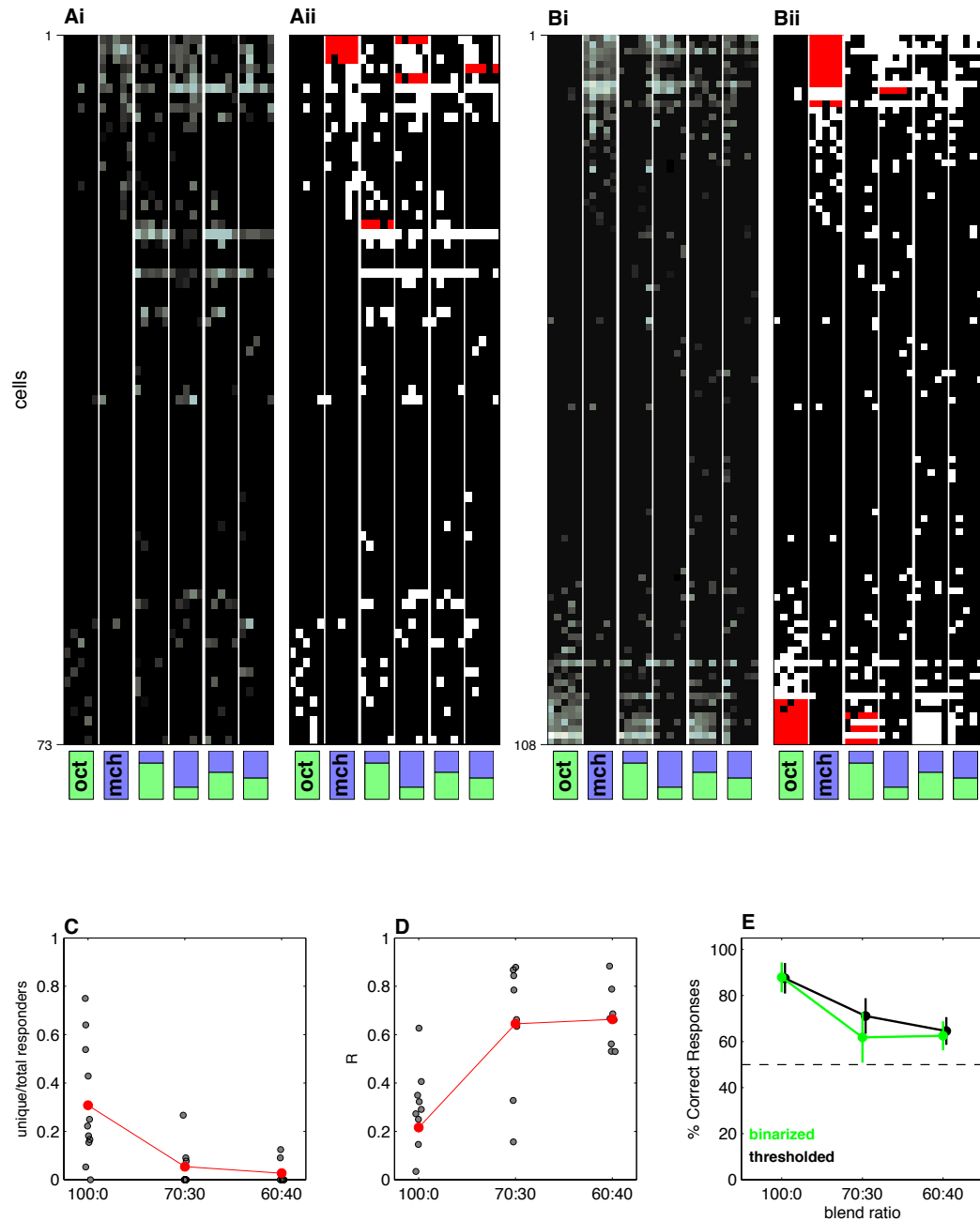


Figure 4.6: A binary code in MB is sufficient to account for learned odor discrimination. **Ai**, Response matrix showing mean evoked dF/F for the pure odors, the 70:30 blends, and the 60:40 blends from one fly. Each row is a different cell and each column a different trial. Non-significant responses are set to zero. **Aii**, Binarized version of **Ai**. Significantly responding cells have a value of 1. Red indicates cells which responded uniquely to one stimulus of each pair. **B**, As **A** but from a different experimental animal. **C**, Proportion of neurons responding uniquely (see main text) to just one odor at each blend ratio. **D**, Correlation coefficients between each blend pair. **E**, Neurometric curves from all flies based upon thresholded (black) and binarized (green) KC response patterns. Error bars show 95% confidence intervals for the mean. Classification based on binarized patterns is not significantly different from that based on thresholded analog inputs.

Part III

Conclusions and perspectives

Chapter 5

Conclusions and perspectives

5.1 *In vivo* imaging of population responses

We have developed a two-photon calcium imaging platform for simultaneously tracking the activity of many single cells in the *Drosophila* MB. This development has allowed us to achieve two experimental aims thus far. First, we have tested the prediction that KC responses should remain sparse when challenged with diverse, intense, and complex odorants. To my knowledge this is the first true description of population sparseness in a substantial portion of a brain area (~5% of MB). By *true* description, I mean that it was calculated within each trial, rather than as an aggregate measure across the experiment. This is important, as correlated changes in activity can be significant for the animal, but are lost by pooling responses across trials. It allowed us, for example, to observe that sparseness actually changes depending on whether the previous stimulus was a higher or lower concentration of the odor (Figure 3.6). This process may facilitate certain aspects of concentration invariant odor perception, or aid in odor gradient tracking. Second, we have identified what we believe are neural determinants of perceptual odor discriminability in the fly. Surprisingly, we find that we are able to predict the behavioral performance of the animal quite well based on the activity of small numbers of MB neurons (Figures 4.4&4.5). This seems to be true even for difficult perceptual discriminations. This is perhaps due to the highly non-overlapping nature of MB representations. The sparse code for odors in the MB may function to minimize overlap between response patterns to different stimuli, thus allowing the use of simple binary plasticity (whether or not a KC fired in response to an odor) for high-accuracy linear classification.

Our ability to address these questions fundamentally relied on our ability to acquire the signals of many neurons simultaneously. This advantage allows us to evaluate the features of the MB neural

code that are actually available for use by the fly on a moment-to-moment basis. This approach does not suffer from the same limitations as pooled single-cell recordings, which, because of their independence, may not accurately reflect the information truly available to the animal to make a perceptual decision.

5.2 Sparseness is a fundamental feature of the MB code

Our results indicate that MB responses to odor will seemingly always be sparser than their AL inputs. Even when driven with complex, intense, and ethologically relevant odors, the KC population responds sparsely. This may seem like a trivial conclusion, but before starting the experiments we wondered whether there actually were some odor features capable of eliciting dense MB responses. Perhaps we just hadn't tried enough stimuli, or the right types of stimuli. We now feel more confident that sparseness is truly an invariant feature of MB responses, and not an artifact of using impoverished experimental stimuli. The real question now is: *What is the significance of sparse MB representation for the fly?*

We believe that sparsening of AL inputs facilitates easier pattern separation by downstream ENs, which then leads to more accurate stimulus associations. This can be illustrated by considering how difficult it would be to learn multiple patterns (odors) using PN responses as input, versus using KC responses as input (Figure 5.1). As more odors are presented, the probability of finding PN synaptic input unique to a particular stimulus drops precipitously, while the probability of finding such input from the KC population remains high as many stimuli are presented. This means that a decoder wanting to respond to only a single one of those stimuli would be more likely to find a useful binary input from KCs than from PNs. Of course, there can always be more than one function for a feature of a neural code. It will be interesting in coming years to see what other roles sparse MB coding plays in the behavior of the fly.

5.3 MB pattern overlap is predictive of simple learned olfactory behaviors

By imaging the population activity of MB on individual trials, we were able to ask how well our ideal observer models corresponded to the behavioral abilities of actual *Drosophila*. It turns out that the neurometric and psychometric functions obtained by using similar odor blends correspond quite closely.

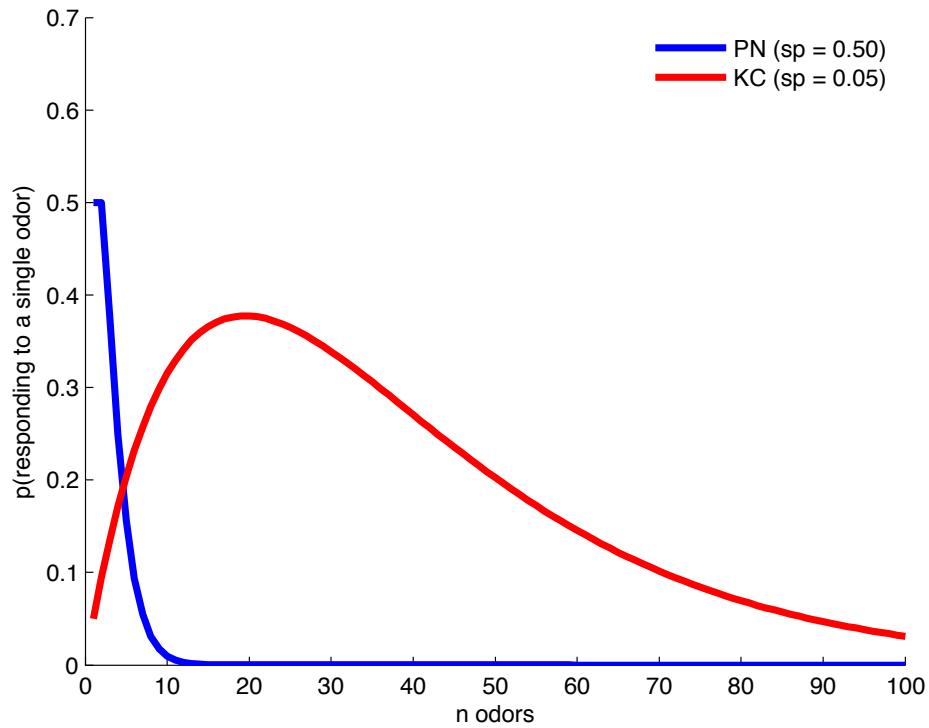


Figure 5.1: Probability of responding to a single odor, as a function of the number of odors. To illustrate the effects of sparse coding, we imagine the PN and KC populations as binary units, with a probability of response, sp . We know that PNs are more likely to respond to a given odor than KCs, approximating $sp = 0.50$ for PNs, and $sp = 0.05$ for KCs (Turner et al. 2008; Honegger et al. 2011). We would like to know how overlapping these binary responses would become if several odors were presented. This is equivalent, in this simple case, to asking what the probability is of responding to a single odor out of n odors. Assuming that responses are independent across odors, we can illustrate this simply as a plot of the binomial distribution, with $k = 1$ success, $n = n$ odors, and $p(\text{success}) = sp$ for each population. We see that the sparsely responding KC population (red line) maintains more unique responses than the less sparse PN population (blue line) as multiple odors are presented.

Interestingly, the classification scheme bearing the closest resemblance to behavioral performance was the perceptron algorithm, which behaves in a way that seems quite similar to how (we think) ENs are decoding KC activity. I will avoid further speculation, but will return below to the role of linear classification in odor discrimination. Another surprising result was that we could predict, based solely on the overlap in MB activity patterns, chemically distinct molecules that flies will generalize between. This means that, were we to image a larger set of odorant representations in MB, we could conceivably map *neural distances* onto *perceptual distances* and predict the stimulus-driven behavior of the fly from neural representations alone. This would represent a substantial inversion of the standard psychophysical model, where one observes behavioral metrics to make predictions about the underlying perceptual and neural metrics. Furthermore, behavioral performance on a difficult discrimination task is predicted well by the overlap between MB responses, indicating that when the perceptual distances between stimuli are reduced, this corresponds to a reduction of neural distance. These findings together serve to highlight the role that we think pattern overlap plays in setting the limits of perceptual discriminability.

This also underscores the importance of how responses to different stimuli are distributed in the population. As Kanerva argued, it is important that items stored in memory minimize, but not completely abolish, overlap. If no neurons were shared between representation of two stimuli, there would be no basis for generalization. Animals need to generalize between stimuli all the time. Even if the same stimulus is presented twice, noise in the neural activity will make the representations in the brain slightly different. Thus, at least a small degree of generalization is expected to be necessary for recognition.

5.4 Associative memory as template matching

One slightly surprising idea to emerge from this work is the conceptualization of associative memory formation as template matching. Often, we think of neural activity as a complicated amorphous substance of the brain, consisting of ever-changing parallel processes. But it seems rather incredible that we could have taken one static snapshot of the activity of ~5% of the MB population and discerned the identity of very similar stimuli about as well as the fly. This makes one wonder: *what if that is all it takes?* The MB is perhaps unique among brain areas, in that there is virtually no spontaneous activity,

and the sparse activity evoked by stimuli shows very little evidence of temporal patterning. I can't help but speculate: *what if that is all there is to odor coding in the MB?* Maybe simple pattern matching suffices to read out odor identity because the system actually is simply pattern matching. It is fairly easy to imagine a biochemical scheme for incrementing KC presynaptic weights onto a broadly-sampling downstream neuron based on neuromodulation. If a synapse was active before the reinforcer arrived, the weight would increase by some fixed amount. In a way, this is similar to the operation of our binary perceptron, which performed at levels comparable to the flies. Of course, the biological implementation of this would be slightly different than our statistical techniques, but still it is an intriguing possibility that the architecture and neural coding in this system have evolved to facilitate the type of learning supported by a perceptron-like decoder.

5.5 Toward a signal processing view of the olfactory system

Extending the above ideas a bit further, I believe we are making substantial strides towards understanding the *Drosophila* olfactory system from a signal processing perspective. The goal of such an approach, as advocated by Barlow, is ultimately to understand the neural activity we observe in terms of the function it serves for the animal. Correspondingly, the transformations observed in the olfactory system should be relatable to some sensory processing steps that selectively accentuate, or extract, certain features of the stimuli. Currently, I think this view could include several stages of neural processing that encompass the full range of steps in *Drosophila* olfaction, from receptor activation, to selective formation of learned associations. It may be briefly summarized as follows.

A large number of broadly tuned receptor neurons at the periphery ensure complete and overlapping coverage of the fly's olfactory receptive range. OSNs ultimately converge onto a relatively tiny number of AL PNs. This anatomical convergence of many independent stimulus encoders, and the properties of the synapse, serve to selectively amplify weak responses and average out noise. Thus, the dynamic range and the signal-to-noise ratio of the output should be enhanced. At the same time, mechanisms for normalizing the response of individual processing channels by the total sensory input to the system serve as a form of global gain control, ensuring that overall output of the AL is in a range that is neither too weak, nor saturating. This potentially functions to preserve sparse representation of

the stimulus in the MB. Upon passing through the AL, the sensory representation is fanned-out to the MB at a ratio of roughly 1:13. This dramatic divergence corresponds to the projection of these representations into a much higher-dimensional coding space. Sparse representation in this space serves to reasonably minimize the overlap between representations, while preserving some degree of relatedness. This minimal overlap sets the limits for making both stimulus discriminations and generalizations. This high-dimensional representation may now be more easily read out by simple linear decoders than a dense compressed representation. The weights of a decoder for classification of certain stimuli may be set using a simple plasticity rule that discards temporal and rate information and thus corresponds to learning a template by example.

While this model may seem fairly complete there are many gaps in our knowledge. For instance, we do not know how the sparse representations are generated from dense PN inputs in the MB of *Drosophila*. This could be through a certain connectivity scheme, local processing with the MB, or some form of unidentified global inhibition. There remains much work ahead to fill in these gaps, but the insight they will provide into the function of this relatively simple nervous system will surely be enlightening.

5.6 Future directions

I remain hopeful that the methods we have developed for addressing population-level questions about MB odor coding will be useful for answering several pressing questions in the field, some of which are discussed below.

Do MB odor representations change after learning? Our studies to date have only imaged odor responses in naïve flies. Given the highly dynamic requirements for different KC classes during different phases in memory processing, it is expected that a conditioned odor would be represented by activity in changing groups of KCs over time. Calcium imaging results from trained flies seem to indicate that the magnitude of the output of MB lobes changes after conditioning, but it remains unclear whether the identity of the KCs that respond to the odor are changing.

Is information about the stimulus encoded in the fine timing of KC responses? It is worth noting that in the experiments presented in preceding chapters, we discarded any temporal information that might have been present in the calcium responses and simply averaged the change in fluorescence over a period of several seconds. Surprisingly, we did quite well at classifying the odor based on these dynamically impoverished responses. Though electrophysiological recordings seem to indicate that KC odor responses are not highly dynamic, it is still possible that information about the odor is present in the timing of KC responses. In future studies, it will be interesting to determine whether fine differences in the timing of KC responses indicates anything about the odor stimulus, such as intensity or odor quality.

At what MB neural distance do flies draw the boundary between perceived stimulus and a stored template? We observed that flies are able to generalize learned associations across odors that have similar representations in the MB. Using our calcium imaging approach, we can calculate the neural distance between different pairs of odors and predict on average the stimuli to which an animal will generalize. By coupling measurement of single fly generalization behavior with imaging of a series of odorants with different neural distances within the same fly, we could map the generalization boundary that is used to determine whether the animal will display a generalized response. Do two stimuli need to overlap by 20% in the MB, or by 80% to retrieve the stored memory? This would be an important addition to our understanding of how activity in circuits for storing memories are decoded into useful behavior.

What is the circuit mechanism for making KC responses sparse? We still know very little about the circuit mechanism for generating sparse responses in the MB. From our results, we know that sparseness seems to be important for the system, but how is it maintained across changing stimulus parameters? Is sparseness enforced by feedback or feedforward inhibition? Does sparse connectivity with PNs play a role? This is an important question because neural codes in many systems, including sensory cortex, are sparser than their inputs, and the circuit mechanisms for achieving this transformation may be quite general.

Appendix A - Odor concentration and KC response magnitude

The results presented in Chapter 3 indicate that the proportion of responsive KCs does not change drastically as odor concentration is increased. The animal nonetheless must be able to perceive changes in odor concentration as distinctive. For example, *Drosophila* can be conditioned to avoid a certain odorant concentration (Masek and Heisenberg 2008). Information about the odor concentration could therefore be represented in either the pattern of responding KCs, or in the intensity of responses. The topic of whether odor concentration affects KC response magnitude was not explicitly addressed in the original study, appearing in Chapter 3. This outstanding question is addressed here. Overall, I find that KC response magnitude is significantly different for only the highest odor concentration presented (10% saturated vapor). I have analyzed for *all cells* in a field of view 1) the *total summed* change in fluorescence during the odor epoch and 2) the *mean* fluorescence change across cells during the odor epoch. Similarly, I have also calculated these parameters using *only significantly responding* cells.

Results of analysis I have analyzed the KC calcium signals from the data set shown in Figure 3.6 to examine whether KC response magnitude, rather than the proportion of responsive KCs, varies as a function of odor concentration. There were no differences between the two odors used (fresh banana and isoamyl acetate) so the data sets were pooled. Since we knew from the results of 3.4.5 that there was a significant interaction between concentration and the session type (high-to-low or low-to-high; see Figure 3.6 for illustration) I also pooled across session type. The experimental groups were balanced so there should be no bias towards the effect of one session type or the other. For all four metrics tested, all odor concentrations (1%, 2%, 4%, and 10% saturated vapor) differed significantly from clean air (0% saturated vapor). Since I was interested in the difference between odor concentrations, I excluded clean

air trials from the analyses.

I first looked at the total summed change in fluorescence (dF/F) over all cells in the field of view. Overall, there was a significant effect of odor concentration on total calcium change in MB ($p < 0.0001$, $F_{(3,466)} = 9.73$) (Figure A 1). Only the highest concentration (10% saturated vapor), however, differed from the rest ($p < 0.05$, Tukey-Kramer HSD). I then looked at the mean fluorescence change across all cells during the odor epoch. Similarly, there was a significant effect of concentration on the mean change in fluorescence across all cells ($p < 0.0001$, $F_{(3,466)} = 10.99$) (Figure A 2). Again, only the highest concentration differed from the other concentrations ($p < 0.05$, Tukey-Kramer HSD). I then limited the analysis to cells that were detected as having significant responses on each trial (see Chapter 3.3 Methods for details). Doing this presumably eliminates imaging noise and enriches for true responses. These results also indicate a significant effect of concentration on both total summed change ($p < 0.0001$, $F_{(3,459)} = 8.61$) and mean change ($p < 0.0001$, $F_{(3,459)} = 8.61$) in fluorescence (Figures A 3-4). But, again, for both measures the only significant contrast is between the highest concentration and the other three ($p < 0.05$, Tukey-Kramer HSD).

Overall, these analyses reveal that only the highest concentration of odor elicited significantly different KC response magnitudes. This concentration (10%) was ten times greater than the lowest concentration (1%), and 2.5 times greater than the next lowest (4%). It is interesting, then, that concentration differences of comparable order in the lower concentration range (i.e. 1% vs 4%; a 4-fold difference) produced KC responses of indistinguishable magnitude.¹ This suggests that there may be a range, outside of which, changes in concentration differentially affect the strength of MB responses. It is worth noting that 10% saturated vapor is an extremely high concentration. Experiments done in most *Drosophila* olfaction labs are done at ~1% or less. Since these experiments were originally performed with the goal of maximally driving input to the MB, we considered this high concentration to be a strong, if not entirely physiologically relevant, stimulus.

It still remains quite possible that the *identities* of responsive KCs, rather than the response intensities, change as a function of odor concentration. This is, in fact, what has been observed in the locust MB (Stopfer et al. 2003). Unfortunately, since we were originally interested in calculating the proportion of responding KCs, we were not concerned with tracking the identities of those cells

¹Note, this was *not* because they produced uniformly weak responses. The average response magnitude in significant KCs observed for even the lowest (1%) concentration (mean $dF/F = 0.46$) was 82% of the average response to the highest (10%) concentration (mean $dF/F = 0.56$).

throughout the experiment. So the rather extensive data set we collected did not include many cases where the same set of KCs was tracked throughout the experiment. This makes us unable to analyze this data set for changes in patterns. Future work should be able to clearly determine whether odor concentration affects the identities of responding KCs.

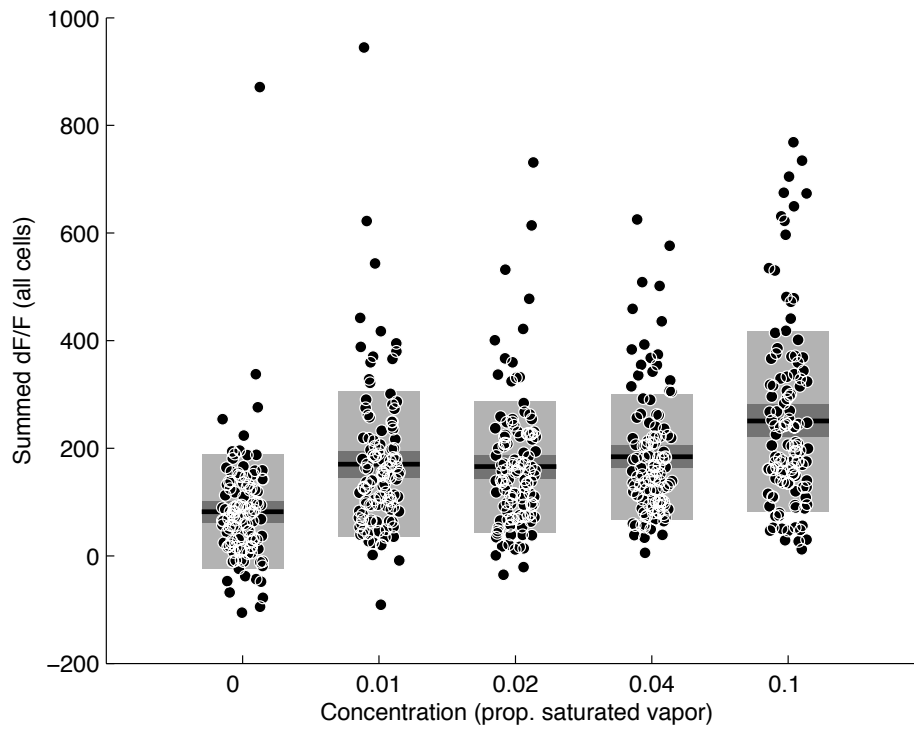


Figure A 1: Total summed dF/F during odor epoch over all cells as a function of odor concentration. Each point is a single trial from a single animal. Light gray boxes indicate standard deviations around the mean and dark boxes indicate the 95% confidence interval.

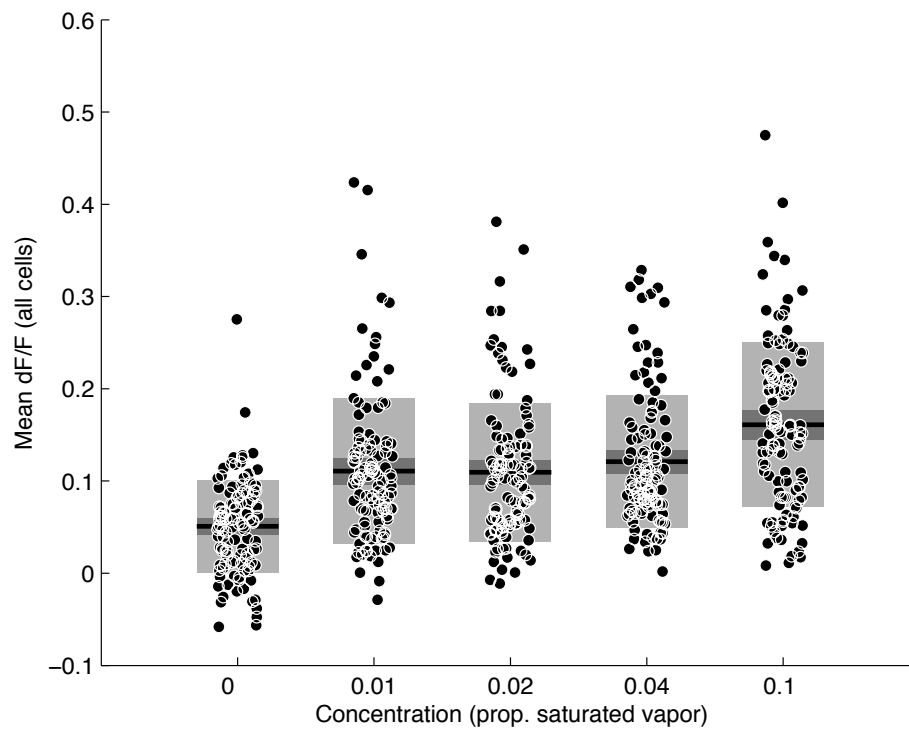


Figure A 2: Mean dF/F during odor epoch averaged over all cells as a function of odor concentration. Each point is a single trial from a single animal. Light gray boxes indicate standard deviations around the mean and dark boxes indicate the 95% confidence interval.

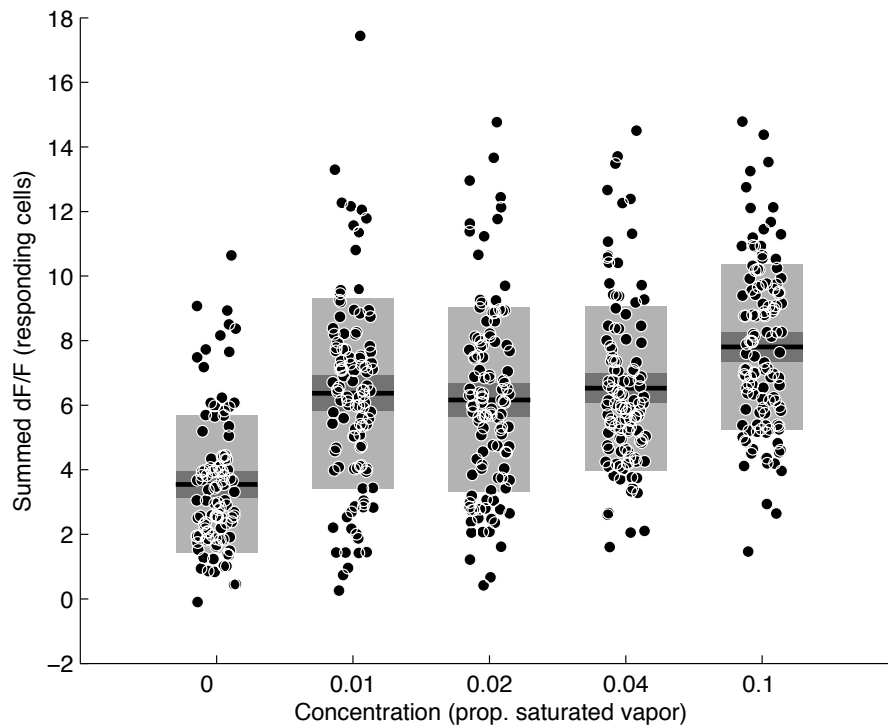


Figure A 3: Total summed dF/F in KCs over all significantly responding cells as a function of odor concentration. Each point is a single trial from a single animal. Light gray boxes indicate standard deviations around the mean and dark boxes indicate the 95% confidence interval.

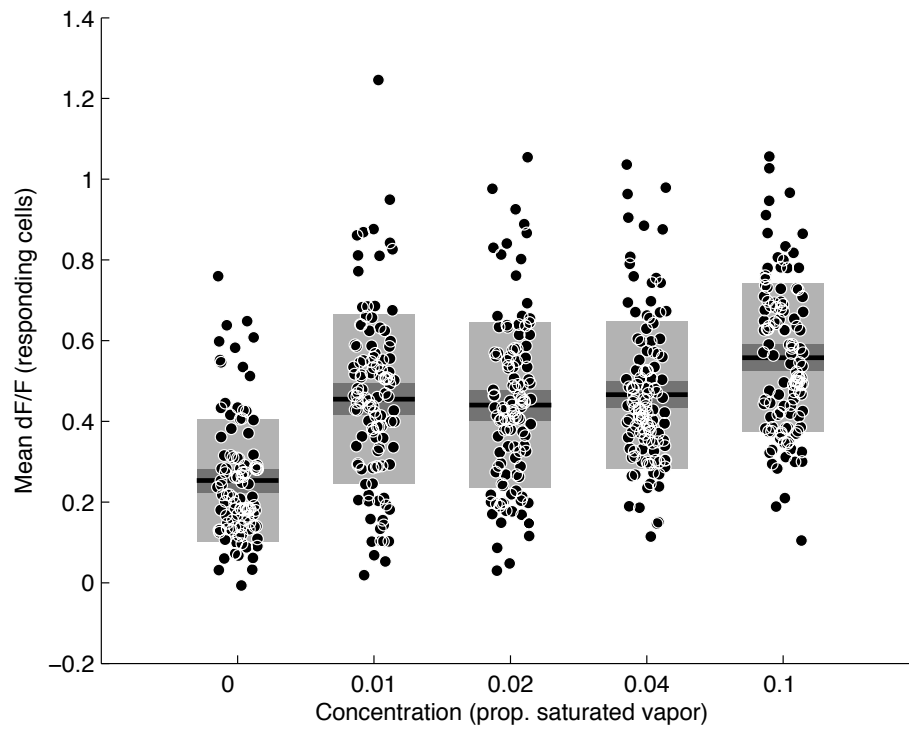


Figure A 4: Total summed dF/F during odor epoch over all significantly reponding cells as a function of odor concentration. Each point is a single trial from a single animal. Light gray boxes indicate standard deviations around the mean and dark boxes indicate the 95% confidence interval.

References

- Abuin L, Bargeton B, Ulbrich MH, Isacoff EY, Kellenberger S, Benton R. 2011. Functional architecture of olfactory ionotropic glutamate receptors. *Neuron* **69**: 44–60.
- Adrian ED. 1926. The impulses produced by sensory nerve endings: Part I. *J Physiol* **61**: 49–72.
- Adrian ED, Matthews R. 1927. The action of light on the eye: Part I. The discharge of impulses in the optic nerve and its relation to the electric changes in the retina. *J Physiol* **63**: 378–414.
- Adrian ED, Matthews R. 1928. The action of light on the eye: Part III. The interaction of retinal neurones. *J Physiol* **65**: 273–298.
- Adrian ED, Zotterman Y. 1926. The impulses produced by sensory nerve-endings: Part II. The response of a Single End-Organ. *J Physiol* **61**: 151–171.
- Akalal DBG, Yu D, Davis RL. 2010. A late-phase, long-term memory trace forms in the γ neurons of *Drosophila* mushroom bodies after olfactory classical conditioning. *J Neurosci* **30**: 16699–16708.
- Akalal DBG, Yu D, Davis RL. 2011. The long-term memory trace formed in the *Drosophila* α/β mushroom body neurons is abolished in long-term memory mutants. *J Neurosci* **31**: 5643–5647.
- Arzi A, Sobel N. 2011. Olfactory perception as a compass for olfactory neural maps. *Trends in cognitive sciences* **15**: 537–545.
- Aso Y, Grubel K, Busch S, Friedrich A, Siwanowicz I, Tanimoto H. 2009. The Mushroom Body of Adult *Drosophila* Characterized by GAL4 Drivers. *J Neurogenet* **23**: 156–172.
- Aso Y, Siwanowicz I, Bräcker L, Ito K, Kitamoto T, Tanimoto H. 2010. Specific dopaminergic neurons for the formation of labile aversive memory. *Curr Biol* **20**: 1445–1451.
- Attwell D, Laughlin SB. 2001. An energy budget for signaling in the grey matter of the brain. *J Cereb Blood Flow Metab* **21**: 1133–1145.
- Averbeck BB, Latham PE, Pouget A. 2006. Neural correlations, population coding and computation. *Nat Rev Neurosci* **7**: 358–366.
- Baldassi C, Braunstein A, Brunel N, Zecchina R. 2007. Efficient supervised learning in networks with binary synapses. *Proc Natl Acad Sci USA* **104**: 11079–11084.
- Barlow HB. 1953. Summation and inhibition in the frog's retina. *J Physiol* **119**: 69–88.
- Barlow HB. 1972. Single units and sensation: a neuron doctrine for perceptual psychology? *Perception* **1**: 371–394.

- Barlow H. 1961. Possible principles underlying the transformation of sensory messages. in *Sensory Communication* (ed. Rosenblith W), pp. 217–234. MIT Press, Cambridge, MA.
- Barlow H. 1994. The neuron doctrine in perception. in *The Cognitive Neurosciences* (ed. Gazzaniga M), pp. 415–435. MIT Press, Cambridge, MA.
- Barlow HB, Parker AJ, Singer W, Thorpe SJ. 2009. Barlow’s 1972 paper. *Perception* **38**: 795–807.
- Benton R, Sachse S, Michnick SW, Vosshall LB. 2006. Atypical membrane topology and heteromeric function of *Drosophila* odorant receptors in vivo. *PLoS Biol* **4**: e20.
- Benton R, Vannice KS, Gomez-Diaz C, Vosshall LB. 2009. Variant ionotropic glutamate receptors as chemosensory receptors in *Drosophila*. *Cell* **136**: 149–162.
- Bhandawat V, Olsen S, Gouwens N, Schlief M, Wilson R. 2007. Sensory processing in the *Drosophila* antennal lobe increases reliability and separability of ensemble odor representations. *Nat Neurosci* **10**: 1474–1482.
- Bhandawat V, Maimon G, Dickinson MH, Wilson RI. 2010. Olfactory modulation of flight in *Drosophila* is sensitive, selective and rapid. *J Exp Biol* **213**: 3625–3635.
- Blum AL, Li W, Cressy M, Dubnau J. 2009. Short- and long-term memory in *Drosophila* require cAMP signaling in distinct neuron types. *Curr Biol* **19**: 1341–1350.
- Briggman KL, Abarbanel HDI, Kristan WB. 2005. Optical imaging of neuronal populations during decision-making. *Science* **307**: 896–901.
- Britten KH, Newsome WT, Shadlen MN, Celebrini S, Movshon JA. 1996. A relationship between behavioral choice and the visual responses of neurons in macaque MT. *Vis Neurosci* **13**: 87–100.
- Brooks ES, Greer CL, Romero-Calderón R, Serway CN, Grygoruk A, Haimovitz JM, Nguyen BT, Najibi R, Tabone CJ, de Belle JS, Krantz DE. 2011. A Putative Vesicular Transporter Expressed in *Drosophila* Mushroom Bodies that Mediates Sexual Behavior May Define a Neurotransmitter System. *Neuron* **72**: 316–329.
- Broome BM, Jayaraman V, Laurent G. 2006. Encoding and decoding of overlapping odor sequences. *Neuron* **51**: 467–482.
- Budick SA, Dickinson MH. 2006. Free-flight responses of *Drosophila melanogaster* to attractive odors. *J Exp Biol* **209**: 3001–3017.
- Busch S, Selcho M, Ito K, Tanimoto H. 2009. A map of octopaminergic neurons in the *Drosophila* brain. *J Comp Neurol* **513**: 643–667.
- Butcher NJ, Friedrich AB, Lu Z, Tanimoto H, Meinertzhagen IA. 2012. Different classes of input and output neurons reveal new features in microglomeruli of the adult *Drosophila* mushroom body calyx. *J Comp Neurol* **520**: 2185–2201.
- Cachero S, Jefferis GSXE. 2008. *Drosophila* olfaction: the end of stereotypy? *Neuron* **59**: 843–845.
- Campbell RAA, King AJ, Nodal FR, Schnupp JWH, Carlile S, Doubell TP. 2008. Virtual adult ears reveal the roles of acoustical factors and experience in auditory space map development. *J Neurosci* **28**: 11557–11570.

- Carlsson MA, Diesner M, Schachtner J, Nässel DR. 2010. Multiple neuropeptides in the *Drosophila* antennal lobe suggest complex modulatory circuits. *J Comp Neurol* **518**: 3359–3380.
- Cassenaer S, Laurent G. 2012. Conditional modulation of spike-timing-dependent plasticity for olfactory learning. *Nature* **482**: 47–52.
- Cayirlioglu P, Kadow IG, Zhan X, Okamura K, Suh GSB, Gunning D, Lai EC, Zipursky SL. 2008. Hybrid neurons in a microRNA mutant are putative evolutionary intermediates in insect CO₂ sensory systems. *Science* **319**: 1256–1260.
- Chechik G, Anderson MJ, Bar-Yosef O, Young ED, Tishby N, Nelken I. 2006. Reduction of information redundancy in the ascending auditory pathway. *Neuron* **51**: 359–368.
- Chiang AS, Lin CY, Chuang CC, Chang HM, Hsieh CH, Yeh CW, Shih CT, Wu JJ, Wang GT, Chen YC, Wu CC, Chen GY, Ching YT, Lee PC, Lin CY, Lin HH, Wu CC, Hsu HW, Huang YA, Chen JY, Chiang HJ, Lu CF, Ni RF, Yeh CY, Hwang JK. 2011. Three-dimensional reconstruction of brain-wide wiring networks in *Drosophila* at single-cell resolution. *Curr Biol* **21**: 1–11.
- Chou YH, Spletter ML, Yaksi E, Leong JCS, Wilson RI, Luo L. 2010. Diversity and wiring variability of olfactory local interneurons in the *Drosophila* antennal lobe. *Nat Neurosci* **13**: 439–449.
- Christiansen F, Zube C, Andlauer TFM, Wichmann C, Fouquet W, Oswald D, Mertel S, Leiss F, Tavosanis G, Luna AJF, Fiala A, Sigrist SJ. 2011. Presynapses in Kenyon Cell Dendrites in the Mushroom Body Calyx of *Drosophila*. *J Neurosci* **31**: 9696–9707.
- Claridge-Chang A, Roorda RD, Vrontou E, Sjulson L, Li H, Hirsh J, Miesenböck G. 2009. Writing memories with light-addressable reinforcement circuitry. *Cell* **139**: 405–415.
- Connolly JB, Roberts IJ, Armstrong JD, Kaiser K, Forte M, Tully T, O’Kane CJ. 1996. Associative learning disrupted by impaired Gs signaling in *Drosophila* mushroom bodies. *Science* **274**: 2104–2107.
- Couto A, Alenius M, Dickson BJ. 2005. Molecular, anatomical, and functional organization of the *Drosophila* olfactory system. *Curr Biol* **15**: 1535–1547.
- Cury K, Uchida N. 2010. Robust odor coding via inhalation-coupled transient activity in the mammalian olfactory bulb. *Neuron* **68**: 570–585.
- Dacks AM, Green DS, Root CM, Nighorn AJ, Wang JW. 2009. Serotonin modulates olfactory processing in the antennal lobe of *Drosophila*. *J Neurogenet* **23**: 366–377.
- Daniels RW, Gelfand MV, Collins CA, DiAntonio A. 2008. Visualizing glutamatergic cell bodies and synapses in *Drosophila* larval and adult CNS. *J Comp Neurol* **508**: 131–152.
- Davis RL. 2005. Olfactory memory formation in *Drosophila*: from molecular to systems neuroscience. *Annual review of neuroscience* **28**: 275–302.
- Davis RL. 2011. Traces of *Drosophila* memory. *Neuron* **70**: 8–19.
- de Belle J, Heisenberg M. 1994. Associative odor learning in *Drosophila* abolished by chemical ablation of mushroom bodies. *Science* **263**: 692–695.
- de Bruyne M, Clyne PJ, Carlson JR. 1999. Odor coding in a model olfactory organ: the *Drosophila* maxillary palp. *J Neurosci* **19**: 4520–4532.

- de Bruyne M, Foster K, Carlson JR. 2001. Odor coding in the *Drosophila* antenna. *Neuron* **30**: 537–552.
- Demmer H, Kloppenburg P. 2009. Intrinsic membrane properties and inhibitory synaptic input of kenyon cells as mechanisms for sparse coding? *J Neurophysiol* **102**: 1538–1550.
- Dobritsa AA, van der Goes van Naters W, Warr CG, Steinbrecht RA, Carlson JR. 2003. Integrating the molecular and cellular basis of odor coding in the *Drosophila* antenna. *Neuron* **37**: 827–841.
- Dubnau J, Grady L, Kitamoto T, Tully T. 2001. Disruption of neurotransmission in *Drosophila* mushroom body blocks retrieval but not acquisition of memory. *Nature* **411**: 476–480.
- Duistermars BJ, Chow DM, Frye MA. 2009. Flies require bilateral sensory input to track odor gradients in flight. *Curr Biol* **19**: 1301–1307.
- Erber J, Masuhr T, Menzel R. 1980. Localization of short-term memory in the brain of the bee, *Apis mellifera*. *Physiological Entomology* **5**: 343–358.
- Fernandez PC, Locatelli FF, Person-Rennell N, Deleo G, Smith BH. 2009. Associative conditioning tunes transient dynamics of early olfactory processing. *J Neurosci* **29**: 10191–10202.
- Fiete IR, Hahnloser RHR, Fee MS, Seung HS. 2004. Temporal sparseness of the premotor drive is important for rapid learning in a neural network model of birdsong. *J Neurophysiol* **92**: 2274–2282.
- Fisher RA. 1936. The Use of Multiple Measurements in Taxonomic Problems. *Annals of Eugenics* **7**: 179–188.
- Fishilevich E, Domingos AI, Asahina K, Naef F, Vosshall LB, Louis M. 2005. Chemotaxis behavior mediated by single larval olfactory neurons in *Drosophila*. *Curr Biol* **15**: 2086–2096.
- Fishilevich E, Vosshall LB. 2005. Genetic and functional subdivision of the *Drosophila* antennal lobe. *Curr Biol* **15**: 1548–1553.
- Földiák P, Young M. 1995. Sparse coding in the primate cortex. in *The Handbook of Brain Theory and Neural Networks* (ed. Arbib M). MIT Press, Cambridge, MA.
- Friedrich RW, Laurent G. 2001. Dynamic optimization of odor representations by slow temporal patterning of mitral cell activity. *Science* **291**: 889–894.
- Galizia CG, Rössler W. 2010. Parallel olfactory systems in insects: anatomy and function. *Annual Review of Entomology* **55**: 399–420.
- Garcia-Lazaro JA, Ahmed B, Schnupp JWH. 2006. Tuning to natural stimulus dynamics in primary auditory cortex. *Curr Biol* **16**: 264–271.
- Ghosh S, Larson SD, Hefzi H, Marnoy Z, Cutforth T, Dokka K, Baldwin KK. 2011. Sensory maps in the olfactory cortex defined by long-range viral tracing of single neurons. *Nature* **472**: 217–220.
- Göpfert MC, Humphris ADL, Albert JT, Robert D, Hendrich O. 2005. Power gain exhibited by motile mechanosensory neurons in *Drosophila* ears. *Proc Natl Acad Sci USA* **102**: 325–330.
- Göpfert MC, Robert D. 2003. Motion generation by *Drosophila* mechanosensory neurons. *Proc Natl Acad Sci USA* **100**: 5514–5519.

- Gross CG. 2002. Genealogy of the "grandmother cell". *The Neuroscientist* **8**: 512–518.
- Guerrieri F, Schubert M, Sandoz JC, Giurfa M. 2005. Perceptual and neural olfactory similarity in honeybees. *PLoS biology* **3**: e60.
- Guizar-Sicairos M, Thurman ST, Fienup JR. 2008. Efficient subpixel image registration algorithms. *Optics letters* **33**: 156–158.
- Hallem E, Carlson J. 2006. Coding of odors by a receptor repertoire. *Cell* **125**: 143–160.
- Hamel LH. 2009. *Knowledge Discovery With Support Vector Machines*. Wiley-Interscience, Hoboken, NJ.
- Han KA, Millar NS, Grotewiel MS, Davis RL. 1996. DAMB, a novel dopamine receptor expressed specifically in *Drosophila* mushroom bodies. *Neuron* **16**: 1127–1135.
- Hansson BS, Stensmyr MC. 2011. Evolution of insect olfaction. *Neuron* **72**: 698–711.
- Hartline H. 1938. The response of single optic nerve fibers of the vertebrate eye to illumination of the retina. *American Journal of Physiology* **121**: 400–415.
- Hartline H, Graham C. 1932. Nerve impulses from single receptors in the eye. *J Cell Comp Physiol* **1**: 277–295.
- Hastie T, Tibshirani R, Friedman J. 2009. *The Elements of Statistical Learning: Data Mining, Inference, and Prediction*. Springer, New York, NY.
- Hattori D, Chen Y, Matthews BJ, Salwinski L, Sabatti C, Grueber WB, Zipursky SL. 2009. Robust discrimination between self and non-self neurites requires thousands of Dscam1 isoforms. *Nature* **461**: 644–648.
- Heeger DJ. 1992. Normalization of cell responses in cat striate cortex. *Vis Neurosci* **9**: 181–197.
- Heisenberg M, Borst A, Wagner S, Byers D. 1985. *Drosophila* mushroom body mutants are deficient in olfactory learning. *J Neurogenet* **2**: 1–30.
- Heisenberg M. 2003. Mushroom body memoir: from maps to models. *Nat Rev Neurosci* **4**: 266–275.
- Hekmat-Scafe DS, Scafe CR, McKinney AJ, Tanouye MA. 2002. Genome-wide analysis of the odorant-binding protein gene family in *Drosophila melanogaster*. *Genome Res* **12**: 1357–1369.
- Honegger KS, Campbell RAA, Turner GC. 2011. Cellular-resolution population imaging reveals robust sparse coding in the *Drosophila* mushroom body. *J Neurosci* **31**: 11772–11785.
- Houweling AR, Brecht M. 2008. Behavioural report of single neuron stimulation in somatosensory cortex. *Nature* **451**: 65–68.
- Hubel DH, Wiesel TN. 1968. Receptive fields and functional architecture of monkey striate cortex. *J Physiol* **195**: 215–243.
- Hubel D, Wiesel T. 1959. Receptive fields of single neurones in the cat's striate cortex. *J Physiol* **148**: 574–591.
- Hubel D, Wiesel T. 1962. Receptive fields, binocular interaction and functional architecture in the cat's visual cortex. *J Physiol* **160**: 106–154.

- Hung CP, Kreiman G, Poggio T, DiCarlo JJ. 2005. Fast readout of object identity from macaque inferior temporal cortex. *Science* **310**: 863–866.
- Ignell R, Root CM, Birse RT, Wang JW, Nässel DR, Winther AME. 2009. Presynaptic peptidergic modulation of olfactory receptor neurons in *Drosophila*. *Proc Natl Acad Sci USA* **106**: 13070–13075.
- Ito I, Ong R, Raman B, Stopfer M. 2008. Sparse odor representation and olfactory learning. *Nat Neurosci* **11**: 1177–1184.
- Ito K, Suzuki K, Estes P, Ramaswami M, Yamamoto D, Strausfeld NJ. 1998. The organization of extrinsic neurons and their implications in the functional roles of the mushroom bodies in *Drosophila melanogaster*. *Learning & memory* **5**: 52–77.
- Jayaraman V, Laurent G. 2007. Evaluating a genetically encoded optical sensor of neural activity using electrophysiology in intact adult fruit flies. *Front Neural Circuits* **1**: 3.
- Jefferis G, Potter C, Chan A, Marin E, Rohlfsing T, Maurer C, Luo L. 2007. Comprehensive maps of *Drosophila* higher olfactory centers: spatially segregated fruit and pheromone representation. *Cell* **128**: 1187–1203.
- Johard HAD, Enell LE, Gustafsson E, Trifilieff P, Veenstra JA, Nässel DR. 2008. Intrinsic neurons of *Drosophila* mushroom bodies express short neuropeptide F: relations to extrinsic neurons expressing different neurotransmitters. *J Comp Neurol* **507**: 1479–1496.
- Jones WD, Cayirlioglu P, Kadow IG, Vosshall LB. 2007. Two chemosensory receptors together mediate carbon dioxide detection in *Drosophila*. *Nature* **445**: 86–90.
- Jortner RA, Farivar SS, Laurent G. 2007. A simple connectivity scheme for sparse coding in an olfactory system. *J Neurosci* **27**: 1659–1669.
- Kamikouchi A, Inagaki HK, Effertz T, Hendrich O, Fiala A, Göpfert MC, Ito K. 2009. The neural basis of *Drosophila* gravity-sensing and hearing. *Nature* **458**: 165–171.
- Kanerva P. 1988. *Sparse Distributed Memory*. MIT Press, Cambridge, MA.
- Kazama H, Wilson R. 2009. Origins of correlated activity in an olfactory circuit. *Nat Neurosci* **12**: 1136–44.
- Kazama H, Wilson RI. 2008. Homeostatic matching and nonlinear amplification at identified central synapses. *Neuron* **58**: 401–413.
- Keene A, Waddell S. 2007. *Drosophila* olfactory memory: single genes to complex neural circuits. *Nat Rev Neurosci* **8**: 341–354.
- Kenyon F. 1896. The Meaning and Structure of the So-Called "Mushroom Bodies" of the Hexapod Brain. *The American Naturalist* **30**: 643–650.
- Kim YC, Lee HG, Han KA. 2007. D1 dopamine receptor dDA1 is required in the mushroom body neurons for aversive and appetitive learning in *Drosophila*. *J Neurosci* **27**: 7640–7647.
- Krashes M, Keene A, Leung B, Armstrong J, Waddell S. 2007. Sequential use of mushroom body neuron subsets during *Drosophila* odor memory processing. *Neuron* **53**: 103–115.

- Krashes MJ, DasGupta S, Vreede A, White B, Armstrong JD, Waddell S. 2009. A neural circuit mechanism integrating motivational state with memory expression in *Drosophila*. *Cell* **139**: 416–427.
- Kuffler S. 1953. Discharge patterns and functional organization of mammalian retina. *J Neurophysiol* **16**: 37–68.
- Laissue PP, Vosshall LB. 2008. The olfactory sensory map in *Drosophila*. *Adv Exp Med Biol* **628**: 102–114.
- Larsson MC, Domingos AI, Jones WD, Chiappe ME, Amrein H, Vosshall LB. 2004. Or83b encodes a broadly expressed odorant receptor essential for *Drosophila* olfaction. *Neuron* **43**: 703–714.
- Lee T, Lee A, Luo L. 1999. Development of the *Drosophila* mushroom bodies: sequential generation of three distinct types of neurons from a neuroblast. *Development* **126**: 4065–4076.
- Leiss F, Groh C, Butcher N, Meinertzhagen I, Tavosanis G. 2009. Synaptic organization in the adult *Drosophila* mushroom body calyx. *J Comp Neurol* **517**: 808–824.
- Lettvin JY, Maturana HR, McCulloch WS, Pitts WH. 1959. What the frog's eye tells the frog's brain. *Proc Inst Radio Engr* **47**: 1940–1951.
- Levy WB, Baxter RA. 1996. Energy efficient neural codes. *Neural Comput* **8**: 531–543.
- Lin H, Lai J, Chin A, Chen Y, Chiang A. 2007. A map of olfactory representation in the *Drosophila* mushroom body. *Cell* **128**: 1205–1217.
- Liu X, Davis R. 2008. The GABAergic anterior paired lateral neuron suppresses and is suppressed by olfactory learning. *Nat Neurosci* **12**: 53–59.
- Machens CK, Stemmler MB, Prinz P, Krahe R, Ronacher B, Herz AV. 2001. Representation of acoustic communication signals by insect auditory receptor neurons. *J Neurosci* **21**: 3215–3227.
- MacLeod K, Bäcker A, Laurent G. 1998. Who reads temporal information contained across synchronized and oscillatory spike trains? *Nature* **395**: 693–698.
- Malnic B, Hirono J, Sato T, Buck LB. 1999. Combinatorial receptor codes for odors. *Cell* **96**: 713–723.
- Mamiya A, Beshel J, Xu C, Zhong Y. 2008. Neural representations of airflow in *Drosophila* mushroom body. *PLoS ONE* **3**: e4063.
- Mamiya A, Straw AD, Tómasson E, Dickinson MH. 2011. Active and passive antennal movements during visually guided steering in flying *Drosophila*. *J Neurosci* **31**: 6900–6914.
- Margulies C, Tully T, Dubnau J. 2005. Deconstructing memory in *Drosophila*. *Curr Biol* **15**: R700–13.
- Marin EC, Jefferis GSXE, Komiyama T, Zhu H, Luo L. 2002. Representation of the glomerular olfactory map in the *Drosophila* brain. *Cell* **109**: 243–255.
- Marr D. 1969. A theory of cerebellar cortex. *J Physiol* **202**: 437–470.
- Martinez W, Martinez A. 2005. *Exploratory data analysis with Matlab*. Chapman and Hall, London.
- Masek P, Heisenberg M. 2008. Distinct memories of odor intensity and quality in *Drosophila*. *Proc Natl Acad Sci USA* **105**: 15985–15990.

- Mazor O, Laurent G. 2005. Transient dynamics versus fixed points in odor representations by locust antennal lobe projection neurons. *Neuron* **48**: 661–673.
- McGuire SE, Le PT, Davis RL. 2001. The role of *Drosophila* mushroom body signaling in olfactory memory. *Science* **293**: 1330–1333.
- Meredith M. 1986. Patterned response to odor in mammalian olfactory bulb: the influence of intensity. *J Neurophysiol* **56**: 572–597.
- Moskowitz HR, Barbe CD. 1977. Profiling of odor components and their mixtures. *Sens Processes* **1**: 212–226.
- Murmu MS, Stinnakre J, Réal E, Martin JR. 2011. Calcium-stores mediate adaptation in axon terminals of olfactory receptor neurons in *Drosophila*. *BMC Neuroscience* **12**: 105.
- Murthy M, Turner GC. 2010. In vivo whole-cell recordings in the *Drosophila* brain. in *Drosophila neurobiology methods: a laboratory manual* (eds. Zhang B, Waddell S, Freeman M). Cold Spring Harbor Laboratory Press, Cold Spring Harbor, NY.
- Murthy M, Fiete I, Laurent G. 2008. Testing odor response stereotypy in the *Drosophila* mushroom body. *Neuron* **59**: 1009–1023.
- Nagel KI, Wilson RI. 2011. Biophysical mechanisms underlying olfactory receptor neuron dynamics. *Nat Neurosci* **14**: 208–216.
- Newsome WT, Britten KH, Movshon JA. 1989. Neuronal correlates of a perceptual decision. *Nature* **341**: 52–54.
- O'Connor DH, Wittenberg GM, Wang SSH. 2005. Graded bidirectional synaptic plasticity is composed of switch-like unitary events. *Proc Natl Acad Sci USA* **102**: 9679–9684.
- Okada R, Awasaki T, Ito K. 2009. Gamma-aminobutyric acid (GABA)-mediated neural connections in the *Drosophila* antennal lobe. *J Comp Neurol* **514**: 74–91.
- Olsen S, Bhandawat V, Wilson R. 2007. Excitatory interactions between olfactory processing channels in the *Drosophila* antennal lobe. *Neuron* **54**: 89–103.
- Olsen SR, Bhandawat V, Wilson RI. 2010. Divisive normalization in olfactory population codes. *Neuron* **66**: 287–299.
- Olsen SR, Wilson RI. 2008. Lateral presynaptic inhibition mediates gain control in an olfactory circuit. *Nature* **452**: 956–960.
- Olshausen BA, Field DJ. 1996. Emergence of simple-cell receptive field properties by learning a sparse code for natural images. *Nature* **381**: 607–609.
- Olshausen BA, Field DJ. 2004. Sparse coding of sensory inputs. *Current opinion in neurobiology* **14**: 481–487.
- Pascual A, Pr eat T. 2001. Localization of long-term memory within the *Drosophila* mushroom body. *Science* **294**: 1115–1117.
- Perez-Orive J, Mazor O, Turner G, Cassenaer S, Wilson R, Laurent G. 2002. Oscillations and sparsening of odor representations in the mushroom body. *Science* **297**: 359–365.

- Petersen CC, Malenka RC, Nicoll RA, Hopfield JJ. 1998. All-or-none potentiation at CA3-CA1 synapses. *Proc Natl Acad Sci USA* **95**: 4732–4737.
- Pfeiffer BD, Jenett A, Hammonds AS, Ngo TTB, Misra S, Murphy C, Scully A, Carlson JW, Wan KH, Lavery TR, Mungall C, Svirskas R, Kadonaga JT, Doe CQ, Eisen MB, Celniker SE, Rubin GM. 2008. Tools for neuroanatomy and neurogenetics in *Drosophila*. *Proc Natl Acad Sci USA* **105**: 9715–9720.
- Pinheiro J, Bates D. 2000. *Mixed-effects models in S and S-plus*. Springer, New York, NY.
- Purushothaman G, Bradley DC. 2005. Neural population code for fine perceptual decisions in area MT. *Nat Neurosci* **8**: 99–106.
- Qin H, Cressy M, Li W, Coravos J, Izzi S, Dubnau J. 2012. Gamma Neurons Mediate Dopaminergic Input during Aversive Olfactory Memory Formation in *Drosophila*. *Curr Biol* **22**: 608–614.
- Rieke F, Bodnar DA, Bialek W. 1995. Naturalistic stimuli increase the rate and efficiency of information transmission by primary auditory afferents. *Proc Biol Sci* **262**: 259–265.
- Root C, Semmelhack J, Wong A, Flores J, Wang J. 2007. Propagation of olfactory information in *Drosophila*. *Proc Natl Acad Sci U S A* **104**: 11826–11831.
- Root CM, Ko KI, Jafari A, Wang JW. 2011. Presynaptic facilitation by neuropeptide signaling mediates odor-driven food search. *Cell* **145**: 133–144.
- Root CM, Masuyama K, Green DS, Enell LE, Nässel DR, Lee CH, Wang JW. 2008. A presynaptic gain control mechanism fine-tunes olfactory behavior. *Neuron* **59**: 311–321.
- Rosenblatt F. 1958. The perceptron: a probabilistic model for information storage and organization in the brain. *Psychol Rev* **65**: 386–408.
- Roy B, Singh AP, Shetty C, Chaudhary V, North A, Landgraf M, Vijayraghavan K, Rodrigues V. 2007. Metamorphosis of an identified serotonergic neuron in the *Drosophila* olfactory system. *Neural Development* **2**: 20.
- Ruta V, Datta SR, Vasconcelos ML, Freeland J, Looger LL, Axel R. 2010. A dimorphic pheromone circuit in *Drosophila* from sensory input to descending output. *Nature* **468**: 686–690.
- Salzman CD, Britten KH, Newsome WT. 1990. Cortical microstimulation influences perceptual judgments of motion direction. *Nature* **346**: 174–177.
- Sanes JR, Zipursky SL. 2010. Design principles of insect and vertebrate visual systems. *Neuron* **66**: 15–36.
- Schwaerzel M, Heisenberg M, Zars T. 2002. Extinction antagonizes olfactory memory at the subcellular level. *Neuron* **35**: 951–960.
- Schwaerzel M, Monastirioti M, Scholz H, Friggi-Grelin F, Birman S, Heisenberg M. 2003. Dopamine and octopamine differentiate between aversive and appetitive olfactory memories in *Drosophila*. *J Neurosci* **23**: 10495–10502.
- Séjourné J, Plaçais PY, Aso Y, Siwanowicz I, Trannoy S, Thoma V, Tedjakumala SR, Rubin GM, Tchénio P, Ito K, Isabel G, Tanimoto H, Preat T. 2011. Mushroom body efferent neurons responsible for aversive olfactory memory retrieval in *Drosophila*. *Nat Neurosci* **14**: 903–910.

- Semmelhack JL, Wang JW. 2009. Select *Drosophila* glomeruli mediate innate olfactory attraction and aversion. *Nature* **459**: 218–223.
- Shanbhag SR, Müller B, Steinbrecht RA. 2000. Atlas of olfactory organs of *Drosophila melanogaster* 2. Internal organization and cellular architecture of olfactory sensilla. *Arthropod structure & development* **29**: 211–229.
- Shanbhag S, Müller B, Steinbrecht R. 1999. Atlas of olfactory organs of *Drosophila melanogaster*: 1. Types, external organization, innervation and distribution of olfactory sensilla. *International Journal of Insect Morphology and Embryology* **28**: 377–397.
- Shang Y, Claridge-Chang A, Sjulson L, Pypaert M, Miesenbock G. 2007. Excitatory local circuits and their implications for olfactory processing in the fly antennal lobe. *Cell* **128**: 601–612.
- Shiraiwa T. 2008. Multimodal chemosensory integration through the maxillary palp in *Drosophila*. *PLoS ONE* **3**: e2191.
- Silbering AF, Galizia CG. 2007. Processing of odor mixtures in the *Drosophila* antennal lobe reveals both global inhibition and glomerulus-specific interactions. *J Neurosci* **27**: 11966–11977.
- Silbering AF, Rytz R, Grosjean Y, Abuin L, Ramdya P, Jefferis GSXE, Benton R. 2011. Complementary function and integrated wiring of the evolutionarily distinct *Drosophila* olfactory subsystems. *J Neurosci* **31**: 13357–13375.
- Sosulski DL, Bloom ML, Cutforth T, Axel R, Datta SR. 2011. Distinct representations of olfactory information in different cortical centres. *Nature* **472**: 213–216.
- Stensmyr MC, Giordano E, Balloi A, Angioy AM, Hansson BS. 2003. Novel natural ligands for *Drosophila* olfactory receptor neurones. *J Exp Biol* **206**: 715–724.
- Stettler DD, Axel R. 2009. Representations of odor in the piriform cortex. *Neuron* **63**: 854–864.
- Stopfer M, Laurent G. 1999. Short-term memory in olfactory network dynamics. *Nature* **402**: 664–668.
- Stopfer M, Jayaraman V, Laurent G. 2003. Intensity versus identity coding in an olfactory system. *Neuron* **39**: 991–1004.
- Störtkuhl KF, Hovemann BT, Carlson JR. 1999. Olfactory adaptation depends on the Trp Ca²⁺ channel in *Drosophila*. *J Neurosci* **19**: 4839–4846.
- Su CY, Martelli C, Emonet T, Carlson JR. 2011. Temporal coding of odor mixtures in an olfactory receptor neuron. *Proc Natl Acad Sci USA* **108**: 5075–5080.
- Szyszka P, Ditzen M, Galkin A, Galizia CG, Menzel R. 2005. Sparsening and temporal sharpening of olfactory representations in the honeybee mushroom bodies. *J Neurophysiol* **94**: 3303–3313.
- Szyszka P, Galkin A, Menzel R. 2008. Associative and non-associative plasticity in kenyon cells of the honeybee mushroom body. *Front Syst Neurosci* **2**: 3.
- Tabor R, Yaksi E, Weislogel JM, Friedrich RW. 2004. Processing of odor mixtures in the zebrafish olfactory bulb. *J Neurosci* **24**: 6611–6620.
- Tan Y, Yu D, Pletting J, Davis RL. 2010. Gilgamesh is required for rutabaga-independent olfactory learning in *Drosophila*. *Neuron* **67**: 810–820.

- Tanaka N, Awasaki T, Shimada T, Ito K. 2004. Integration of chemosensory pathways in the *Drosophila* second-order olfactory centers. *Curr Biol* **14**: 449–457.
- Tanaka NK, Ito K, Stopfer M. 2009. Odor-evoked neural oscillations in *Drosophila* are mediated by widely branching interneurons. *J Neurosci* **29**: 8595–8603.
- Tanaka NK, Tanimoto H, Ito K. 2008. Neuronal assemblies of the *Drosophila* mushroom body. *J Comp Neurol* **508**: 711–755.
- Thum AS, Jenett A, Ito K, Heisenberg M, Tanimoto H. 2007. Multiple memory traces for olfactory reward learning in *Drosophila*. *J Neurosci* **27**: 11132–11138.
- Tian L, Hires SA, Mao T, Huber D, Chiappe ME, Chalasani SH, Petreanu L, Akerboom J, McKinney SA, Schreiter ER, Bargmann CI, Jayaraman V, Svoboda K, Looger LL. 2009. Imaging neural activity in worms, flies and mice with improved GCaMP calcium indicators. *Nature methods* **6**: 875–881.
- Todi SV, Sharma Y, Eberl DF. 2004. Anatomical and molecular design of the *Drosophila* antenna as a flagellar auditory organ. *Microsc Res Tech* **63**: 388–399.
- Tomer R, Denes AS, Tessmar-Raible K, Arendt D. 2010. Profiling by image registration reveals common origin of annelid mushroom bodies and vertebrate pallium. *Cell* **142**: 800–809.
- Tootoonian S, Coen P, Kawai R, Murthy M. 2012. Neural representations of courtship song in the *Drosophila* brain. *J Neurosci* **32**: 787–798.
- Tully T, Quinn WG. 1985. Classical conditioning and retention in normal and mutant *Drosophila melanogaster*. *J Comp Physiol A* **157**: 263–277.
- Turner GC, Bazhenov M, Laurent G. 2008. Olfactory representations by *Drosophila* mushroom body neurons. *J Neurophysiol* **99**: 734–746.
- Turner SL, Ray A. 2009. Modification of CO₂ avoidance behaviour in *Drosophila* by inhibitory odorants. *Nature* **461**: 277–281.
- Uchida N, Mainen ZF. 2003. Speed and accuracy of olfactory discrimination in the rat. *Nat Neurosci* **6**: 1224–1229.
- van der Goes van Naters W, Carlson JR. 2007. Receptors and neurons for fly odors in *Drosophila*. *Curr Biol* **17**: 606–612.
- Venables WN, Ripley B. 1999. *Modern Applied Statistics with S*. Springer-Verlag, New York, NY, 4th edition.
- Vosshall LB, Wong AM, Axel R. 2000. An olfactory sensory map in the fly brain. *Cell* **102**: 147–159.
- Walker KMM, Ahmed B, Schnupp JWH. 2008. Linking cortical spike pattern codes to auditory perception. *Journal of cognitive neuroscience* **20**: 135–152.
- Wang Y, Chiang A, Xia S, Kitamoto T, Tully T, Zhong Y. 2003. Blockade of neurotransmission in *Drosophila* mushroom bodies impairs odor attraction, but not repulsion. *Curr Biol* **13**: 1900–1904.
- Wang Y, Wright NJ, Guo H, Xie Z, Svoboda K, Malinow R, Smith DP, Zhong Y. 2001. Genetic manipulation of the odor-evoked distributed neural activity in the *Drosophila* mushroom body. *Neuron* **29**: 267–276.

- Wang Y, Guo HF, Pologruto TA, Hannan F, Hakker I, Svoboda K, Zhong Y. 2004. Stereotyped odor-evoked activity in the mushroom body of *Drosophila* revealed by green fluorescent protein-based Ca²⁺ imaging. *J Neurosci* **24**: 6507–6514.
- Wang Y, Mamiya A, shyn Chiang A, Zhong Y. 2008. Imaging of an early memory trace in the *Drosophila* mushroom body. *J Neurosci* **28**: 4368–4376.
- Willmore B, Tolhurst DJ. 2001. Characterizing the sparseness of neural codes. *Network* **12**: 255–270.
- Willmore BDB, Mazer JA, Gallant JL. 2011. Sparse coding in striate and extrastriate visual cortex. *J Neurophysiol* **105**: 2907–2919.
- Wilson R, Laurent G. 2005. Role of GABAergic inhibition in shaping odor-evoked spatiotemporal patterns in the *Drosophila* antennal lobe. *J Neurosci* **25**: 9069–9079.
- Wilson R, Turner G, Laurent G. 2004. Transformation of olfactory representations in the *Drosophila* antennal lobe. *Science* **303**: 366–370.
- Wu CL, Shih MFM, Lai JSY, Yang HT, Turner GC, Chen L, Chiang AS. 2011. Heterotypic gap junctions between two neurons in the *Drosophila* brain are critical for memory. *Curr Biol* **21**: 848–854.
- Yaksi E, Wilson RI. 2010. Electrical coupling between olfactory glomeruli. *Neuron* **67**: 1034–1047.
- Yao CA, Ignell R, Carlson JR. 2005. Chemosensory coding by neurons in the coeloconic sensilla of the *Drosophila* antenna. *J Neurosci* **25**: 8359–8367.
- Yarali A, Mayerle M, Nawroth C, Gerber B. 2008. No evidence for visual context-dependency of olfactory learning in *Drosophila*. *Die Naturwissenschaften* **95**: 767–774.
- Yasuyama K, Meinertzhagen IA, Schürmann FW. 2002. Synaptic organization of the mushroom body calyx in *Drosophila melanogaster*. *J Comp Neurol* **445**: 211–226.
- Yorozu S, Wong A, Fischer BJ, Dankert H, Kernan MJ, Kamikouchi A, Ito K, Anderson DJ. 2009. Distinct sensory representations of wind and near-field sound in the *Drosophila* brain. *Nature* **458**: 201–205.
- Yu D, Akalal DBG, Davis RL. 2006. *Drosophila* alpha/beta mushroom body neurons form a branch-specific, long-term cellular memory trace after spaced olfactory conditioning. *Neuron* **52**: 845–855.
- Yu D, Keene AC, Srivatsan A, Waddell S, Davis RL. 2005. *Drosophila* DPM neurons form a delayed and branch-specific memory trace after olfactory classical conditioning. *Cell* **123**: 945–957.
- Yu HH, Chen CH, Shi L, Huang Y, Lee T. 2009. Twin-spot MARCM to reveal the developmental origin and identity of neurons. *Nat Neurosci* **12**: 947–953.
- Zhu S, shyn Chiang A, Lee T. 2003. Development of the *Drosophila* mushroom bodies: elaboration, remodeling and spatial organization of dendrites in the calyx. *Development* **130**: 2603–2610.
- Zohary E, Shadlen M, Newsome W. 1994. Correlated neuronal discharge rate and its implications for psychophysical performance. *Nature* **370**: 140–143.